

INFORMATION TO USERS

This manuscript has been reproduced from the microfilm master. UMI films the text directly from the original or copy submitted. Thus, some thesis and dissertation copies are in typewriter face, while others may be from any type of computer printer.

The quality of this reproduction is dependent upon the quality of the copy submitted. Broken or indistinct print, colored or poor quality illustrations and photographs, print bleedthrough, substandard margins, and improper alignment can adversely affect reproduction.

In the unlikely event that the author did not send UMI a complete manuscript and there are missing pages, these will be noted. Also, if unauthorized copyright material had to be removed, a note will indicate the deletion.

Oversize materials (e.g., maps, drawings, charts) are reproduced by sectioning the original, beginning at the upper left-hand corner and continuing from left to right in equal sections with small overlaps. Each original is also photographed in one exposure and is included in reduced form at the back of the book.

Photographs included in the original manuscript have been reproduced xerographically in this copy. Higher quality 6" x 9" black and white photographic prints are available for any photographs or illustrations appearing in this copy for an additional charge. Contact UMI directly to order.

UMI

A Bell & Howell Information Company
300 North Zeeb Road, Ann Arbor MI 48106-1346 USA
313/761-4700 800/521-0600

**PREDICTION OF BIODIESEL FUEL ATOMIZATION
CHARACTERISTICS BASED ON MEASURED PROPERTIES**

by
Cecil A. W. Allen

A Thesis Submitted to the
Faculty of Engineering
In Partial Fulfilment of the Requirements
for the Degree of

DOCTOR OF PHILOSOPHY
Major Subject: Agricultural Engineering

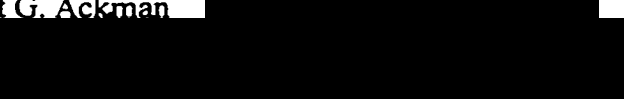
APPROVED:



Dr. K. Chris Watts, Supervisor



Dr. Robert G. Ackman



Dr. Michael J. Pegg



Dr. Ken I. Wilkie



Dr. Charles L. Peterson, University of Idaho, External Examiner

DALHOUSIE UNIVERSITY - DALTECH
Halifax, Nova Scotia

1998



**National Library
of Canada**

**Acquisitions and
Bibliographic Services**

**395 Wellington Street
Ottawa ON K1A 0N4
Canada**

**Bibliothèque nationale
du Canada**

**Acquisitions et
services bibliographiques**

**395, rue Wellington
Ottawa ON K1A 0N4
Canada**

Your file Votre référence

Our file Notre référence

The author has granted a non-exclusive licence allowing the National Library of Canada to reproduce, loan, distribute or sell copies of this thesis in microform, paper or electronic formats.

The author retains ownership of the copyright in this thesis. Neither the thesis nor substantial extracts from it may be printed or otherwise reproduced without the author's permission.

L'auteur a accordé une licence non exclusive permettant à la Bibliothèque nationale du Canada de reproduire, prêter, distribuer ou vendre des copies de cette thèse sous la forme de microfiche/film, de reproduction sur papier ou sur format électronique.

L'auteur conserve la propriété du droit d'auteur qui protège cette thèse. Ni la thèse ni des extraits substantiels de celle-ci ne doivent être imprimés ou autrement reproduits sans son autorisation.

0-612-31516-9

Canada

DALTECH LIBRARY

“AUTHORITY TO DISTRIBUTE MANUSCRIPT THESIS”

TITLE:

**Prediction of Biodiesel Fuel Atomization Characteristics Based on
Measured Properties**

The above library may make available or authorize another library to make available individual photo/microfilm copies of this thesis without restrictions.

Full Name of Author: Cecil A. W. Allen

Signature of Author:

A solid black rectangular box redacting the author's signature.

Date:

June 30, 1998

TABLE OF CONTENTS

LIST OF TABLES	vii
LIST OF FIGURES	x
LIST OF SYMBOLS	xiii
ACKNOWLEDGEMENTS	xvi
ABSTRACT	xvii
1 INTRODUCTION	1
1.1 Rationale	3
1.2 Thesis Objectives	4
2 LITERATURE REVIEW	5
2.1 Diesel Engines	5
2.1.1 Basic Operational Principles of the Diesel Engine	5
2.1.2 Combustion in the Diesel Engine	6
2.2 Fats and Oils	7
2.2.1 The Transesterification Process	11
2.3 Biodiesel CI Engine	14
2.3.1 Neat Vegetable Oils as Diesel Fuels	15
2.3.2 Vegetable Oil / Diesel Fuel Blends	16
2.3.3 The Use of Esters of Vegetable Oils as Diesel Fuel	17
2.4 Droplet Measurement Techniques	21
2.4.1 Capture by Immersion in Liquids	21
2.4.2 Still Photography	23
2.4.3 Particle Measuring Systems (PMS)	23
2.4.4 Laser Diffraction Technique (Malvern Analyser)	24
2.4.5 Summary of Droplet Measuring Techniques	27

3	THEORETICAL CONSIDERATIONS	28
3.1	Droplet Formation	28
3.2	Droplet Evaporation and Combustion	30
3.3	Sensitivity Analysis of Properties Affecting Atomization	32
3.3.1	Atomization Characteristic Model [Msipa <i>et al.</i> , 1983]	33
3.3.2	SMD Model [Hiroyasu <i>et al.</i> , 1989]	36
3.3.3	Sensitivity Analysis Procedure	36
3.3.4	Results of Sensitivity Analysis	37
4	RESEARCH PROCEDURES	45
4.1	Overview of the Four Phases of the Research	45
4.2	Sample Preparation	46
4.2.1	The Transesterification Procedure	50
4.3	Measurement of Properties	53
4.3.1	Viscosity	53
4.3.2	Surface Tension	53
4.4	Atomization Characteristics	54
5	MODELS FOR PREDICTING BIODIESEL PROPERTIES	63
5.1	Viscosity	63
5.1.1	Predicting Viscosities of Mixtures using a Simplified Logarithmic Equation	66
5.2	Surface Tension	68
5.2.1	Predicting Surface Tension of Mixtures using a Weighted Mass Average Method	71
5.3	Atomization Models	72

6 RESULTS AND DISCUSSION	75
6.1 Viscosity	75
6.1.1 Viscosity of Methyl and Ethyl Ester GC Standards	75
6.1.2 Viscosity of Mixtures of Methyl and Ethyl Ester GC Standards ..	79
6.1.3 Prediction of the Viscosities of Vegetable Oil Biodiesel Fuels ...	82
6.2 Surface Tension	93
6.2.1 Surface Tension of Methyl and Ethyl Ester GC Standards	93
6.2.2 Surface Tension of Mixtures of Methyl and Ethyl Ester GC Standards	
.....	98
6.2.3 Prediction of the Surface Tension of Vegetable Oil Biodiesel Fuels	
.....	101
6.3 Atomization	107
6.3.1 Spray System Preliminary Results	107
6.3.2 Atomization of Biodiesel Fuels	117
6.3.3 Predicting the Rosin-Rammler Parameters and SMD using Regression	
Models	126
6.3.4 Dimensional Analysis of SMD Regression Model	137
6.4 Review of Experimental Results	142
7 APPLICATION OF PREDICTION MODELS TO BIODIESEL FUELS.....	143
7.1 Inferences on Biodiesel Fuel Atomization Based on Predicted Parameters..	157
8 CONCLUSIONS	158
9 RECOMMENDATIONS	160
REFERENCES	162
APPENDIX A Design of an Engine Test Facility for Biodiesel Fuels	172
APPENDIX B Sensitivity Analysis of Thermal Properties	180

APPENDIX C	C - Programs Used to Carry Out Sensitivity Analysis on Biodiesel Properties	185
APPENDIX D	Viscosities of Natural Vegetable Oil Methyl Esters Predicted using the Measured Viscosities of GC Standards	195
APPENDIX E	Surface Tension of Natural Vegetable Oil Methyl Esters Predicted using the Measured Surface Tension of GC Standards	196
APPENDIX F	Regression Analyses for Atomization Parameters SMD, 'X', and 'n'	197

LIST OF TABLES

- Table 2.2.1 Fatty Acid Composition of Some Naturally Occurring Fats and Oils
- Table 3.3.4.1 Typical Properties of Mixtures of Canola, Peanut and Coconut Oil Methyl Esters
- Table 3.3.4.2 Mean Value of Properties used for Sensitivity Analysis
- Table 3.3.4.3 Parameters used in Sensitivity Analysis
- Table 5.1.1 Group Contribution for G_{ij} at 298K (25 °C)
- Table 5.2.1 Structural Contributions for the Computation of the Parachor (Quale, 1953)
- Table 5.2.2 Structural Contributions for the Computation of the Parachor (Meissner and Michaels, 1949)
- Table 6.1.2.1 Viscosities of Binary, Ternary and Quaternary Mixtures of Fatty Acid Ethyl Ester GC Standards at 25°C
- Table 6.1.2.2 Viscosities and Mass Fraction of Simulated Vegetable Oil Methyl Esters at 40 °C - (using measured viscosities of pure components)
- Table 6.1.3.1 Viscosities of Methyl Ester Biodiesel Fuels at 40 °C - (using viscosities of pure components taken from Swern (1979) and lumped mass fractions)
- Table 6.1.3.2 Biodiesel Fuel Methyl Ester Composition Obtained by TLD-FID Analysis
- Table 6.1.3.3 Viscosities of Methyl Ester Biodiesel Fuels at 40 °C - {using viscosities of pure components taken from Swern (1979) and mass fractions taken from Ackman (1996)}
- Table 6.2.1.1 Surface Tension of Saturated Methyl Esters at 40 °C
- Table 6.2.2.1 Surface Tension of Binary, Ternary and Quaternary Mixtures of Fatty Acid Ethyl Ester GC Standards at 25°C
- Table 6.2.2.2 Surface Tension of Simulated Vegetable Oil Methyl Esters at 40 °C

- Table 6.2.3.1 Surface Tension of Pure Methyl Esters Calculated Using the Sugden's Parachor
- Table 6.2.3.2 Surface Tension of Methyl Ester Biodiesel Fuels at 40 °C (using component surface tension calculated by the Sugden's Parachor method)
- Table 6.2.3.3 Surface Tension of Methyl Ester Biodiesel Fuels at 40 °C (using mass fractions given by Ackman (1996) and component surface tension calculated by the Sugden's Parachor method)
- Table 6.3.1.1 Comparison of Log-Differences for Four Droplet Distribution Models (taken at spray tip for medium flow pump rack position)
- Table 6.3.2.1 SMD of Biodiesel and Diesel Fuels
- Table 6.3.2.2 Rosin-Rammler 'X' Parameters for Biodiesel ME and Diesel Fuels
- Table 6.3.2.3 Rosin-Rammler 'n' Parameters for Biodiesel ME and Diesel Fuels
- Table 6.3.3.1 Regression Analysis for SMD of Methyl Ester Biodiesel Fuels using Three Coefficients and a Constant
- Table 6.3.3.2 Regression Analysis for SMD of Methyl Ester Biodiesel Fuels using Two Coefficients and No Constant
- Table 6.3.3.3 Fitted Data and Confidence Limits for SMD
- Table 6.3.3.4 Regression Analysis for the 'X' Parameter of Methyl Ester Biodiesel Fuels
- Table 6.3.3.5 Fitted Data and Confidence Limits for 'X'
- Table 6.3.3.6 Regression Analysis for the 'n' Parameter for Methyl Ester Biodiesel Fuels
- Table 6.3.3.7 Fitted Data and Confidence Limits for 'n'
- Table 6.3.4.1 Typical Values for Atomization Parameters
- Table 7.1 Fatty Acid Composition of 15 Fats and Oils (Ackman, 1996)
- Table 7.2 Predicted Viscosities for 15 Biodiesel Fuel Types (40 °C)
- Table 7.3 Predicted Surface Tension for 15 Biodiesel Fuel Types (40 °C)
- Table 7.4 Sensitivity Analysis of SMD Regression Model #1 (Equation 6.3.3.9)
- Table 7.5 Sensitivity Analysis of SMD Regression Model #2 (Equation 6.3.3.10)

Table 7.6	SMD Predicted for 15 Biodiesel Fuel Types Based on Specific Atomization Parameters
Table 7.7	Regression Analysis for SMD of Methyl Ester Biodiesel Fuels using Viscosity as the only Independent Variable
Table B.1	Mean Value of Thermal Properties used for Sensitivity Analysis
Table D.1	Viscosities of Methyl Ester Biodiesel Fuels at 40 °C - (using measured viscosities of GC standards and lumped mass fractions)
Table E.1	Surface Tension of Methyl Ester Biodiesel Fuels at 40 °C (using measured surface tension of GC Standards)

LIST OF FIGURES

- Figure 2.4.4.1 Schematic of a Malvern Droplet Analyser
- Figure 3.3.5.1 Variation of Normalized Atomization Characteristic (Ka_i / Ka_{max}) with 5% Variation of Surface Tension for Constant Density and Viscosity
- Figure 3.3.5.2 Variation of Normalized Atomization Characteristic (Ka_i / Ka_{max}) with 5% Variation Density for Constant Surface Tension and Viscosity
- Figure 3.3.5.3 Variation of Normalized Atomization Characteristic (Ka_i / Ka_{max}) with 5% Variation of Viscosity for Constant Surface Tension and Density
- Figure 3.3.5.4 Variation of Normalized Atomization Characteristic (Ka_i / Ka_{max}) with 30% Variation of Viscosity for Constant Surface Tension and Density
- Figure 3.3.5.5 Variation of Normalized Sauter Mean Diameter (SMD_i / SMD_{max}) with 5% Variation of Surface Tension for Constant Density and Viscosity
- Figure 3.3.5.6 Variation of Normalized Sauter Mean Diameter (SMD_i / SMD_{max}) with 5% Variation of Density for Constant Surface Tension and Viscosity
- Figure 3.3.5.7 Variation of Normalized Sauter Mean Diameter (SMD_i / SMD_{max}) with 5% Variation of Viscosity for Constant Density and Surface Tension
- Figure 3.3.5.8 Variation of Normalized Sauter Mean Diameter (SMD_i / SMD_{max}) with 30% Variation of Surface Tension for Constant Density and Viscosity
- Figure 4.2.1 Schematic of Batch Transesterification Unit
- Figure 4.2.2 Overall View of Batch Transesterification Unit
- Figure 4.2.2.1 TLC-FID Chromatogram showing ME Separation
- Figure 4.4.1 Diesel Pump and Electric Motor
- Figure 4.4.2 Diesel Pump and Fuel Injectors
- Figure 4.4.3 Fuel Injector and its Coupling
- Figure 4.4.4 Precision X-Y-Z Computer Controlled Traversing Mechanism
- Figure 4.4.5 Electronic Components for Timing Pulsed Spray

- Figure 4.4.6 A Typical Spray as Visualized using the Timed Stroboscope**
- Figure 6.1.1.1 Viscosities of Fatty Acid Methyl and Ethyl Ester GC Standards at 40°C**
- Figure 6.1.1.2 Viscosity Trend Lines for Methyl and Ethyl Ester GC Standards at 40°C**
- Figure 6.1.3.1 Rheograms for Vegetable Oil Methyl Ester Biodiesel Fuels at 40 °C Plotted on a Linear Scale**
- Figure 6.1.3.2 Rheograms for Vegetable Oil Methyl Ester Biodiesel Fuels at 40 °C Plotted on a Log Scale**
- Figure 6.1.3.3 Viscosities of Pure Methyl Ester Biodiesel Fuel Components at 40 °C [Swern, 1979)**
- Figure 6.2.1.1 Surface Tension of Fatty Acid Methyl and Ethyl Ester GC Standards at 40°C**
- Figure 6.2.1.2 Surface Tension Trend Lines for Saturated Methyl and Ethyl Ester GC Standards at 40 °C**
- Figure 6.2.3.1 Surface Tension of Pure Methyl Ester Biodiesel Fuel Components at 40 °C**
- Figure 6.3.1.1 Diesel Fuel Droplet Distribution for Ten Runs**
- Figure 6.3.1.2 Canola ME Biodiesel Fuel Droplet Distribution for Ten Runs**
- Figure 6.3.1.3 Coconut ME Biodiesel Fuel Droplet Distribution for Ten Runs**
- Figure 6.3.1.4 Soya ME Biodiesel Fuel Droplet Distribution for Ten Runs**
- Figure 6.3.1.5 Peanut ME Biodiesel Fuel Droplet Distribution for Ten Runs**
- Figure 6.3.1.6 Palm ME Biodiesel Fuel Droplet Distribution for Ten Runs**
- Figure 6.3.1.7 Diesel Fuel Droplet Distribution Using Different Models**
- Figure 6.3.1.8 Canola Oil Droplet Distribution Using Different Models**
- Figure 6.3.1.9 Verification of the Rosin-Rammler Distribution**
- Figure 6.3.2.1 Droplet Distribution of Diesel Fuel, Neat Canola Oil and Canola Oil Methyl Ester**
- Figure 6.3.2.2 Droplet Distributions of Biodiesel ME and Diesel Fuels**
- Figure 6.3.2.3 Measured SMD of Methyl Ester Biodiesel Fuels**

Figure 6.3.2.4 Percent Difference of the Measured SMD of Methyl Ester Biodiesel Fuels Compared with Diesel Fuel

- Figure 7.1 Predicted Viscosities at 40 °C for 15 Methyl Ester Biodiesel Fuels**
- Figure 7.2 Predicted Surface Tension at 40 °C for 15 Methyl Ester Biodiesel Fuels**
- Figure 7.3 Predicted Sauter Mean Diameter for 15 Methyl Ester Biodiesel Fuels**
- Figure 7.4 Predicted SMD for 15 Biodiesel Types Compared with Diesel Fuel**
- Figure 7.5 Predicted Droplet Distribution for 15 Methyl Ester Biodiesel Fuels**
- Figure A.1 Schematic of Circuit Diagram for D.C. Machines**
- Figure A.2 Schematic of Optical Speed Sensor**
- Figure A.3 Schematic Layout of Test Unit**
- Figure A.4 Overall View of the Engine and D.C Motor Setup**
- Figure B.1 Variation of Normalized Burning Rate Constant (Kb_i / Kb_{max}) with 5% Variation of Density for Constant Specific Heat Capacity, Thermal Conductivity and Latent Heat of Vaporization**
- Figure B.2 Variation of Normalized Burning Rate Constant (Kb_i / Kb_{max}) with 5% Variation of Specific Heat Capacity for Constant Density, Thermal Conductivity and Latent Heat of Vaporization**
- Figure B.3 Variation of Normalized Burning Rate Constant (Kb_i / Kb_{max}) with 5% Variation of Latent Heat of Vaporization for Constant Density, Thermal Conductivity and Specific Heat Capacity**
- Figure B.4 Variation of Normalized Burning Rate Constant (Kb_i / Kb_{max}) with 5% Variation of Thermal Conductivity for Constant Density, Latent Heat of Vaporization and Specific Heat Capacity**

LIST OF SYMBOLS

c	-	constant in surface tension weight function
cr	-	compression ratio
C_p	-	specific heat capacity (J/kg.K)
d	-	diameter (m)
D	-	capillary diameter for rolling-ball viscometer (m)
E	-	nozzle efficiency
g	-	acceleration due to gravity (m/s^2)
Ka	-	atomization characteristic
Kb	-	burning rate constant (m/s)
K_1, K_2, K_3, K_4	-	regression constants
G	-	viscosity interaction parameter
L	-	latent heat of vaporization (J/kg)
m	-	slope
M	-	molecular weight (g/mol)
n	-	Rosin-Rammler distribution parameter
N	-	number of droplets
P	-	pressure (Pa)
[P]	-	surface tension Parachor { $(N/m)^{1/4} (m^3/mol)$ }
Q	-	volume flow rate (m^3/s)
R	-	gas constant (J/mol.K)
Re	-	Reynolds number { $(\rho V d)/\mu$ }
R_{over}	-	fraction of droplets over diameter d
s	-	standard error
t	-	time (s)
T	-	temperature (K)

V	-	velocity (m/s)
w	-	surface tension weight factor
We	-	Weber number $[(\rho V^2 d)/\sigma]$
x	-	mass fraction
X	-	Rosin-Rammler distribution parameter
y	-	mole fraction

Greek Symbols

γ	-	polytropic index
$\dot{\gamma}$	-	shear rate in viscous flow (1/s)
θ	-	rolling-ball viscometer angle (deg)
λ	-	thermal conductivity (W/m ² K)
μ	-	dynamic viscosity (mPa.s)
ν	-	kinematic viscosity (m ² /s)
ρ	-	density (kg/m ³)
σ	-	surface tension (mN/m)
τ	-	shear stress in viscous flow (Pa)
ϕ	-	nozzle length to diameter ratio $[L_o/d_o]$ (m)
ψ	-	fuel to air density ratio ρ_f/ρ_g

Subscripts

f	-	fuel
g	-	gas atmosphere into which fuel is injected
L	-	fuel injector line
o	-	nozzle orifice

Abbreviations

CI	-	compression ignition
DI	-	direct injection
IDI	-	indirect injection
EE	-	ethyl esters
FAME	-	fatty acid methyl esters
FFA	-	free fatty acids
GC	-	gas chromatography
MA	-	mass average
ME	-	methyl esters
NDB	-	number of double bonds in a carbon chain
PMS	-	particle measuring system
SMD	-	Sauter Mean Diameter
TG	-	triglyceride
ST	-	surface tension
TLC-FID	-	thin layer chromatography with flame ionization detection
VO	-	vegetable oil
VOME	-	vegetable oil methyl ester

ACKNOWLEDGEMENTS

The author wishes to express his sincere gratitude to all those persons who may have contributed in one way or another to the successful completion of this thesis.

Special thanks to Dr. K. Chris Watts for his invaluable support and encouragement throughout the thesis work. His supervision and guidance were superb. The financial support provided by him through his Natural Science and Engineering Research Council (NSERC) operating grant is very highly appreciated.

The author wishes to acknowledge the excellent guidance provided by Doctors Robert G. Ackman, Michael J. Pegg, and Ken I. Wilkie throughout the thesis activities. Special thanks to these professors for providing research material and invaluable advice during the thesis work.

The work of Messrs. Jack Vissers and Albert Murphy, mechanical technologists, was of a very high class. Congratulation and special thanks to both of them for their superb work. Mr. Greg Jollimore provided excellent assistance with all of the electronics and his work is highly appreciated. The assistance given by Mr. John Pyke in various areas is also highly appreciated.

Thanks to Dr. Alan Paulson, Dr. Alex Speers, Mr. John Thompson and Mr. Doug Singer for providing viscosity and surface tension equipment and supplies. Special thanks to Ms. Anne Timmins and Ms. Ena MacPherson for their invaluable technical assistance given during chemical analysis of the biodiesel fuels.

Most important of all, deepest gratitude to my wife, Giselle; my mother, Waveney; my sons Stefan and Steven; and all my family for giving tremendous support and encouragement throughout my study career.

ABSTRACT

Biodiesel fuels are the acyl esters of triglycerides that originate from vegetable or animal sources. The most common of these are the vegetable oil methyl ester (VOME) biodiesel fuels. These oils are from renewable sources and have great potential as fuels for the compression ignition engine.

The relationship between the fatty acid composition of the VOME, their viscosity and surface tension, and their atomization characteristics were investigated in this study. Models for predicting the viscosity and surface tension were established by considering biodiesel fuels as being mixtures of fatty acid methyl esters (FAME). The mixture equation for viscosity predicted the fuel's viscosity within 3.5% on average of the measured values. Surface tension was also predicted within 3.5% on average. These mixture equations were developed and verified using controlled mixtures of gas chromatography injection standards.

Atomization characteristics of five VOME biodiesels were measured using a Malvern Laser Diffraction Droplet Analyzer. These characteristics were compared with each other and with diesel #2 fuel, and were correlated with surface tension and viscosity. Regression models for atomization were developed with viscosity and surface tension as independent variables; all other parameters being held constant. The model for predicting the Sauter Mean Diameter (SMD) had an accuracy of approximately $0.8 \mu\text{m}$ on average. The parameters of this model were related to dimensional parameters developed using dimensional analyses. The droplet distribution of all the VOMEs was found to follow a Rosin-Rammler distribution model and regression models to predict the two parameters of this model were also developed.

The viscosity, surface tension and atomization characteristics of 15 common oils /fats were predicted using their fatty acid compositions taken from the literature. It was found that most of the oils had similar atomization characteristics because they contained mainly C18 unsaturated fatty acids. In general, it was found that oils containing mainly fatty acids with carbon numbers less than or equal to C14 had good atomization characteristics (less than 15% higher SMD) that were statistically similar to diesel fuel. Oils with mainly C18 unsaturates had moderate atomization characteristics (up to 25% higher SMD) compared to diesel fuel. Oils with mainly saturated fatty acids with carbon numbers greater than or equal to C16 had poorer atomization characteristics (greater than 25% higher SMD) compared with diesel fuel.

1 INTRODUCTION

Energy requirements for field equipment and transport vehicles have conventionally been provided mainly by liquid petroleum fuels. In 1973 the organization of petroleum exporting countries (OPEC) increased the price of oil from US\$2/barrel to US\$10/barrel resulting in what was known as the “first energy crisis”. In 1979 the price again went up to US\$30/barrel and since then there has only been a slight reduction in this price. Studies carried out by various authors, including Buckley-Golder and Langley (1985), conclude that with the current trend of oil consumption from known reserves, the supply of oil has an approximate 30 year life from 1985 to 2014. This prediction does not explicitly mean that the oil supply will come to an abrupt end at that time but it is just an estimation based on the ratio of known reserves to current utilization.

In developing countries, like Guyana, the high prices of petroleum based products are a great burden on their economy. Petroleum products are normally imported by these countries and usually consume in excess of 50% of their foreign currency earnings. The cost of living in developing countries is also affected by the price of petroleum products since almost all economic activities, including agriculture, are reliant on petroleum products.

Due to the general concern regarding the future availability of fossil fuels, environmental concerns regarding its use, and the negative impact of the high prices of petroleum products on the economy of developing countries, there exists a need for the increased use of liquid alternative fuels in the future. Promising candidates for this are vegetable oil fuels which are particularly applicable to compression ignition engines. Vegetable oils are derived from renewable sources and their production can be undertaken by developing countries. Many workers have sought to use neat (unprocessed) vegetable oils in diesel engines; even the engine’s inventor Rudolf Diesel used peanut oil in the early stages of the engine’s development. However, as fuel for diesel engines, vegetable oils are now almost exclusively used in the form of methyl or ethyl esters. The conversion of vegetable oils to their acyl

esters results in the removal of the glycerol moiety of the oil which leads primarily to a marked reduction in its viscosity, usually from approximately 40-60 mPa.s to 2 - 8 mPa.s depending on the oil and its fatty acid composition. The surface tension of the oils is also slightly reduced.

Biodiesel fuels in the form of esters of vegetable oils have the potential to compete with standard diesel fuels in most respects, as will be discussed in Chapter 2. However, in order to realize biodiesels' maximum potential, a clear understanding of how its characteristics affect the performance of compression ignition engines is essential. There are two broad categories into which the tests of fuel performance can be placed; one based on engine performance characteristics, and the other based on the fuel atomization and combustion characteristics. Extensive work has been done on engine tests and varied results have been reported (Chapter 2). An engine test facility was designed and commissioned in the preliminary stages of this doctorate (Appendix A). This test facility is well equipped for measuring engine performance in terms of power, fuel consumption, exhaust and fuel temperatures, and emissions. However, due to the varied results in the proliferation of papers dealing with engine tests it was concluded that a systematic study of the biodiesel fuel characteristics was required, covering particularly the atomization aspects of their application to the compression ignition engine. The efficiency and rate of combustion of a fuel in a compression ignition engine is a function of the atomization of the fuel, i.e., the magnitude and spread of droplet sizes. Therefore, this fundamental process was selected as the basis of this doctorate. Blends of biodiesel and petroleum based diesel fuels were not considered in this study.

1.1 Rationale

Since it is well established that biodiesel fuels are potentially viable alternatives to petroleum-based fuels (Chapter 2), a clear understanding of the relationship between the chemical, physical and combustion properties of these fuels is essential. In Chapter 3 several existing theoretical models relating these properties to atomization and combustion were investigated by means of sensitivity analyses to determine the critical properties to be considered when investigating the applicability of biodiesel as a fuel. It became apparent that the two main physical properties that affect atomization are the fuel's surface tension and viscosity. Thus a complete analysis of these two properties was carried out. Methods for experimentally analyzing the atomization characteristics of the fuels (and their individual components) and the two main properties affecting atomization are discussed in Chapter 4. Since the biodiesel type varied widely due to the variety of vegetable and animal oils that are available, there existed a need to link the two main properties that affect atomization to the fatty acid composition of the oil. Models for predicting the viscosity and surface tension are discussed in Chapter 5. Verification of these models was accomplished through utilization of a wide range of experimental analyses. Chapter 6 discusses the results of these experiments and the results of experimentally determined atomization characteristics of five different biodiesel types. These atomization characteristics were then linked to the surface tension and viscosity of the biodiesel fuels through regression models. The coefficients of one regression model was linked to physical parameters through dimensional analysis.

Due to the varying engine test results reported on the performance of a variety of biodiesel fuels, there existed a need to predict the atomization characteristics of these fuels based on their fatty acid composition. With the various models developed in Chapters 5 and 6, this capability was established. This system of models was applied to 15 different types of vegetable and animal oils to determine their atomization characteristics (Chapter 7).

1.2 Thesis Objectives

Thus the specific objectives of this thesis were to:

1. Determine which physical properties were most relevant to the atomization of fatty acid methyl ester biodiesel fuels
2. Obtain experimentally these properties for component fatty acid methyl esters
3. Develop and verify empirical and/or theoretical models to predict these physical properties
4. Obtain experimentally the atomization characteristics of fatty acid methyl ester biodiesel fuels
5. Develop and verify empirical and/or theoretical models to predict the atomization characteristics of biodiesel fuels based upon their fatty acid composition
6. Use the models developed to establish whether or not the spray characteristics of compositionally different biodiesels are significantly different and identify the sources of these differences if any.

2 LITERATURE REVIEW

2.1 Diesel Engines

Vegetable oils are used almost entirely in compression ignition engines, commonly known as diesel engines. These engines are usually classified into two categories: direct, and indirect injection engines.

Direct injection diesel engines have the fuel injected directly into the combustion chamber. The fuel is injected under high pressure through a nozzle with single or multiple tiny orifices. This results in a fuel spray with very fine droplets thus making it easier for the fuel to evaporate and burn.

In the indirect injection engine, the fuel is injected into an auxiliary chamber that is adjacent and connected to the main combustion chamber. Most combustion starts sooner in this chamber and burning gases exit the chamber with high velocities giving a greater ability for mixing of fuel and air. Fuels of poorer qualities can be used with this type of engine.

2.1.1 Basic Operational Principles of the Diesel Engine

Diesel engines are commonly four-stroke cycle engines. With the four-stroke cycle, air is drawn into the cylinder during the first stroke followed by high compression during the second. Fuel is injected and burnt during the third stroke and the products of combustion are exhausted during the fourth.

The diesel engine relies on a high compression ratio, typically greater than 14:1, for combustion to occur. This compression ratio is made high in order to bring the temperature of the air near the end of the compression stroke to a level where autoignition is promoted when the fuel is injected into the cylinder. A principal requirement of a fuel for diesel engines is that it must be autoignited easily [Ferguson, 1986].

2.1.2 Combustion in the Diesel Engine

The combustion process in compression ignition engines is divided into four stages [Benson and Whitehouse, 1979]:

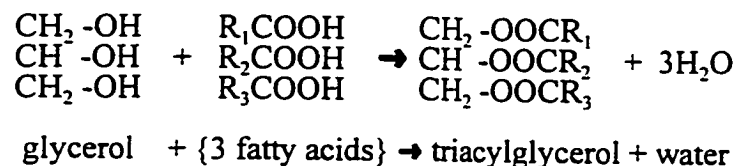
- 1 Ignition Delay; this is the period between the start of injection and the start of combustion.
- 2 Rapid, uncontrollable combustion due to the presence of many ignition points and the high temperature present in the combustion chamber. This stage extends to the point of maximum pressure.
- 3 A lower rate of combustion after the peak pressure.
4. A very low rate of combustion occurring well down the expansion stroke.

During the ignition delay period many processes occur within the cylinder. Fuel has to be broken down into droplets, heated, vaporized, and mixed with air. Both physical and chemical delays are present and these two delays are not additive since they are usually overlapping [Ferguson, 1986].

Due to the high compression ratio the temperature and pressure of the air at the time of injection are normally well above those required to support chain-reactions in a uniform fuel-air mixture. Under these conditions, ignition of any element of the charge does not require transfer of energy from another portion but will occur when the local temperature, pressure, and mixing of fuel and air make combustion possible [Taylor, 1985a]. In general the combustion of the fuel in the compression-ignition engine depends on the local condition in each part of the charge and does not depend on the spread of the flame through the charge as with spark ignition engines. However, the local flames may assist the ignition of adjacent sections if the local conditions (e.g., fuel-air ratio) support combustion. Local flames may also reduce the reaction time of adjacent sections by raising their temperature and pressure. The combustion rate is thus a function of the state and distribution of the fuel as well as the pressure and temperature in the chamber, where the latter is initially dictated by the compression ratio [Taylor, 1985b]. Other factors that influence the combustion process are injection timing, turbulence in the combustion chamber, engine rpm, along with several other fuel properties.

2.2 Fats and Oils

Plant and animal fats consist mainly of triacylglycerols (triglycerides) and minor quantities of accompanying polar lipids and sterols. Their chemical structure consists of three fatty acid residues connected to glycerol through ester linkages [Engler *et al.* 1992]. This arrangement is shown below:



The type of triglyceride and its complexity is determined by: the number, kind, and mode of arrangement of the individual fatty acids attached to the glycerol skeleton to form the specific glyceride; and the number and relative proportion of these glycerides that form the specific fat or oil. The fatty acids part of the triglyceride account for 90 to 94% of the compound's total molecular weight. These acids are usually aliphatic compounds ranging from C6 to C24. The vegetable oil itself consists of several triglycerides in which the three fatty acid residues may vary.

The difference between a fat and an oil is their physical state. The term fat usually defines the solid state and oil the liquid state. These terms are reversible depending on the temperature to which the compound is exposed. When the state is unimportant, the term fat is usually used.

Naturally occurring fatty acids are classified into two categories based on the presence or absence of multiple bonds in their hydrocarbon chain. These two categories of fatty acids are termed "saturated" and "unsaturated." Saturated fatty acids are those with no multiple bonds present and unsaturated fatty acids are those with multiple bonds. The degree of unsaturation of the unsaturated fatty acid group is determined by the number of double or triple bonds present in the structure, with a higher number of multiple bonds representing a higher degree of unsaturation. Markley (1960) and Ralston (1948) have an extensive nomenclature and insight to fatty acids. Ackman (1996) gives an insight to fatty acids in newer fats and oils. Table 2.2.1 gives the fatty acid composition of some commonly available vegetable oils.

The unsaturated fatty acid residues in a triglyceride can undergo either oxidative or thermal polymerization reactions among themselves producing high molecular weight, cross-linked

gel structures that are difficult to burn. Oils with a greater degree of unsaturation exhibit a greater tendency to polymerize [Engler *et al.*, 1992].

The iodine number/value is a measure of unsaturation. Vegetable oils are reported to have iodine numbers in the intermediate range 100-140 and in this range fouling problems in the combustion chamber may occur [Engler *et al.*, 1992]. Apart from having intermediate iodine numbers, triglycerides are also highly nonvolatile compounds.

Table 2.2.1 Fatty Acid Composition of Some Naturally Occurring Fats and Oils

Common Name	C #	Percent Composition of Oil (Fat) Type												
		PNO	RSO	OLO	COO	CRO	PO	PKO	SAO	SUO	SBO	TLO		
Caproic	6:0	-	-	-	0-0.8	-	-	tr-1.5	-	-	-	-	-	
Caprylic	8:0	-	-	-	5-9	-	tr	3-5	-	-	-	-	-	
Capric	10:0	-	-	-	6-10	-	tr	3-7	-	-	tr	-	-	
Lauric	12:0	-	-	-	44-52	-	tr	40-52	-	-	tr	tr-0.2	-	
Myristic	14:0	tr-1	-	0.1-1.2	13-19	tr-1.7	0.5-6	14-18	tr	-	tr	2-8	-	
Palmitic	16:0	6-9	1-3	7-16	8-11	8-12	32-45	7-9	3-6	3-6	7-11	24-37	-	
Stearic	18:0	3-6	0.4-3.5	1-3	1-3	2-5	2-7	1-3	1-4	1-3	2-6	14-29	-	
Arachidic	20:0	2-4	0.5-2.4	0.1-0.3	0-0.4	tr	tr	tr-1	tr-0.2	0.6-4	0.3-3	tr-1.2	-	
Behenic	22:0	1-3	0.6-2.1	-	-	tr	-	-	-	tr-0.8	tr	-	-	
Palmitoleic	16:1	tr-1.7	0.2-3	tr	0-1	0.2-1.6	0.8-1.8	tr-1	-	tr	tr	1.9-2.7	-	
Oleic	18:1	53-71	12-24	65-85	5-8	19-49	38-52	11-19	13-21	14-43	15-33	40-50	-	
Gadoleic	20:1	-	4-12	-	-	-	-	-	-	-	-	-	-	
Erucic	22:1	-	40-55	-	-	-	-	-	-	-	-	-	-	
Linoleic	18:2	13-27	12-16	4-15	tr-2.5	34-62	5-11	0.5-2	73-79	44-75	43-56	1-5	-	
Linolenic	18:3	tr	7-10	tr-1	-	tr	tr	-	tr	tr	5-11	-	-	
Oil Content of Seed		44-55	22-49	35-75	65-68		45-55	44-53	25-37	22-36	15-25			

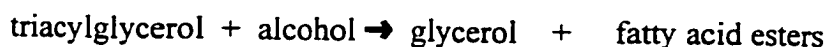
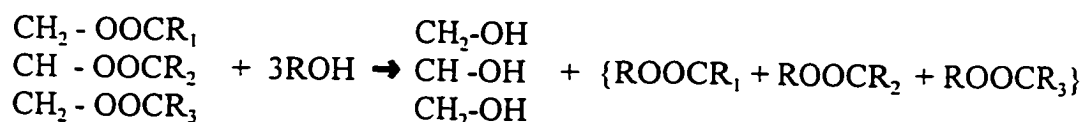
PNO - Peanut Oil; RSO - Rapeseed Oil; OLO - Olive Oil; COO - Coconut Oil; CRO - Corn Oil; PO - Palm Oil; PKO - Palm Kernel Oil
 SAO - Safflower Oil; SUO - Sunflower Oil; SBO - Soybean Oil; TLO - Tallow (from Bailey's Industrial Oil & Fat Products, 1979)

2.2.1 The Transesterification Process

The transesterification process is widely used in the field of biodiesel engineering. In fact the term “biodiesel” is now being used almost entirely to define acyl esters of vegetable oils produced by the transesterification process.

In the esterification of an acid, an alcohol acts as a nucleophilic reagent, that is, the alcohol either transfers its electrons or shares them with outside atoms or ions. The displacement of an alcohol from an ester by a different alcohol is called transesterification [Morrison and Boyd, 1971]. Glycerol in triglycerides is the alcohol which is replaced by a lower molecular weight alcohol.

The transesterification process can take place with or without the presence of a catalyst. Either an acid or alkali catalyst can be applied in the process and methyl, ethyl, or butyl esters of the carboxylic acids are normally produced. The stoichiometry of this reaction is 3 mol of alcohol per mol of vegetable oil to produce 3 mol of fatty acid esters and 1 mol of glycerol [Freedman *et al.*, 1984a]. The reaction is as follows:



Kusy (1982) investigated two processes of transesterifying triglycerides with ethanol. Both methods, the first developed by Bradshaw and Meuly of the Dupont company and the other by Trent of the Colgate-Palmolive Peat company, were found to be successful. In the Bradshaw and Meuly method, as reported by Kusy (1982), 1.75 equivalents of the alcohol were used along with 25 percent of the catalyst solution. The catalyst was made of

approximately 0.5 percent (by weight of vegetable oil) of sodium methoxide in methanol. The Trent's method used the same catalyst but three to five times the stoichiometric amount of alcohol was used. An organic or inorganic acid was applied after the transesterification process to render the catalyst inert.

Freedman *et al.* (1984a) investigated the variables that affect the yields and purity of esters produced by way of the transesterification process. Sixty grams (0.0682 mol) of edible-grade vegetable oil was mixed with 16.572 mL (13.115 g or 0.4093 mol) of methanol. Sodium methoxide (0.5%, by weight of oil) was used as the catalyst. It was reported that 98% of the reaction was completed in approximately one hour. Several factors were found to significantly affect the yield and quality of the ester. The water content of all materials, including the catalyst and triglyceride, and the acid value of the triglyceride were required to be very low. An acid value of less than one (i.e., free fatty acid content of less than 0.5%) and a water content of less than 0.3% (i.e., substantially anhydrous materials) were recommended. Acid and water contents above those values were reported to cause a significant decrease in the ester yield.

The molar fraction of alcohol to vegetable oil was also found to be a significant variable in determining the ester yield. A molar ratio of 6:1 of alcohol to vegetable oil resulted in the highest yields of esters (93-98%) and glycerol yields were also reported to be highest at this ratio. Increasing the recommended ratio of 6:1 complicated the separation of the glycerol from the fatty esters with no significant increase in the yield.

The time required for the reaction to be completed was estimated to be 1 hr by Freedman *et al.* (1984a). The temperature depended on the type of alcohol being used and was recommended to be a few degrees below the boiling point of the alcohols (examples of reaction temperatures are: methanol 60 °C, ethanol 75 °C, and butanol 114 °C). Nouredini

and Zhu (1997) found that increasing the reaction temperature for methyl esters from 30 to 70 °C led to significant increases in the reaction rate with temperatures up to 50 °C, but little increase in reaction rate after 50 °C. Work done by Allen and Watts (1996) showed that reaction times in the range 15-30 minutes were adequate for greater than 98% conversion when canola oil was transesterified with methanol at 60 °C.

The use of crude vegetable oils was found to adversely affect the ester yields due to the presence of solids and other extraneous materials. For biodiesel it has been suggested that degummed, filtered crude vegetable oils may be adequate, although fully refined oils give the best results [Freedman *et al.*, 1984a]. Using fully refined oils, however, increases the production cost of biodiesel and would have negative effects on its ability to compete with other fuels. Cvengros and Povazeneč (1996) were successful in using cold-pressed, filtered rapeseed oil to produce methyl esters. Their method yielded 34 wt% of oil based on crop weight which accounts for some 83% of the oil content of the seeds. Their transesterification process yielded 96 - 99% conversion of the triglycerides to esters. These results are promising since they show that some of the production costs of biodiesel fuel can be reduced by bypassing the refining stage. Industrial production of biodiesel has been undertaken [Gutsche, 1997 and Krawczyk, 1996] and typical continuous processes are outlined by Nouredini *et al.*, 1996; Krisnangkura and Simamharnop, 1992; and Kusy 1982.

Controlling and quantifying the extent of the transesterification process is very important for biodiesel fuel production. Several standards have been and are being proposed for biodiesel fuels [Knothe *et al.*, 1996 and Mittelbach, 1996] and a handbook outlining analytical methods specifically for biodiesel was also produced [Bailer *et al.*, 1994]. For the determination of the extent of the transesterification reaction three methods are commonly applied: liquid chromatography - gas chromatography (LC-GC) [Lechner *et al.*, 1997; Mittelbach *et al.*, 1996; Plank and Lorbeer, 1994]; thin layer chromatography-flame

ionization detection (TLC-FID) [Freedman *et al.*, 1984b]; and correlation of methyl ester content with physical properties, e.g., viscosity [De Filippis *et al.*, 1995].

2.3 Biodiesel CI Engine

Vegetable oils were used as fuel for diesel engines to some extent since the invention of the compression injection (CI) engine by Rudolf Diesel in the late 1800's. Progress in this area has however fluctuated over the years. During the early stages of the diesel engine strong interest was shown in the use of vegetable oils as fuel but this interest declined in the late 1950's after the supply of petroleum products became abundant. The so called "fuel crisis" during the early 1970's, however, caused a renewed interest in vegetable oil fuels. This interest evolved after it became apparent that the world's petroleum reserves were slowly dwindling. At present, the use of vegetable oils may not seem feasible as a complete replacement for diesel fuels in the developed world but there is tremendous potential in developing countries.

Vegetable oil (VO) fuels are renewable energy sources and significant benefit can be derived from the combustion of biodiesel rather than petroleum based diesel fuels. The carbon dioxide produced by the combustion of the VO fuels balances to some extent that used by the plants from which they originate, therefore, the net gain of CO₂ in the atmosphere is negligible unlike that which occurs with the combustion of petroleum based diesel. Vegetable oils also contain only trace quantities, if any, of sulphur, thus resulting in less SO_x pollution.

When applied as fuels for the CI engine vegetable oils have taken three general forms over the years: neat or pure vegetable oils; blends of vegetable oils and diesel fuel; or

transesterified vegetable oils. Goering *et al.* (1987) gave a summary of authors, to that date, who carried out engine performance and durability tests and the type of vegetable oil fuel used. Bhattacharyya and Reddy (1994) also reviewed the use of vegetable oils as fuels for internal combustion engines.

2.3.1 Neat Vegetable Oils as Diesel Fuels

If neat vegetable oils could work satisfactorily in the CI engine it would represent one of the cheapest alternatives since the processing requirements would be minimal. This was one of the first concepts investigated. Quick (1980) gave a summary of authors, dating postwar to 1980, who carried out engine performance and durability tests on various types of neat vegetable oils and engine types.

Neat vegetable oils unquestionably are able to produce a comparatively good supply of power and torque to the crankshaft. Several authors have reported this by way of experimental results. Engler *et al.* (1992) found that both a direct injection and an indirect injection single cylinder CI engines started and ran well on neat vegetable oils (cottonseed) at various degrees of refining; except oils that were unfiltered. The thermal efficiencies and the brake specific fuel consumptions compared well with diesel #2 fuel. Several authors [Mazed *et al.*, 1985; Fuls *et al.*, 1984; Ryan III *et al.*, 1984; Vinyard *et al.*, 1982; Quick, 1980; among others] showed similar results. Mazed *et al.* (1985), however, found that neat peanut oil produced lower power output when compared with blends and diesel #2 fuel. This was attributed to the higher viscosity and lower heating value of the neat vegetable oils. Similar findings were made by Vinyard *et al.* (1982) where it was found that refined soybean oil and refined peanut oil produced 87% and 97%, respectively, of the power produced by diesel #2 fuel. Despite this lower power the Deutz engine manufacturer honoured factory warranties on their indirect injection engines that operated on degummed sunflower oil [Fuls *et al.*, 1984].

Ryan III *et al.* (1984) did a statistical evaluation of the performance of diesel engines as a function of the fuel's chemical composition. Their results showed that the linolenic-linoleic ratio, iodine number, and nitrogen were the most significant variables for the DI engine whereas the nitrogen content, oxygen content and free fatty acid content were the most significant for the IDI engine.

The generally acceptable power production of the CI engines operated with neat vegetable oils is however overshadowed by some short term problems and its poor long term durability performance. Typical short term problems with four cylinder engines include: engine knock; gumming and blocking of fuel lines, filters and injectors; and cold start difficulties. These problems were attributed to the high viscosity of the oils. Some of the long term problems with the neat vegetable oils, which were more severe than the short term problems, include: injector coking or carbon buildup on injector tip; carbon buildup in the combustion chamber; wear of cylinder liners, piston and rings; and thickened and/or contaminated lubricating oil [Reid *et al.*, 1989; Peterson, 1986; Mazed *et al.*, 1985; Fuls *et al.*, 1984; Pryde, 1983]. Most authors used the Engine Manufacturers Association (EMA) 200 hours test for long term durability evaluation.

2.3.2 Vegetable Oil / Diesel Fuel Blends

The tremendous long term difficulties when using neat vegetable oils as diesel fuel led to the investigation of other alternatives by many authors. One such alternative was vegetable oil/diesel fuel blends. Various authors used several blends ratios with some degree of success but most of them reported that blends of 50% or less vegetable oil were the most suitable. Barhey (1992) reported that a 50/50 palm kernel oil/diesel blend had the best applicability. Lague and Stanley (1987) also concluded that a 50/50 blend of waste vegetable oil/diesel was most applicable to the CI engine.

In general, as the percentage of vegetable oil increases in the blend with diesel fuel, problems tend toward that of the neat vegetable oils. These problems are usually the progressive formation of excessive carbon deposits in the engine [Goering *et al.*, 1987; Korus and Jo, 1985; Borgelt and Harris, 1982]. However, Lague and Stanley (1987) found that 50:50 and 20:80 waste vegetable oil/diesel blends passed the EMA 200 hr durability test with slightly better results in some areas of performance than the same indirect injection engine operating on diesel fuel. Carbon buildup on all parts was not higher than that of the diesel fuel and wear was also comparable.

Schumacher (1994) investigated, among other things, the density of the smoke produced by a direct injection engine using an 80:20 blend of low sulphur diesel/soydiesel. It was found that the density of the smoke decreased with an increase in concentration of soydiesel in the blends while the reverse occurred for oxides of nitrogen. Increased concentration of soydiesel also resulted in reduced carbon monoxide and hydrocarbon content of the exhaust emission.

2.3.3 The Use of Esters of Vegetable Oils as Diesel Fuel

The most promising applications of vegetable oils as diesel fuels is that of acyl esters of the oils. Methyl, ethyl or butyl esters produced by means of the transesterification process are usually used with methyl esters being the most common. In sections 2.3.1 and 2.3.2 above, the problems associated with the long term performance of diesel engines fueled by vegetable oil substitutes were attributed mainly to the fuel's viscosity. Esters of vegetable oils have significantly lower viscosities than the neat or blended vegetable oil fuels thus the viscosity related problems are greatly reduced.

The application of acyl esters of vegetable oils as diesel engine fuels was studied by several authors [Goodrum *et al.*, 1996; Peterson and Reece, 1996; Peterson *et al.*, 1992; Schumacher *et al.*, 1992; Mittelbach and Trillhart, 1988; Goering *et al.*, 1987; Peterson *et al.*, 1987; Peterson and Mora, 1985; Clarke *et al.*, 1984; Wagner *et al.*, 1984; Zubik *et al.*, 1984; Hassett and Hasan, 1982; Hawkins and Fuls, 1982; Pischinger *et al.*, 1982; Siekmann *et al.*, 1982; Tahir *et al.*, 1982]. Most of their findings were similar, and typical ones are given below.

Peterson *et al.* (1992) found that the engine performance of a diesel engine fueled with methyl and ethyl esters of rapeseed oil was comparable to standard diesel #2 fuel with the esters showing slightly lower power output and associated higher brake specific fuel consumption. The methyl ester was reported to produce slightly more power than the ethyl ester. Schumacher (1992) found that 100% soydiesel (methyl ester of soybean oil) produced slightly more power on average than low sulphur diesel fuel.

Results of tests done by Zubik *et al.* (1984) showed that the methyl esters of sunflower oil produced higher maximum cylinder pressure and rate of pressure rise than diesel #2 fuel. The combustion process was also analyzed to be the same as diesel fuel, with a delay period followed by rapid combustion and then a slower diffusion controlled phase. Ali *et al.* (1996) investigated in-cylinder characteristics of methyl esters of beef tallow and blends with diesel fuel and ethanol. They found that the peak pressures of the 100% esters and some of the blends were 5-9% lower than that for diesel #2 fuel. The same was found for the rate of pressure rise.

Wagner *et al.* (1984) reported that the cetane rating of esters of soybean oil was higher than that of diesel #2 fuel and thus a shorter delay period was assumed to be present although no cylinder pressure monitoring was done. The cetane rating was positively proportional to the

molecular weight of the alcohol used in the transesterification process. Van Gerpen (1996) found that longer fatty acid carbon chains and saturated fatty acid molecules resulted in higher cetane values.

Mittelbach and Trillhart (1988) investigated the use of transesterified used-frying-oil in diesel engines. They tested these methyl esters on a 1.6 litre Volkswagen car and reportedly found no significant difference in the performance of the engine when compared with diesel fuel.

One of the reported problems with the methyl ester fuels is the dilution of the lubricating oil. Clark *et al.* (1984) found that the viscosity of the lubricating oil decreased continuously with engine operation during the 200 hour EMA durability test suggesting that the esters caused some amount of dilution. This problem was also observed by Wagner *et al.* (1984). It should be noted that these results are opposite to the results previously discussed with the neat vegetable oils where polymerization occurred causing the lubricating oils to thicken.

Goering *et al.* (1987) found that methyl, ethyl, and butyl esters of soybean oil all produced wear that was considered normal during the 200 hour EMA test. The methyl and butyl esters produced slightly higher piston and top-ring-groove deposits compared with the ethyl esters and diesel fuel.

Peterson *et al.* (1992) found that the ethyl esters of rapeseed oil produced the same amount of injector coking as diesel fuel while the methyl esters of the oil produced slightly higher amounts. The viscosities of these two esters types (methyl and ethyl) were approximately twice that of the diesel #2 fuel. Goodrum *et al.* (1996) also investigated fuel injector tip deposits with tricaprylin (C8:0), tributyrin (C4:0) and peanut oil. The coking indices, derived from pixel counts of a photo image, were 0.77, 0.56 and 1.26 respectively compared to diesel

#2 fuel which was given an index of 1.00. Therefore, one could deduce that shorter chained fatty acids have a lesser tendency to coke than longer chain fatty acids. Lower viscosity and surface tension usually indicate better atomization and burning of the fuel in the CI engine.

Mittelbach and Trillhart (1988) in their tests with methyl esters of used frying oil found that the level of oxides of nitrogen was high due to the high combustion temperature. This high temperature was attributed to the high oxygen content of the ester fuel. However, all other emissions, including polycyclic aromatic hydrocarbons (PAH), were low. Peterson and Reece (1996) did on-road tests with a pickup truck and found that rapeseed oil methyl and ethyl esters produced lower HC, CO and NO_x emissions compared to diesel #2 fuel. However, particulate matter emissions were higher. The ethyl ester produced less HC, CO, and NO_x compared to its methyl ester counterpart. Ali *et al.* (1995) found similar results for blends of methyl tallowate, methyl soyate, and ethanol compared to diesel #2 fuel.

Schumacher *et al.* (1992) found that the use of methyl soyate caused rapid deterioration of components of the fuel system made of rubber. This may be of concern when biodiesel fuels are used in current vehicles and power systems.

Apart from some minor problems, it can be concluded that biodiesel fuels (methyl or ethyl esters of triglycerides) are a potentially viable alternative for petrodiesel fuels.

2.4 Droplet Measurement Techniques

The formation of droplets by a diesel injector is a very complicated process that has received much attention for many years. One of the most widely accepted mechanisms of atomization is the one which describes the breakdown of the surface of a liquid jet into thin sheets as a result of shear interaction with the surrounding gases. These thin sheets then breakdown into droplets in a manner similar to the Raleigh regime. Further theoretical aspects of droplet breakdown are given in Chapter 3.

In order to verify models for atomization one would need an effective method for measuring the atomization parameters. Droplet data can be acquired experimentally by four general means:

- capture by immersion liquids
- still photography
- laser imaging systems (Particle Measuring Systems - PMS)
- laser diffraction systems

2.4.1 Capture by Immersion in Liquids

A relatively simple method of carrying out droplet analysis is by capturing the droplets in an immersion liquid followed by analysis of the droplets using micro photography or some other technique. In applying this capture technique the choice of the immersion liquid is critical. Vander Griend *et al.* (1988) outlined some of the key physical characteristics of the immersion liquid required for successful operation, which include:

- The immersion liquid and test sample should be totally immiscible, that is, they should not mix to form a homogenous mixture.
- The density of the immersion liquid should be lower than the sample.

- The immersion liquid should have a low enough viscosity such that droplet breakup is reduced on impact but high enough to prevent coalescence.
- The surface tension should be low enough to allow penetration of the droplets into the immersion liquid.

Along with these fluid properties, the height of the nozzle above the liquid surface should be sufficient to reduce to occurrence of droplet fragmentation on impact.

Once the nozzle height and immersion liquid characteristics are favourable, the process of capturing the droplets in the immersion liquid is relatively straightforward and simple. However, the analysis of these droplets for size and distribution is usually very time-consuming since each droplet over the entire surface, or over a selected segment that is representative of the whole, has to be measured. Micro photography, with the aid of a microscope for magnification, is usually done as soon as possible after the droplets are captured on the liquid surface. This magnified image is then digitized and a computer program is used to aid in the sizing and counting of droplets. However, manual analysis is not uncommon.

Due to the time required for the analysis of the results and the unavailability of suitable equipment on campus, this method was not suitable for use in this work.

2.4.2 Still Photography

High-speed photographic systems have been used with some degree of success for the analysis of sprays by Chella *et al.* (1986). It was pointed out that photographic systems are

relatively insensitive to the shape and optical properties of the particles and could be used in the determination of droplet velocities by double exposures. Along with these features, errors due to multiple scattering can be easily detected by observation of the photo image.

One of the critical parameters of photographing small particles is the exposure time, which is extremely short for micron size particles. The exposure time was stated [Chella *et al.*, 1986] as being directly proportional to the particle size (diameter) and inversely proportional to the particle velocity. Thus for a 10 micron droplet travelling at 100 m/s, a 10 ns exposure time is required. The required intensity of the incident light increases with the decrease in particle size and increase in particle velocity, therefore, a high intensity, short-duration light source is required.

The sizing of the droplets is usually done by “manual analysis of magnified projections of the negative or by automatic analysis directly from the negative” [Chella *et al.*, 1986]. These are very tedious and time-consuming processes and, coupled with the fact that a system had to be assembled and tested for accuracy and repeatability before this method could have been applied, this system was not applied to this research.

2.4.3 Particle Measuring Systems (PMS)

Particle measuring systems (PMS) are particularly suited for the direct measurement of droplet size. A small laser beam approximately 1mm in diameter [Arnold, 1990] is focused across photo detectors. When an opaque particle passes through the beam it obscures a number of detectors thus a direct measurement of the particle size can be made. The sensors have the capability of blocking out particles that are overlapping, out-of-focus and partially in the beam. This feature reduces sizing errors. The system can also be used to measure particle velocity by measuring the rate at which the cells are obscured. Inferences on spatial

distribution of particles can be also made from the obscuration rate data, but this is not a direct measurement. The PMS system does not rely on any mathematical model for its operation. A PMS may have been ideal for this research program but such a system was expensive and unavailable on campus.

2.4.4 Laser Diffraction Technique (Malvern Analyzer)

The Malvern droplet analyzer is an optical system that relies on Fraunhofer diffraction of a monochromatic laser beam within which forward scattering occurs. Figure 2.4.4.1 shows a schematic of the Malvern particle sizer [Meyer and Chigier, 1986]. A monochromatic laser beam is expanded to an approximate 9mm diameter by a light expander unit. This expanded beam then passes through the spray zone, the droplets within which scatters the beam in the near forward direction. The degree of beam scattering is a direct function of the droplet sizes. A special Fourier-transform lens converges all the rays diffracted at given angles to specific sites on a specially designed receiver. This specially designed receiver has 31 concentric ring sensors with increasing surface areas to accommodate the diffraction pattern from each droplet. By using the Fourier-transform lens, even rays diffracted by moving droplets of the same size and at different locations in the beam have their diffraction pattern focused onto the same stationary sensor on the receiver plate. Since several droplets are in the beam at the same time, the integral effect of all droplets of the same size is recorded at each ring sensor on the receiver plate. Several readings of the sensors are taken over time and this data is then averaged. The volume size distribution of the drops is then deduced by a “process of constrained least square fitting of theoretical scattering characteristics to the observed data” [Meyer and Chigier, 1986].

Light that is not scattered by the spray passes through an aperture at the center of the receiver to another sensor which measures its intensity. The intensity of the unscattered beam is used to determine the sample volume concentration by relating this intensity to the intensity of the original beam.

One of the problems with the Malvern laser diffraction system is multiple diffraction in dense sprays [Gulder, 1990]. This phenomenon occurs when the paths between droplets are so small that a diffracted ray is again diffracted by the neighbouring droplet giving larger angles of diffraction. This leads to results that show smaller diameters and wider distributions. Several secondary diffractions could also occur thus leading to even more inaccuracy. This problem was observed in sprays with obscurations greater than 55% on average [Gulder, 1990]. It was found that the predicted SMD decreased systematically with an increase in obscuration that allowed for a set of empirical equations to be developed to correct for this [Gulder, 1990].

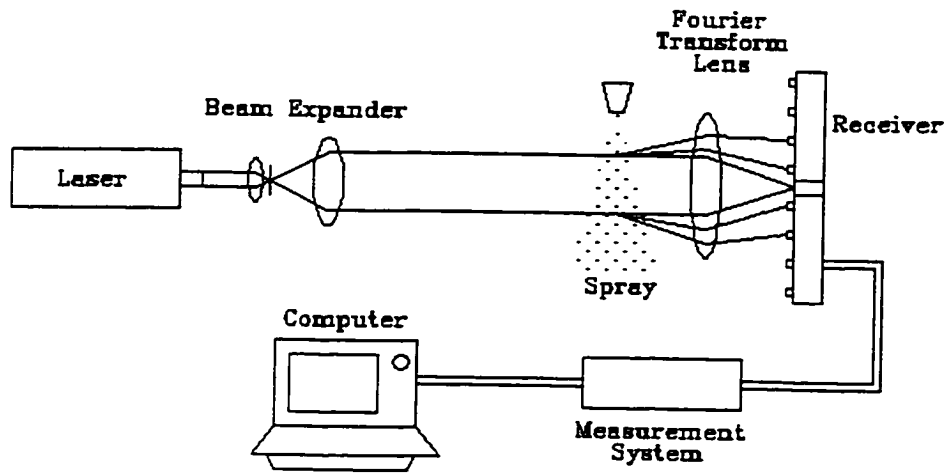


Figure 2.4.4.1 Schematic of a Malvern Droplet Analyzer

Meyer and Chigier (1986) outlined several other limitations of the Malvern droplet sizer. These are:

- The range of droplet sizes that can be analyzed is dependent on the choice of the lens. Inference with regard to the presence or absence of droplets beyond this range cannot be made with any degree of certainty.
- If a distribution model is chosen, an inappropriate choice can lead to erroneous results. Thus, it is usually advisable that the user applies a “model independent” distribution first then compare the results with the selected model. A check for the presence of large particles with the Rosin-Rammler, log normal, and normal distribution functions is usually not recommended.
- Sample-to-lens distances are required to be within the focal length of the lens. This, for typical lenses, may lead to deposition of spray particles on the lens if care is not taken.

The above stated limitations, however, do not take away from ease of use, repeatability and the relatively short time that acceptable results can be obtained with the careful use of the Malvern analyzer.

2.4.5 Summary of Droplet Measuring Techniques

Unlike other imaging and emersion techniques, results from a Malvern analyzer are obtained in a relatively short time and its operation is much less tedious. Repeatability with the Malvern analyzer was also reported to be acceptable [Gulder, 1990]. A Malvern analyzer was obtained and, since the major problem of obscuration can be avoided by careful choice of spray parameters, the theoretical models developed in this work were verified with experimental results obtained from a Malvern 2600 particle sizer.

3 THEORETICAL CONSIDERATIONS

The combustion of fuel in a diesel engine occurs after the fuel is vaporized and mixed with air. To facilitate this vaporization process the fuel is atomized into small droplets. The extent of atomization thus has a direct effect on the vaporization process which in turn affects the combustion process. Therefore, both atomization and evaporation models were considered in this thesis even though the thermal properties have not yet been studied.

3.1 Droplet Formation

There are several publications on the theory of droplet formation, for example, Chigier, 1991; Hiroyasu, 1991; Arai *et al.*, 1984; Msipa *et al.*, 1983; Reitz and Bracco, 1979; Marshall, 1954 and others. In diesel engines, droplet formation can occur in two different modes depending on the engine's injection system design. In the first mode, jet breakup occurs mainly due to interaction with the surrounding atmosphere in the combustion chamber. This is typical of the direct injection engine. With the indirect injection engine, along with the effects of the swirling gas in the auxiliary combustion chamber, jet breakup is augmented by impinging the jet on a solid wall causing some degree of splashing.

Jet breakup regimes are classified according to the jet velocity. The "Raleigh Regime" was one of the first regimes established and applies to low velocity jets where the surroundings have little effect. In this regime jet breakup occurs when the amplitude of the disturbances (axisymmetric waves) is at least half the diameter of the undisturbed jet [Marshall, 1954]. The next regime, referred to as the "First Wind Regime", includes some interaction with the surroundings whereby aerodynamic interaction increases the growth rate of the axisymmetrical waves [Chigier, 1991]. At higher velocities the "Second Wind Regime" is encountered where unstable asymmetric waves are formed on the surface, leading to the

formation of droplets smaller than the jet diameter. In this regime the droplet formation occurs far from the nozzle exit. As the jet velocity is further increased droplet formation occurs closer and closer to the nozzle exit and the “Atomization Regime” is established. The distance from the nozzle tip at which droplet formation occurs is called the breakup length. In the atomization regime aerodynamic interaction between the jet and the surroundings increases instability and has a greater role to play in the droplet sizes. The terms, Laminar Flow Region, Transition Flow Region, Turbulent Flow Region, and Spray Region, respectively, are often used to describe the different regimes previously described.

Atomization is the jet breakup regime which occurs in diesel engines. The fluid's surface tension, viscosity and density along with the jet diameter, the relative velocity between the jet and its surroundings, and turbulence are very important parameters in atomization. The Sauter Mean Diameter (SMD) is commonly used as a measure of the quality of atomization in diesel engines. There have been several models developed using various techniques for SMD and droplet breakup. One of the common ones is the TAB method developed by O'Rourke and Amsden (1987). This model treats the spray system as a “damped, forced harmonic oscillator” and is used in the numerical analysis of spray combustion systems (the KIVA numerical model [Amsden, 1993 and Amsden *et al.*, 1989]). It however requires the determination of constants from experimental data obtained with specialized equipment and parameter setup. Other models available for droplet breakup are given by Wakisaka *et al.*, 1997; Sidahmed, 1996a & 1996b; and Faeth, 1996. Reitz and Diwakar (1987) gave a very simple correlation for SMD as follows:

$$SMD = B \frac{\sigma_f}{\rho_f V_o^2} \quad (3.1.1)$$

where:

σ_f - surface tension of the fuel

- ρ_f - density of the fuel
 V_o - velocity of the fuel jet
 B - a constant.

Equation 3.1.1, however, do not include the fuel's viscosity and may not be applicable to fuels with very different viscosities.

3.2 Droplet Evaporation and Combustion

Evaporation is the first process encountered in the combustion of a droplet. The stages through which evaporation occurs [Strahle, 1993] are:

- An initially cold droplet is heated by its surrounding hot atmosphere mainly through thermal conduction.
- The temperature of the droplet increases up to a point where it remains constant. At this point additional heat is consumed as latent heat and the droplet starts to vaporize.
- As vaporization continues, mass transfer between the atmosphere and the surroundings starts by way of diffusion. This is due to the concentration gradient of the vapour.
- A final state is reached where the rate of mass transfer becomes in equilibrium with the rate of heat transfer and a steady state is achieved.

Basic mathematical analysis of the vaporization of a droplet shows that the square of the droplet diameter decays linearly with time and is commonly known as the d^2 law [Strahle, 1993; Law, 1978; Williams, 1973]. The key factors affecting the evaporation of a droplet are: thermal conductivity, latent heat of vaporization, density, temperature and pressure. The dimensionless Lewis number, which is the ratio of the thermal diffusivity to the mass diffusivity, is also used as a key parameter.

Numerical models for the evaporation of droplets based on several conservation equations have been proposed by many [Fichot *et al.*, 1994; Megaridis and Sirignano, 1990; Belland and Harstad, 1990]. However, care should be taken in applying these models since there are factors, such as droplet interactions, which are absent from many of them.

When the droplet exists in a hot oxidizing atmosphere, the fuel vapour is mixed with the oxidizer and chemical reactions commence. The onset of chemical reactions increases the temperature of the surroundings and the rate of vaporization increases. This continues until a point is reached whereby the rate of heat generation from chemical reaction is much higher than the rate of heat dissipation. When this condition occurs, very rapid or “run-away” chemical reactions develop and the droplet ignites into a flame, that is, combustion occurs.

Williams (1973) presented several models for droplet combustion in his review paper and since then several others have been presented [Fichot *et al.*, 1994; Griffiths *et al.*, 1993; Wong *et al.*, 1993; Law, 1978; Stambuleanu, 1976].

3.3 Sensitivity Analysis of Properties Affecting Atomization

In the references cited on the theory of atomization and droplet burning it is evident that there are some key parameters which are needed to develop any model to predict atomization and burning characteristics. These properties are summarized below.

- Viscosity
- Surface Tension
- Density
- Latent Heat of Vaporization
- Thermal Conductivity
- Specific Heat Capacity
- Boiling Point
- Heat of Combustion

These properties were used directly in most of the models found in the literature. In order to decide which of the above properties were most significant a sensitivity analysis was carried out on selected atomization models (Appendix B outlines this analysis for a selected burning rate model).

There exist in the literature a multitude of models for the prediction of spray characteristics of fuels. Of these models two relatively compact ones were chosen. The first is by Msipa *et al.* (1983). This model produces an atomization characteristic K_a which gives an overall view of the atomization quality. It includes the surface tension, viscosity and density of the fuel.

The second model, developed by Tasanawa, was reported by Hiroyasu *et al.* (1989). This model predicts the Sauter Mean Diameter (SMD) based on the fuel viscosity, surface tension and density. The nozzle hole diameter and the air density in the combustion chamber are also used as key parameters.

The mathematical expressions for these two models are given in the next two sections.

3.3.1 Atomization Characteristic Model [Msipa *et al.*, 1983]

Good atomization in diesel engines was defined to be one which produces a cone shaped spray starting at the nozzle exit. Msipa *et al.* (1983) developed two criteria for which good atomization will occur, one for low viscosity and the other for high viscosity fuels. To define low and high viscosity fuels, Equation 3.3.1.1 below was used, whereby, if its solution resulted in a numeric value greater than one then the viscosity is considered low, and less than one, high viscosity. The data used later in this chapter showed that biodiesel are in the high viscosity category.

$$Visc_{crit} = \frac{\rho_f}{\rho_g} \left(\frac{Re_f}{We_f} \right)^2 \quad (3.3.1.1)$$

where

$Visc_{crit}$ - viscosity criteria

We_f - Weber number for fuel

Re_f - Reynolds number for fuel

ρ - densities for fuel (f) and gas atmosphere (g) [kg/m^3]

For low viscosity the atomization characteristic is:

$$\sqrt{\frac{\rho_f}{\rho_g}} \leq Ka \quad (3.3.1.2)$$

For high viscosity the atomization characteristic is:

$$\left[\frac{\rho_f We_f}{\rho_g Re_f} \right]^{1/3} \leq Ka \quad (3.3.1.3)$$

where the atomization characteristic Ka is given by:

$$Ka = \frac{18.3}{\sqrt{A}} \quad (3.3.1.4)$$

$$A = 3.0 + \frac{(L_o / d_o)}{3.6} \quad (3.3.1.5)$$

where:

- d_o - nozzle diameter (m)
- L_o - nozzle sac length (m)

The Reynolds and Weber numbers are given by:

$$Re_f = \frac{V_o d_o}{\nu_f} \quad (3.3.1.6)$$

$$We_f = \frac{\rho_f V_o^2 d_o}{\sigma_f} \quad (3.3.1.7)$$

where

- σ_f - surface tension of the fuel (N/m)
 ν_f - kinematic viscosity of the fuel (m²/s)

The velocity of the fuel jet V_o was determined by Equation 3.3.1.8 which relates the efficiency (E) of a nozzle in converting pressure (P) energy to kinetic energy:

$$V_o = \left(\frac{2 E (P_L - P_g)}{\rho_f} \right)^{0.5} \quad (3.3.1.8)$$

The gas density, temperature and pressure were determined based on the ideal gas equation and equations for a polytropic processes respectively.

$$\rho_g = \frac{P_g}{R_g T_g} \quad (3.3.1.9)$$

$$P_g = P_{atm} (cr)^\gamma \quad (3.3.1.10)$$

$$T_g = T_{atm} \left(\frac{P_g}{P_{atm}} \right)^{\frac{\gamma-1}{\gamma}} \quad (3.3.1.11)$$

where

- cr - compression ratio
 T_g - compressed gas temperature (K)
 T_{atm} - inlet gas temperature (K)
R - gas constant (kJ/kgK)
 γ - polytropic index

- P_L - fuel line pressure (Pa)
 P_g - compressed gas pressure (Pa)
 P_{atm} - inlet gas pressure (Pa)

3.3.2 SMD Model [Hiroyasu *et al.*, 1989]

This model is an empirical model to predict the Sauter Mean Diameter of fuels. It is given by:

$$SMD = 47 \times 10^{-3} \left(\frac{d_o}{V_o} \right) \left(\frac{\sigma_f}{\rho_g} \right)^{0.25} g^{0.2} \left(1.331 \times 10^5 \frac{\mu_f}{\sqrt{\sigma_f \rho_f d_o}} \right) \quad (3.3.2.1)$$

where:

- SMD - Sauter Mean Diameter (μm)
 μ_f - dynamic viscosity of fuel (Pa.s)
 ρ - density of fuel (f) and combustion chamber compressed gas (g) (kg/m^3)
 σ_f - surface tension of fuel (N/m)
 g - acceleration due to gravity (m/s^2)
 d_o - nozzle diameter (m)
 V_o - jet velocity

3.3.4 Sensitivity Analysis Procedure

In order to determine to what extent the properties should be varied for the sensitivity analysis typical ranges were selected from work done by Allen *et al.* (1996) on mixtures of coconut, peanut and canola oil methyl esters at 25°C. Table 3.3.4.1 shows these typical

values. It can be seen that the density and surface tension did not vary by more than 3-5% on average, while the viscosity varied by 30% on average. Based on these results it was decided to vary all properties to a maximum of $\pm 5\%$ from the mean value. In addition a 30% variation of viscosity was also investigated. The mean value of all properties are given in Table 3.3.4.2. Other parameters used in the analyses are given in Table 3.3.4.3.

3.3.5 Results of Sensitivity Analysis

The sensitivity analysis was carried out using an algorithm written in the C programming language (Appendix C). The results of these analyses are shown graphically in Figures 3.3.5.1 to 3.3.5.4 for normalized atomization characteristic (Ka_i / Ka_{max}) and Figures 3.3.5.5 to 3.3.5.8 for normalized Sauter Mean Diameter (SMD_i / SMD_{max}).

For $\pm 5\%$ variation in **density** the results show that there was no effect on SMD, less than 2% variation from the maximum value of Ka . Therefore, one could conclude that, in terms of atomization, the density has little or no effect in the range over which it is likely to vary.

Varying the **surface tension** over a $\pm 5\%$ level resulted in approximately 3% variation in both SMD and Ka from their maximum values. These values indicate that there was little effect of surface tension for the range over which it is likely to vary. However, the mechanism of jet breakup should be influenced by surface tension. Jet breakup (plane jet without impact) occurs when asymmetric disturbances on the surface of the jet cause parts of the surface to shear off (ligament formation), forming droplets which may also further break down into smaller droplets. Therefore, the surface tension must play a role in the ligament formation at the jet perimeter, and more so the break down of large droplets into smaller ones. This is so because it is the surface tension which holds the droplets and the jet together, therefore, although the sensitivity analysis showed that there was little effect on

atomization with $\pm 5\%$ variation in surface tension, one should investigate if there is any statistically significant difference in the surface tension as a function of fatty acid composition of the biodiesel fuel.

A $\pm 5\%$ variation in the viscosity resulted in a 3% variation in Ka and 9% variation in SMD from their maximum values. However, over the $\pm 30\%$ range in which it is likely to vary, a 18% and 50% variations in Ka and SMD were obtained respectively. These results show that the fluid viscosity is one of the most, if not the most, important property which affects atomization. Therefore, a full and clear understanding of how the viscosity of the biodiesel fuels is affected by the fatty acid composition is necessary.

Table 3.3.4.1 Typical Properties of Mixtures of Canola, Peanut and Coconut Oil Methyl Esters

	Surface Tension (mN/m)	Dynamic Viscosity (mPa.s)	Density (g/mL)
	30	5.05	0.873
	29	5.80	0.886
	29	4.46	0.881
	29	3.10	0.875
	30	4.70	0.872
	30	4.27	0.874
	28	1.90	0.839
Mean	29.2	4.18	0.871
Standard Deviation	0.08	1.2	0.014
Percent Standard Deviation	2.90%	28.72%	1.63%

Table 3.3.4.2. Mean Value of Properties used for Sensitivity Analysis

Property	Mean value
Viscosity	4.18 mPa.s
Density	871.4 kg/m ³
Surface Tension	29.2 mN/m

Table 3.3.4.3. Parameters used in Sensitivity Analysis

Parameter	Value
Injector Line Pressure	35,000 kPa
Cylinder Pressure at BDC	1.01 Bar
Cylinder Temperature at BDC	30 °C
Nozzle Diameter	0.4 mm
Polytropic Index	1.3
Compression Ratio	16
Characteristic Length (L_o / d_o)	2.2
Nozzle Efficiency	0.64

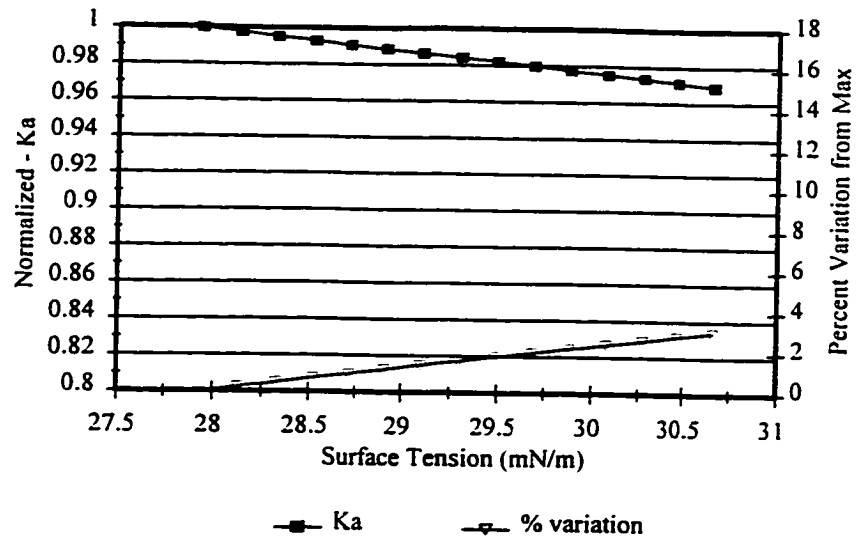


Figure 3.3.5.1 Variation of Normalized Atomization Characteristic (Ka_i / Ka_{max}) with 5% Variation of Surface Tension for Constant Density and Viscosity

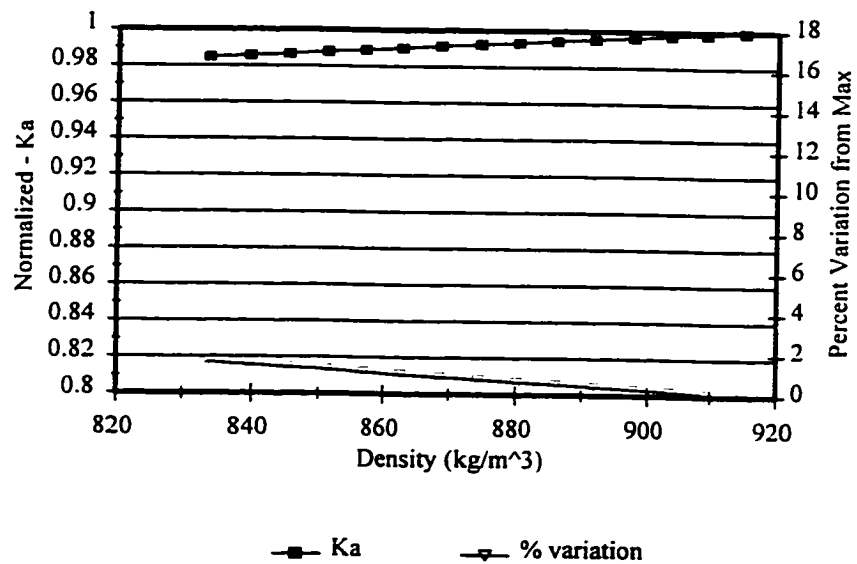


Figure 3.3.5.2 Variation of Normalized Atomization Characteristic (Ka_i / Ka_{max}) with 5% Variation Density for Constant Surface Tension and Viscosity

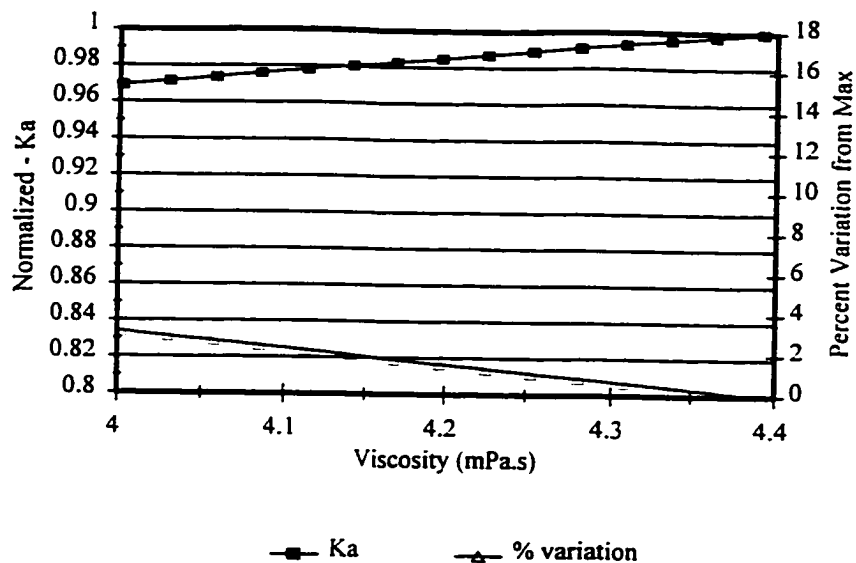


Figure 3.3.5.3 Variation of Normalized Atomization Characteristic ($K_{a_i} / K_{a_{max}}$) with 5% Variation of Viscosity for Constant Surface Tension and Density

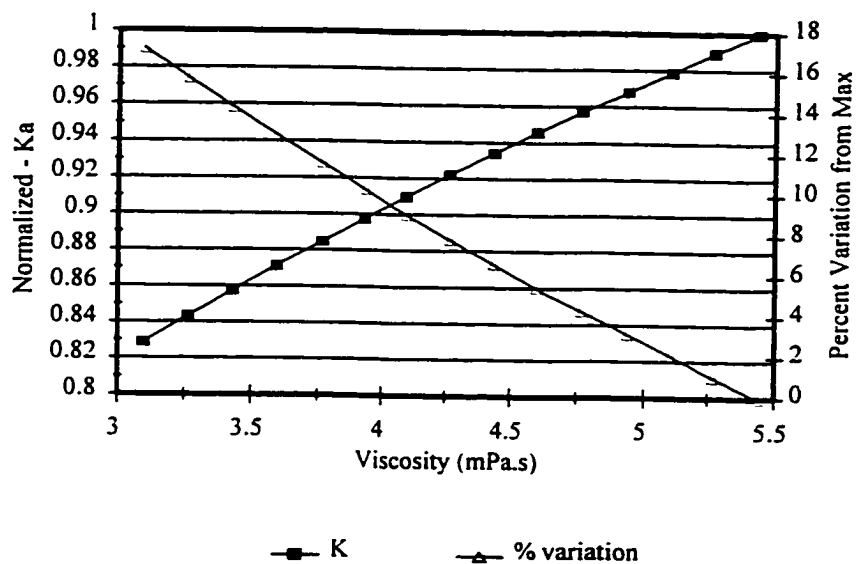


Figure 3.3.5.4 Variation of Normalized Atomization Characteristic ($K_{a_i} / K_{a_{max}}$) with 30% Variation of Viscosity for Constant Surface Tension and Density

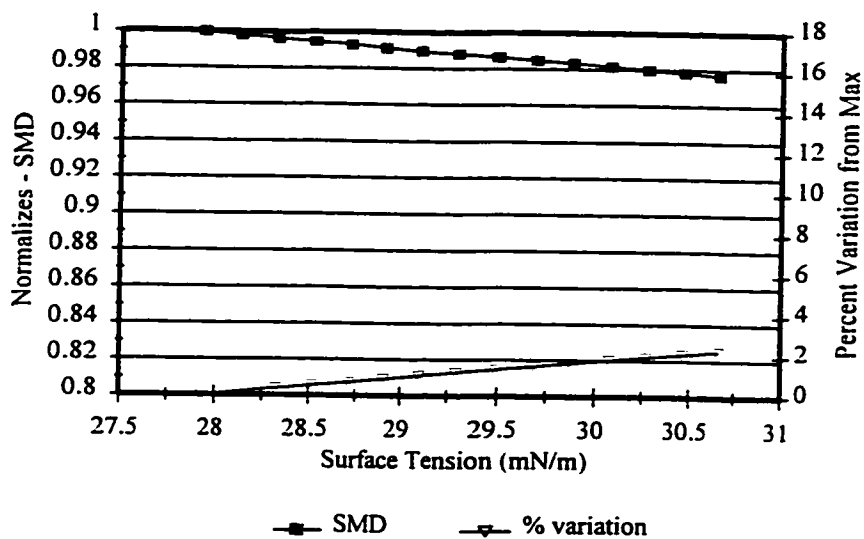


Figure 3.3.5.5 Variation of Normalized Sauter Mean Diameter (SMD_i / SMD_{max}) with 5% Variation of Surface Tension for Constant Density and Viscosity

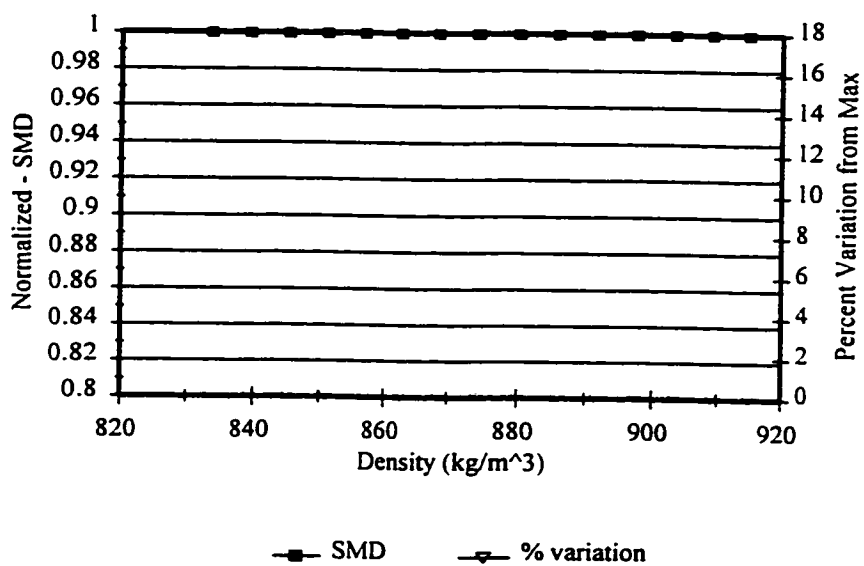


Figure 3.3.5.6 Variation of Normalized Sauter Mean Diameter (SMD_i / SMD_{max}) with 5% Variation of Density for Constant Surface Tension and Viscosity

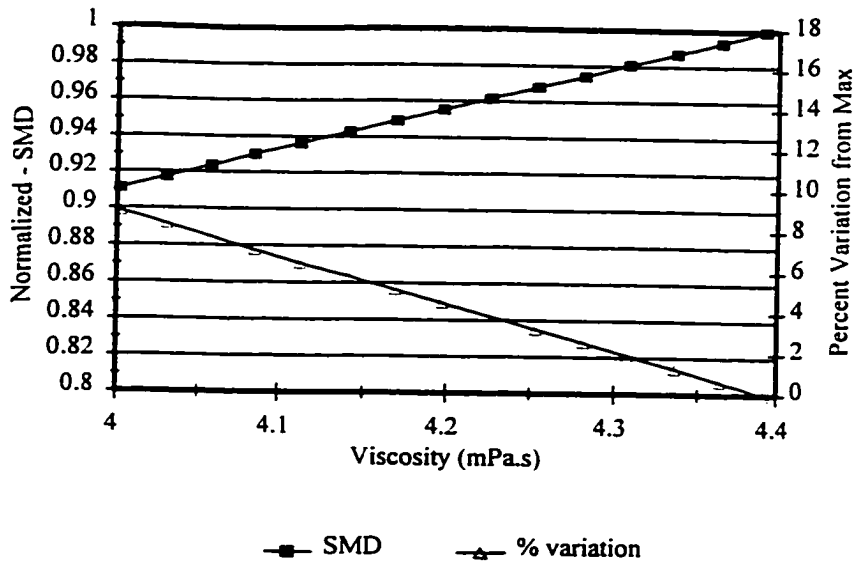


Figure 3.3.5.7 Variation of Normalized Sauter Mean Diameter (SMD_i / SMD_{max}) with 5% Variation of Viscosity for Constant Density and Surface Tension

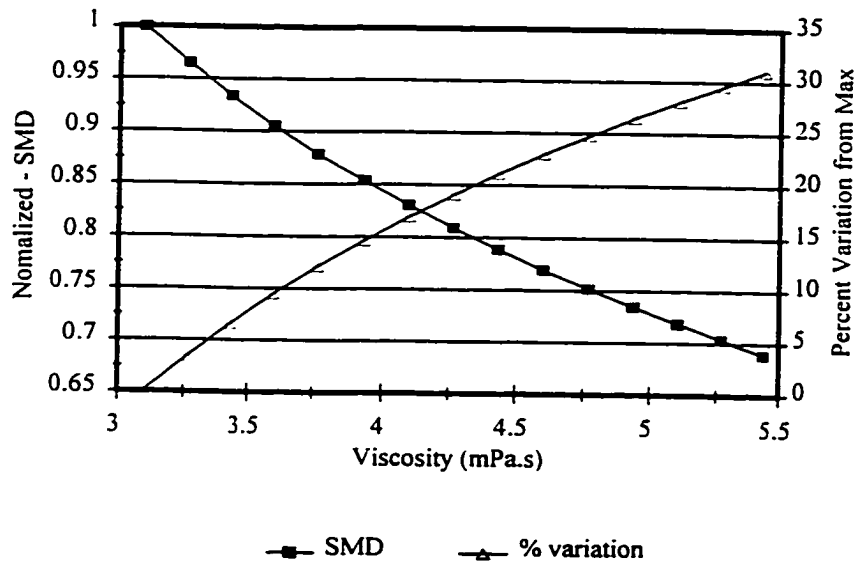


Figure 3.3.5.8 Variation of Normalized Sauter Mean Diameter (SMD_i / SMD_{max}) with 30% Variation of Viscosity for Constant Density and Surface Tension

4 RESEARCH PROCEDURES

4.1 Overview of the Four Phases of the Research

The research activities were carried out in four phases as follows:

- The first phase involved the determination of viscosity and surface tension of binary, ternary and quaternary mixtures of ethyl ester Gas Chromatography (GC) standards at 25 °C. Ethyl esters were chosen for this phase because they were less expensive than methyl esters.
- Having established the applicability of the mixture equations for simple mixtures, phase two involved testing the mixture equations on complex mixtures of methyl ester GC standards which simulated selected vegetable oils. These tests were carried out at a higher temperature of 40 °C to accommodate stearic (18:0) and palmitic acid (16:0) methyl esters which were solid at room temperature.
- Methyl esters of naturally occurring vegetable oils were produced in phase three and their viscosity and surface tension were measured. The previously validated mixture equations were then applied to predict the viscosity and surface tension of the methyl ester biodiesel fuels produced from the naturally occurring vegetable oils. The viscosity and surface tension of the pure components of the natural oils that were required for the mixture equations were obtained from an independent data set taken from the literature. The viscosity and surface tension of the methyl esters of the natural oils were then compared with their measured values to further validate the mixture models.

- Phase four involved measurement of the atomization characteristics of the methyl ester biodiesel fuels produced. These atomization characteristics were then related to the measured viscosity and surface tension of the biodiesel fuels.

4.2 Sample Preparation

Ethyl and methyl ester GC standards were acquired from “Sigma-Aldrich” Chemical Supplies Company. The storage temperatures recommended on the labels for each ester were followed. Edible grade canola, coconut, peanut and soya oils were acquired from a local supplier. Palm oil was also acquired in small quantities from the lipids laboratory on campus.

The vegetable oils (triglycerides) were converted into methyl esters using a batch reactor shown schematically in Figure 4.2.1. This reactor was capable of operating at atmospheric pressure or under a vacuum. The reaction chamber was made of stainless steel and had a transparent high strength glass window through which the reactants were seen. It was 25 cm in diameter on the inside and 30 cm high with a capacity of 12 L. The base of the tank was conical and a transparent drain pipe was attached to its center to view the reactants when separating one phase from another.

A variable speed mixer with replaceable blades was positioned at the center of the unit. Blades to produce down-wash, up-wash, or just swirl were available. The latter was used in these studies. The inner wall of the reactor had a baffle which enhanced the mixing of the contents by breaking the swirl.

Heating and cooling were made possible by adjusting the fluid source using a group of valves operated manually. The reaction chamber was double walled; the cavity between which flowed the heat transfer fluids. A hot water tank provided hot ethylene glycol/water heat transfer fluid at temperatures up to 120 °C. A 2.3 kW heating element was the heat source and the temperature was controlled by a manually adjusted thermostat.

In order to reduce the occurrence of oxidation during the production process, an inert atmosphere within the tank was provided by a nitrogen sparge. The flow of the nitrogen was controlled by a valve and an inert atmosphere was maintained even under vacuum.

Due to the toxic nature of some of the reactants (e.g methanol fumes), all ports were leak tight and any fumes produced were vented through a condenser to atmosphere.

The temperature of the reactants was monitored with a thermometer inserted in the tank and visible through the transparent window. The pH was also monitored using a digital pH meter and probe. A burette for titrating the reactants was in place through an "O"ring sealed port. Figure 4.2.2 shows an overall view of the batch transesterification unit.

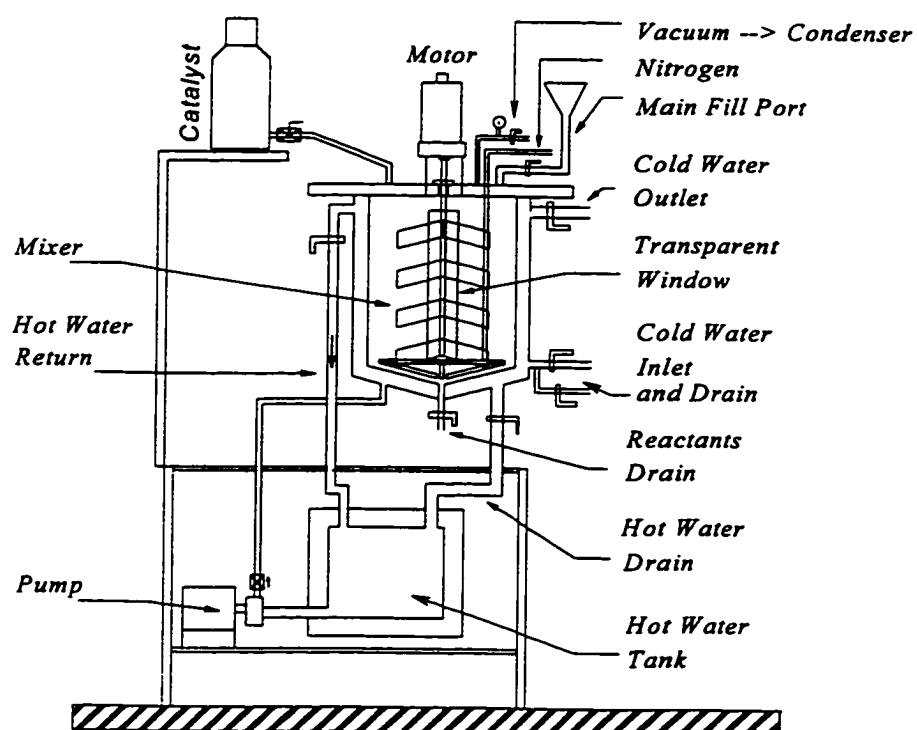


Figure 4.2.1 Schematic of Batch Transesterification Unit

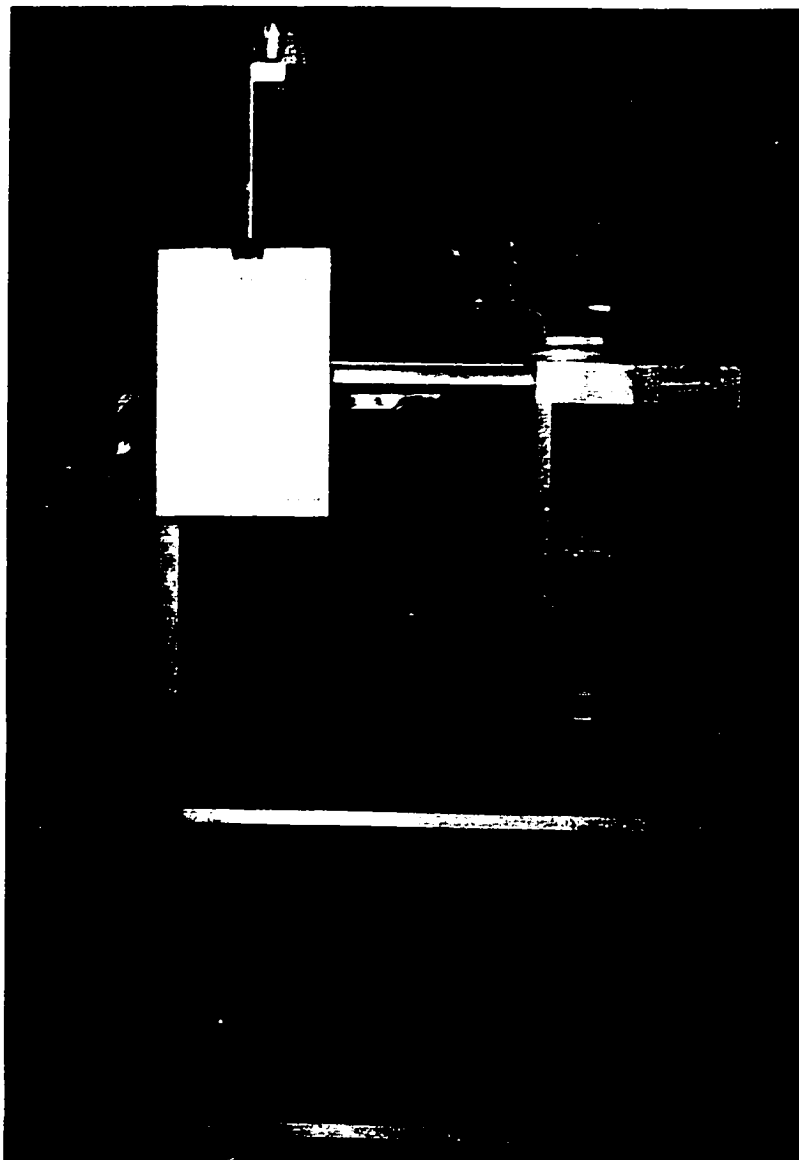


Figure 4.2.2 Overall View of Batch Transesterification Unit

4.2.1 The Transesterification Procedure

Transesterification was carried out using methyl or ethyl alcohol with potassium hydroxide as catalyst. Catalyst levels between 0.5% to 4% by weight of oil can be used depending on the quality and moisture of the oils. A level of 1% by weight was found to provide satisfactory reaction rates and completeness with the edible grade oils used in this study.

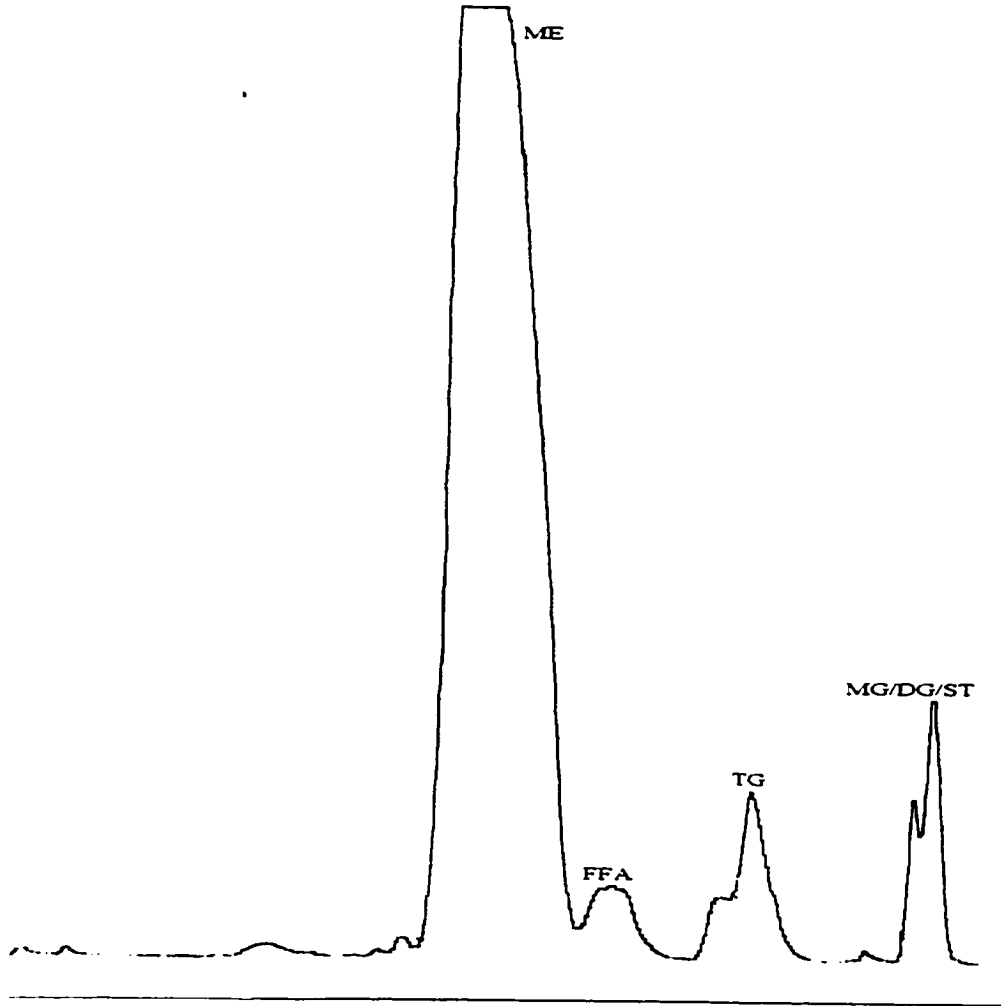
The transesterification reaction was started by heating the vegetable oil to 60 ± 2 °C for methyl esters or 75 ± 2 °C for ethyl esters under a nitrogen atmosphere. For methyl esters 30 mL of methyl alcohol per 100 mL oil was used with 1% w/w_{oil} potassium hydroxide catalyst dissolved in it. For ethyl esters 40 mL of absolute ethanol per 100 mL oil was used with the same catalyst level. The quantity of alcohol used in both cases amounts to slightly greater than a 6:1 molar ratio.

The reaction commenced by adding the alcohol/catalyst mixture to the tank containing the vegetable oil at the reaction temperature. For the first 15 minutes the reactants were mixed vigorously to initiate an intimate mixture of the alcohol and oil. After the first 15 minutes the mixer was stopped and the reaction was allowed to proceed for another 15 minutes. This allowed some time for initial separation of the glycerol layer by gravity. At the end of this time the initial glycerol layer was drained off before the reaction was stopped. Stopping the reaction involved adding 1:1 citric acid (or sulphuric acid) to the reactants to bring the pH to less than 6.5. Removing the glycerol layer before deactivating the catalyst resulted in less acid being required to neutralize the reactants since the glycerol layer carried the majority of the catalyst (96%) [Peterson *et al.*, 1992]. The glycerol layer also contained about 50% of the excess alcohol thus removing this layer reduced the quantity of alcohol to be boiled off. Following the deactivation of the catalyst the alcohol was boiled off under vacuum and nitrogen until no alcohol was seen dripping from the condenser (this took 30-45 minutes

depending on batch size). The reactants were then cooled to approximately 40 °C while any glycerol settled to the bottom of the tank was drained off. The ester layer was then washed twice with distilled water. When washing the ethyl esters an emulsion usually formed, therefore, a 2% sodium sulphate wash water solution was used to ease the emulsion problem. Gentle mixing when washing the ethyl esters was imperative. The ester layer was then dried for 1 hour under vacuum and nitrogen and stored in bottles for testing.

4.2.2 A New TLC-FID Method for Transesterification Quality Checks

The extent of the transesterification reaction was determined using Thin Layer Chromatography with Flame Ionization Detection (TLC-FID) on a Mark III Iatroscan using a **48:48:4:1 hexane:petroleum ether:diethyl ether: formic acid** solvent system. This solvent mixture was derived in these studies. Good separation of methyl and ethyl esters from triglycerides, free fatty acids, and di- and mono-glycerides was observed (Figure 4.2.2.1). The biodiesel produced was first dissolved in chloroform at a concentration of 15 mg ME/ mL. Silica-gel coated Chromarods SII were used and each rod was spotted with 1 μ L of dissolved sample and developed for 25 minutes in a developing tank containing the solvent mixture. Prior to developing, the rods were placed in a constant humidity tank for 10 minutes. After developing they were oven dried at 100 °C for 5 minutes. The Iatroscan Mark-III was then used to analyze the samples for esters, free fatty acids, tri-, di-, and mono-glyceride compositions. Known standards were used to derive the retention times for the various compounds.



ME- methyl ester; FFA - free fatty acids; TG - triglycerides; MG/DG/ST - mono, di- glycerides and sterols

Figure 4.2.2.1 TLC-FID Chromatogram showing ME Separation

4.3 Measurement of Properties

4.3.1 Viscosity

Viscosity measurements were carried out using a “Parr” model AMV 200 micro-viscometer operating on a rolling-ball principle. Since relatively low viscosity fluids were tested, a 30° rolling angle was used in order to increase the rolling time and reduced the average error that may occur in the timing mechanism. A temperature of 40 °C (limited by the specification of the viscometer) was used and a standard calibration fluid was employed to calibrate and constantly check the repeatability of the equipment. Calibration checks were carried out before and after each test sequence and only one replicate for each sample was required since the instrument provided consistently repeatable results. Within the precision of the instrument (two decimal places), the measured viscosities did not vary between replicates.

4.3.2 Surface Tension

A “Kruss” model K8600E Interfacial Tensiometer employing a Du Nouy Ring was used to measure the surface tension of the samples. This tensiometer was equipped with a water bath to control the temperature of the samples at 40 °C. Iso-butanol and benzene were initially used to calibrate the apparatus, then myristic acid methyl ester GC standard (14:0 ME) was used to check the repeatability of the apparatus on a regular basis. The ring was cleaned before each fuel was tested by heating it in the oxidizing part of a propane flame until it was white hot. Only two replicates were required since the instrument gave consistently repeatable results.

4.4 Atomization Characteristics

A Malvern 2600 droplet analyzer was used for all droplet analyses. The operational principles of the Malvern was thoroughly investigated through the review of several papers [Kihm and Caton, 1992; Gulder, 1990; Hirleman and Dellenback, 1989; Dodge *et al.*, 1987; Meyer and Chiger, 1986; Dodge, 1984; Dodge and Cerwin, 1984; Hirleman, 1984; Rizk and Lefebvre, 1984; Hammond Jr., 1981; Swithenbank *et al.*, 1977; Dobbins *et al.*, 1963]. Both theoretical and practical aspects were reviewed and it was concluded that the Malvern, based on its availability and its operational principles, was suitable for this application.

The Malvern 2600 droplet analyzer was installed on a test bench which was designed in this study to accommodate suitable fixtures for a diesel injection system. The diesel injection system (Figure 4.4.1) comprised of an electric motor with a cam shaft attached which drove one of two high pressure diesel fuel pumps (Figure 4.4.2) taken from a “Kubota” single cylinder engine. One of the engines was an indirect injection type and the other was a direct injection engine. The indirect injection engine had a single-orifice injector (Figure 4.4.2) which had a cracking pressure of approximately 14 MPa (2100 psi). The direct injection engine had an injector (Figure 4.4.2) with four orifices and a cracking pressure of approximately 23 MPa (3400 psi). The test injector was attached by means of a coupling (Figure 4.4.3) to a precision X-Y-Z traversing table (Figure 4.4.4) which facilitated the exact, repeatable positioning of the nozzle tip with respect to the laser beam.

The Malvern’s computer system was upgraded to incorporate the use of a hard drive, instead of the two-floppy-drive system it came with. This modification allowed for quicker and safer data storage and program execution. A direct connection with a Pentium computer through the serial interface was also installed. This facilitated the transfer of data files from the Malvern to the Pentium for analysis and presentation.

The injection mode from the diesel pump is pulsatile; thus a special electronic system (Figure 4.4.5) was designed to ensure that the droplet analyzer sampled at a specific angle during the spray period. This electronic control system comprised of an optical shaft encoder and a specially designed “counter” circuit which provided an electrical pulse signal to trigger the droplet analyzer at any given angle. Thus the system was capable of sampling at different stages during the spray period, e.g., at the beginning of the spray, at the end, or any point between those extremes.

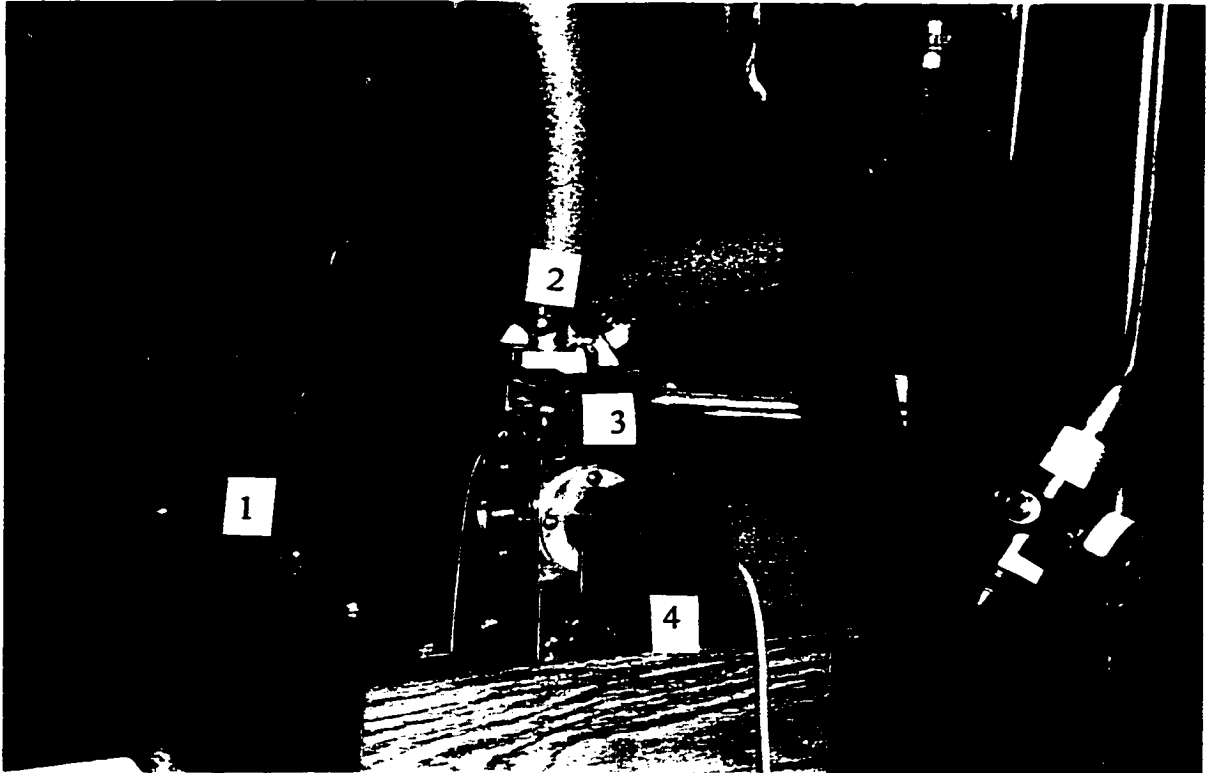
The signal used to trigger the analyzer was also used to trigger a stroboscope which enabled a visual examination of the spray (Figure 4.4.6). With this system, one was able to observe at which shaft position the injection started or ended, and approximately at which position the maximum flow occurred.

The mean drop size and dropsize distribution of atomized biodiesel fuels were measured by first preheating the samples to 40 °C. This temperature coincided with the temperature used for viscosity and surface tension measurements. The fuel types used were methyl esters of coconut, canola, peanut, palm and soya oils. Diesel #2 fuel was also used as reference.

In order to maintain comparability between runs, the pump and injector settings were not changed after initial setup. The pump rack and injector tip were both locked in place after the fuel line was initially bled to remove any air in the system. Once bled, the lines were not cracked since this may have led to either a change in the nozzle position or a change in the flow condition due to air traps. To reduce cross contamination within the fuel pump and lines, they were flushed with the test sample by running the pump for 5 minutes before doing the analysis.

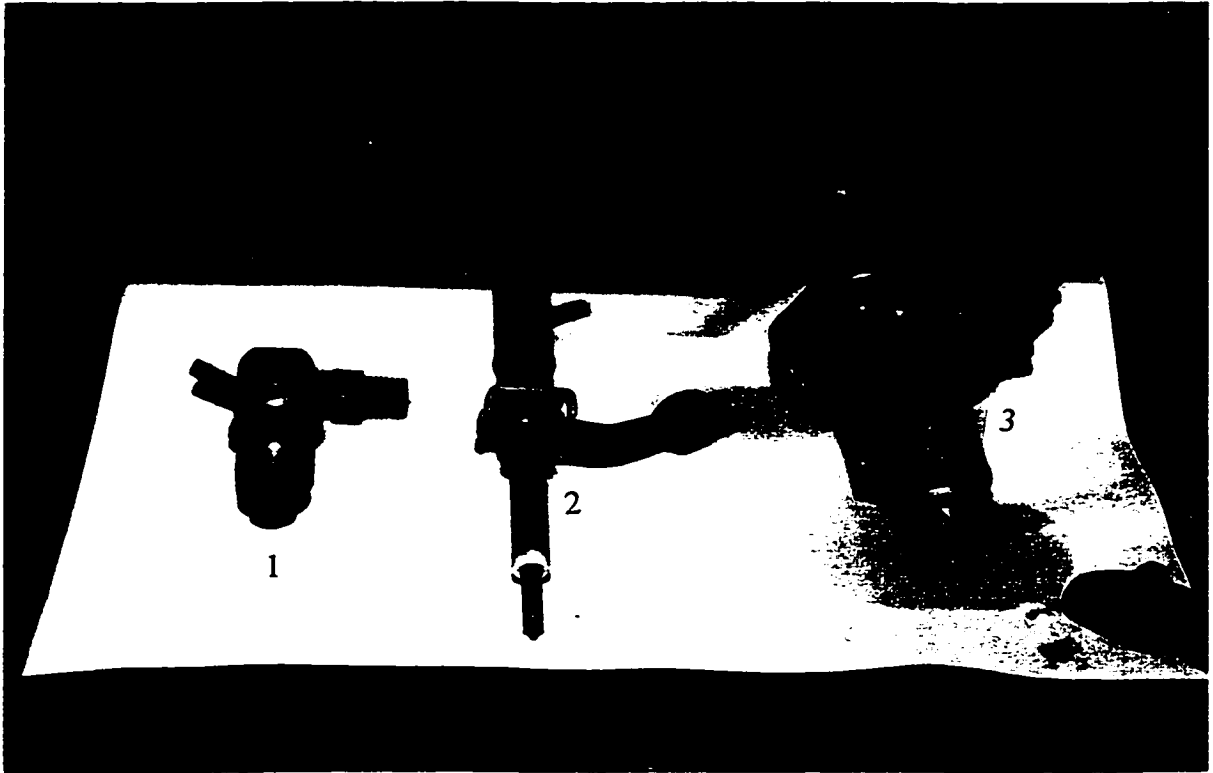
The fuel was stored in an insulated tank and heat loss from the fuel lines was reduced by insulating them. A thermocouple was placed in the fuel tank to monitor the temperature of its contents. The pump body tended to accumulate excess heat after the 5 minutes of flushing. Therefore a cooling fan was put in place and the pump body temperature was monitored with a thermocouple.

Each fuel test procedure comprised of ten runs. At each run the pump was started, allowed to run for 10 seconds then 400 samples of the spray were taken every second revolution of the pump shaft by the Malvern analyzer (shaft speed = 1725 rpm). The position of the spray, the point in time during the spray period, and the pump rack position were chosen to give the optimal condition for analysis by the Malvern. The spray timing was set at mid spray, maximum flow period. The rack position was set to give a spray that was dilute enough to give an obscuration of less than 45% [Gulder, 1990]. The spray was directed so that the laser beam passed through its midpoint in the lateral direction; and the distance between the injector tip and the beam was set at a point where the spray was completely dispersed, but not too far downstream where the spray was unstable (tip to beam distance = 70 mm). All of the above parameters were fixed for all fuel tests. A 300 mm range-lens was used for all tests and the spray to lens distance was 130 mm, within the cut-off distance for that lens.



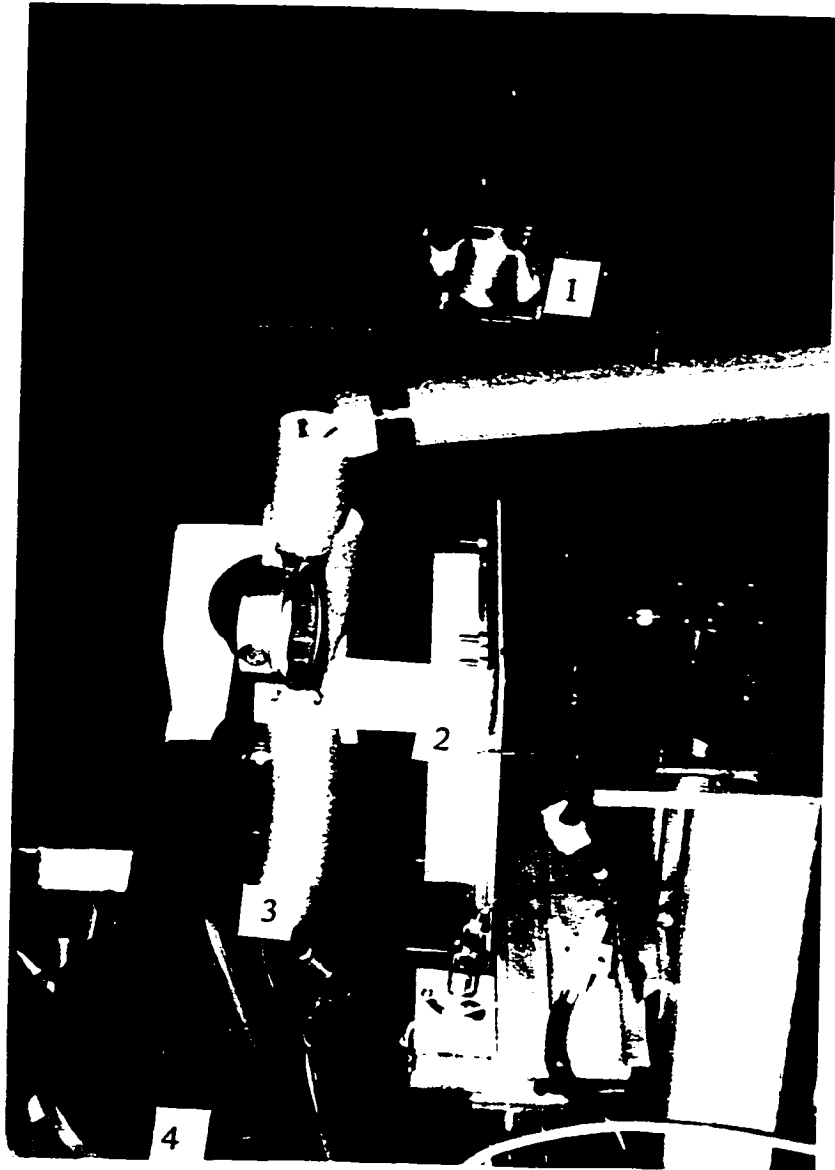
1- Electric Motor, 2- Diesel Pump, 3- Pump Housing, 4- Optical Shaft Encoder

Figure 4.4.1 Diesel Pump and Electric Motor Setup



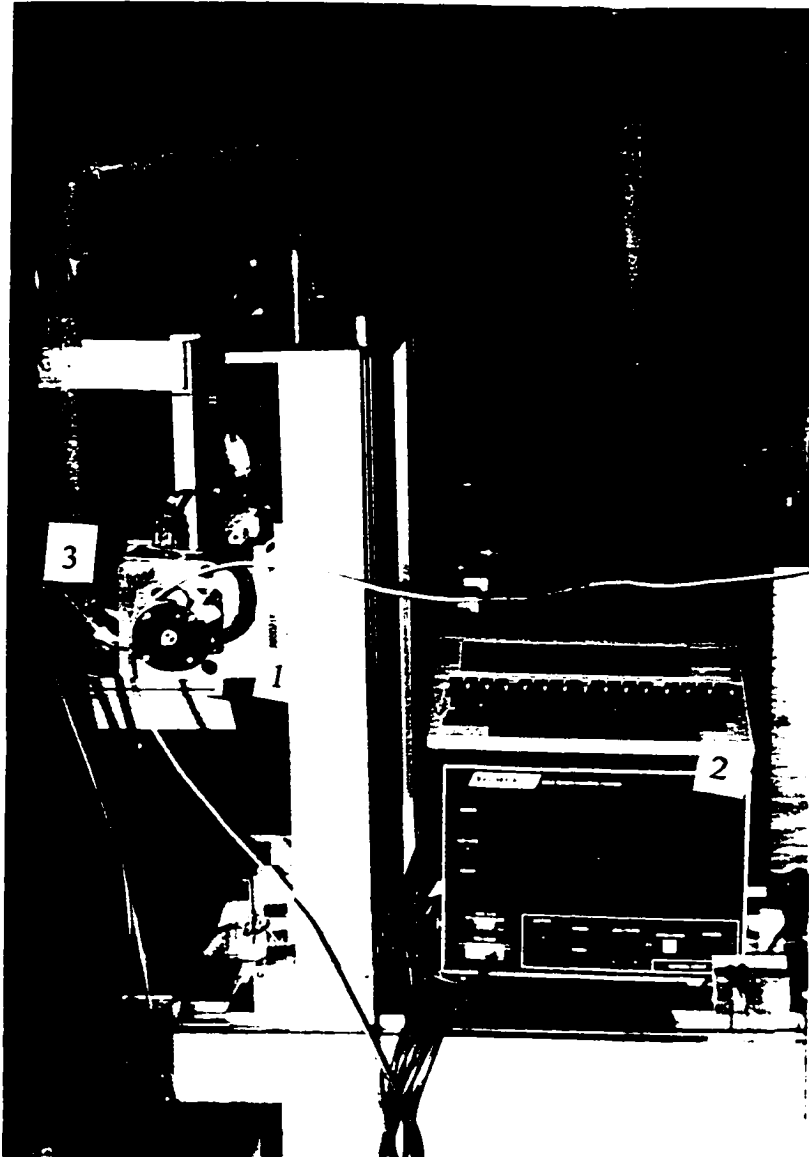
1- Single Orifice Injector, 2- Multiple Orifice Injector, 3- Diesel Pump

Figure 4.4.2 Diesel Pump and Fuel Injectors



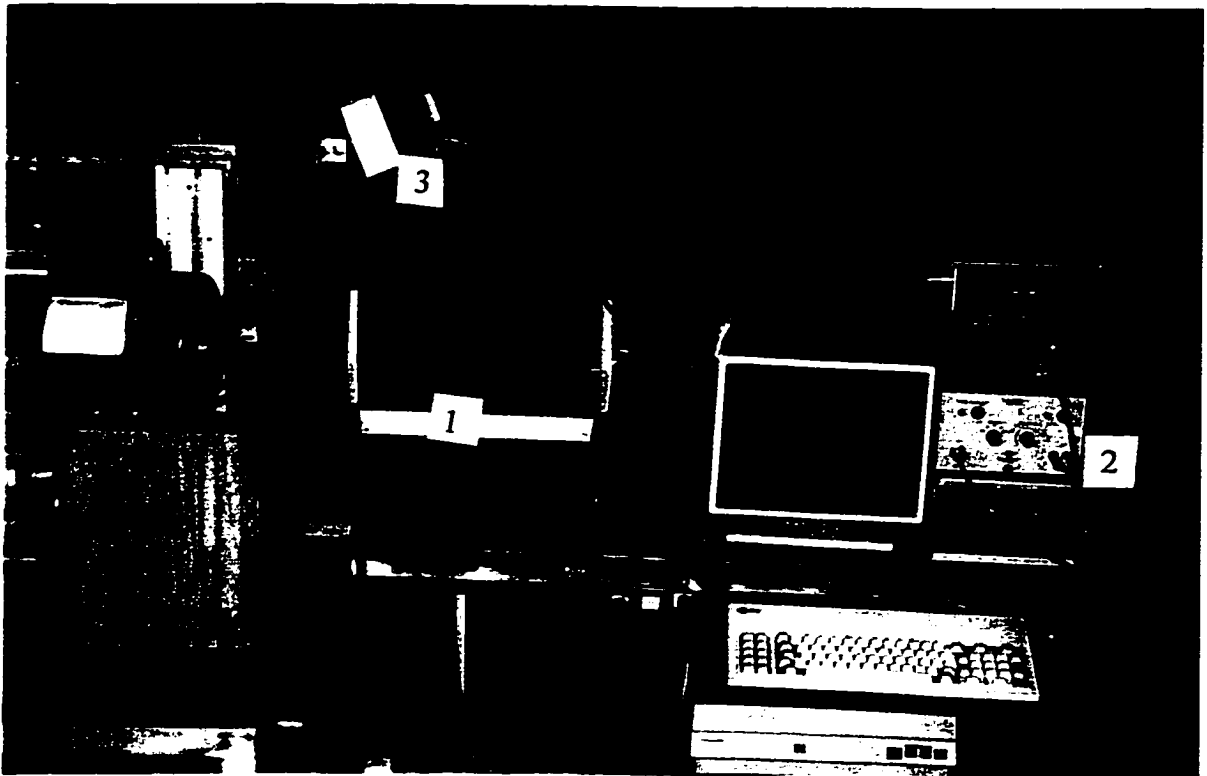
1- Stroboscope. 2- Injector Coupling, 3- Injector, 4- Spray Exhaust

Figure 4.4.3 Fuel Injector and its Coupling



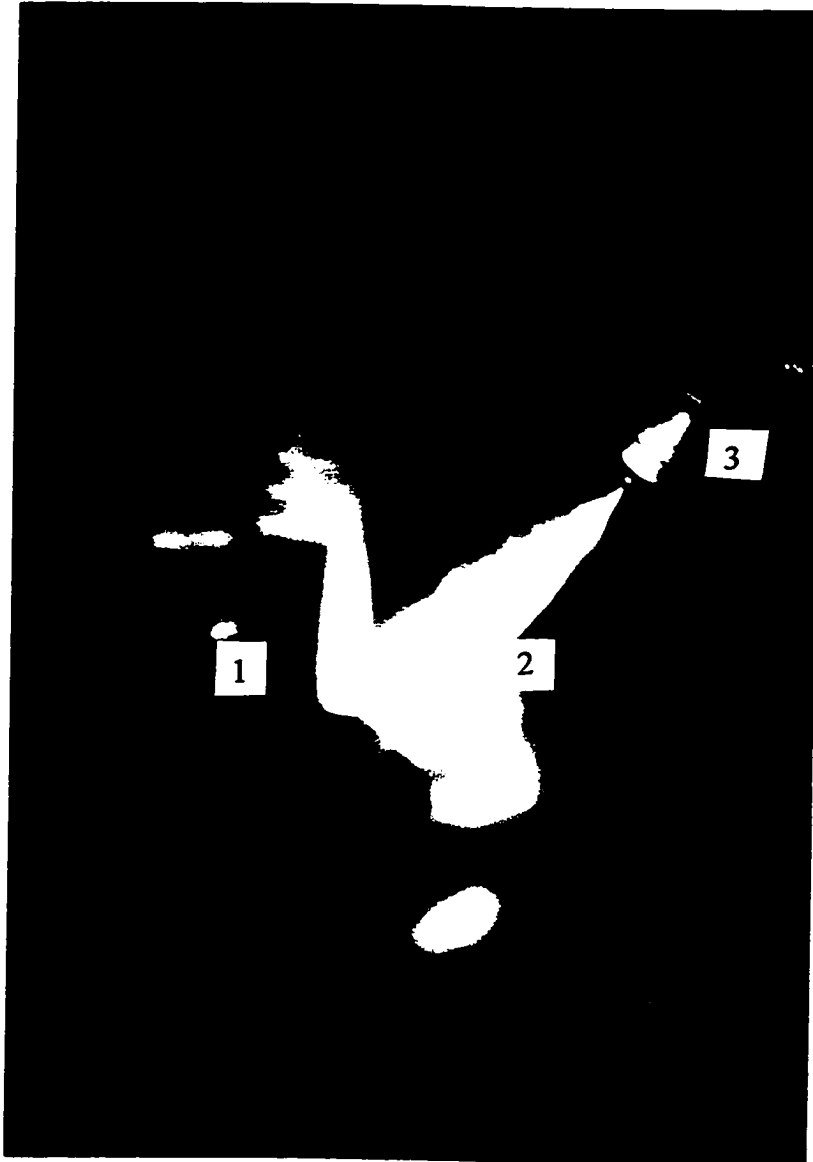
1- XYZ Traversing Unit, 2- Computerised Controller, 3- Fuel Injector

Figure 4.4.4 Precision X-Y-Z Computer Controlled Traversing Mechanism



1- Malvern Analyser, 2- Electronics for Spray Timing, 3- Stroboscope

Figure 4.4.5 Electronic Components for Timing Pulsed Spray



1- He-Ne Laser Beam, 2- Fuel Spray, 3- Fuel Injector

Figure 4.4.6 A Typical Spray as Visualized using the Timed Stroboscope

5 MODELS FOR PREDICTING BIODIESEL PROPERTIES

5.1 Viscosity

There exist in the literature several models for predicting the viscosity of fatty acids. Fisher (1988) described a method based on limiting properties to predict several properties of n-fatty acids. The variation of those properties was attributed to the increments in the methylene group of the homologous series. This method worked fairly well for properties like heat capacity, heat of vaporization, boiling point, molal volume and density but unfortunately the limiting property for viscosity was approximately zero rendering this method inaccurate for viscosity predictions.

Liew *et. al.*, (1991) and Hildebrand (1971) both reported a method for predicting the fluidity (inverse of viscosity) of simple liquids. This method was based on the molal volume and the intrinsic molal volume both of which were predicted based on the chain length and limiting properties. The intrinsic molal volume was that at which the fluidity was zero. This method worked well for non-associated fluids but there is some question about its applicability to associated fluids where there is some amount of intermolecular interaction.

The models mentioned above rely on information on the limiting properties and the intrinsic molal volumes and, since these values are not known, they cannot be applied to the biodiesel components. Several empirical models and data sets for predicting the viscosity of individual fatty acids and neat vegetable oils are also available [Noureddini *et. al.*, 1992; Swern, 1979; Markley, 1960].

The Grunberg - Nissan equation (Grunberg and Nissan, 1949) has been reported (Monnery *et al.*, 1995 and Irving, 1977) to be one of the most suitable equations for computing the viscosity of liquid mixtures. This equation was developed primarily for binary mixtures and worked best with non-associated liquids. However, good results were obtained for some associated fluids with errors less than 5 - 10 %. The Grunberg - Nissan equation can be written as:

$$\ln \mu_m = \sum y_i \ln \mu_i + \sum_{i \neq j} \sum y_i y_j G_{ij} \quad (5.1.1)$$

where

- μ_m mean viscosity of the mixture (Pa.s)
- $\mu_{i,j}$ viscosity of individual components (Pa.s)
- $y_{i,j}$ mole fraction
- G_{ij} interaction parameter (Pa.s)

In an expanded form, Equation 5.1.1 can be written as:

$$\begin{aligned} \ln \mu_m = & y_1 \ln \mu_1 + y_2 \ln \mu_2 + y_3 \ln \mu_3 + y_4 \ln \mu_4 + \dots + y_n \ln \mu_n \\ & + y_1 y_2 G_{1,2} + y_1 y_3 G_{1,3} + y_1 y_4 G_{1,4} + \dots + y_1 y_n G_{1,n} \\ & + y_2 y_3 G_{2,3} + y_2 y_4 G_{2,4} + \dots + y_2 y_n G_{2,n} \\ & + \dots \\ & + y_{n-1} y_n G_{n-1,n} \end{aligned} \quad (5.1.2)$$

It is assumed that the viscosity of the pure components are known.

Reid *et al.* (1987) presented a method which was developed by Isdale to determine the interaction parameters. This method utilized a group contribution method in which the types of chemical groups that make up the compound were given special values. These values were then used in the procedure below to determine the interaction parameter.

1. For the binary interaction parameter $G_{i,j}$, the component to be used as the i^{th} component was selected using the following priority rules:

- a) i = an alcohol if present
- b) i = an acid, if present
- c) i = the component with the most carbon atoms
- d) i = the component with the most hydrogen atoms
- e) i = the component with the most $-\text{CH}_3$ groups

$G_{i,j} = 0$ if none of these rules indicate a priority.

2. $\sum \Delta$ for the i and j components were then calculated from the group contribution values given in Table 5.1.1.

3. Using the Equation 5.1.3, W was calculated using the number of carbon atoms (N) in i and j . ($W=0$ if i or j contains atoms other than C or H)

$$W = \frac{(0.3161)(N_i - N_j)^2}{(N_i + N_j)} - (0.1188)(N_i - N_j) \quad (5.1.3)$$

4. The interaction parameter $G_{i,j}$ was then calculated from Equation 5.1.4.

$$G_{i,j} = \sum \Delta_i - \sum \Delta_j + W \quad (5.1.4)$$

One noticeable omission for Table 5.1.1 is a group contribution factor for the -COO- group. This is an important group in esters and without its value this method cannot be applied to biodiesels.

5.1.1 Predicting Viscosities of Mixtures using a Simplified Logarithmic Equation

It was hypothesised that, since the biodiesel fuel was made up of compounds of similar chemical structure, the interaction parameter is negligible and can be omitted from the Grunberg-Nissan equation. A very simple function was thus derived and is given below:

$$\mu_m = e^{\left(\sum x_i \ln \mu_i \right)} \quad (5.1.1.1)$$

where

μ_m is the viscosity of the mixture (Pa.s)

μ_i is the viscosity of component i (Pa.s)

x_i is the mass fraction of component i

Table 5.1.1 Group Contribution for G_{ij} at 298K (25 °C) [Reid *et al.*, 1987]

Group	Notes	Δ
-CH ₃	--	-0.1
-CH ₂ -	--	0.096
=CH-	--	0.204
=C=	--	0.433
-OH	Methanol	0.887
	Ethanol	-0.023
	Higher aliphatic alcohols	-0.443
	Ketones	1.046
-Cl	--	$0.653 - 0.161 N_{Cl}$
-Br	--	-0.116
-COOH	Acids with:	--
	Non-associated liquids	$-0.411 + 0.06074N_c$
	Ketones	1.13
	Formic acid with ketones	0.167

5.2 Surface Tension

Reid *et al.* (1987) stated that “the surface tension of a liquid mixture is not a simple function of the surface tension of the pure components because in a mixture the composition of the surface is not (necessarily) the same as the bulk”. They also indicated that the surface tension of a mixture calculated using the sum of the mole fraction average is usually less than the measured surface tension. In a review of the literature, no research findings were found on the surface tension of ester mixtures. In fact, very little data was found on surface tension of non-aqueous mixtures.

For pure non-aqueous compounds the Sugden expression, presented by Meissner and Michaels (1949), was reported to give good correlation with experimental data when predicting the surface tension of pure components. The Sugden expression is:

$$\sigma^{\frac{1}{4}} = \frac{[P] \rho}{M} \quad (5.2.1)$$

where

- σ is the surface tension of the pure component (mN/m)
- [P] is a temperature-independent parameter called the “Parachor” of pure component { (N/m)^{1/4} (m³/mol) }
- ρ is the density of the liquid phase in (g/ml)
- M is the molecular weight (g/mol)

Quale (1953) derived a group contribution method in which an additive scheme was proposed to derive the Parachor [P] based on the structure of the components. Values of [P] relevant to this study are given in Table 5.2.1 below. Meissner and Michaels (1949) also presented Parachors for individual components expressed in a slightly different manner. Table 5.2.2 gives the Meissner and Michaels Parachors.

Table 5.2.1 Structural Contributions for the Computation of the Parachor (Quale, 1953)

Component	Parachor [P]
C	9
H	15.5
CH ₃ -	55.5
-CH ₂ -	40.0 {if n > 12 in (-CH ₂) _n [P] is increased to 40.3}
Double (Ethylenic) Bond:	--
Terminal	19.1
2,3 position	17.7
3,4 position	16.3
Triple Bond	40.6
-COO-	63.8
-COOH	73.8
-OH	29.8

Table 5.2.2 Structural Contributions for the Computation of the Parachor (Meissner and Michaels, 1949)

Component	Parachor [P]
C (not in -CH ₂ -)	4.8
H (attached to O)	11.3
H (attached to C)	17.1
-CH ₂ -	39
Double (Ethylenic) Bond:	23.2
Semipolar	-21.6
Triple Bond	46.6
O in ester or -COO-	60

5.2.1 Predicting Surface Tension of Mixtures using a Weighted Mass Average Method

It was previously mentioned that the composition of the surface of a liquid mixture is not necessarily that of the bulk; therefore, a suitable method for predicting the surface tension taking this into account was sought.

It was hypothesized that components with lower surface tensions would have less than their 100% effect in a mixture compared to their pure value thus leading to a higher predicted surface tension. The exact cause of this reduced surface tension is unknown; however, a mechanism for this is proposed herein. It is assumed that components with higher intermolecular attraction in their pure state, thus higher surface tension, would likely have a higher intensity attraction to each other in a mixture thus tending to force the lower surface tension components away from the surface. Assuming this is the case, the lower surface tension components of a mixture will have less influence at the surface compared with the higher surface tension components.

Based on this hypothesis it was assumed that a linear weight-function could be utilized to obtain an effective surface tension for the individual components of a mixture. This 'weight-function' was derived as a function of the numeric value of the surface tension. To obtain the weight-function, the maximum and minimum surface tension of the pure components in the particular mixture were used. A weight factor of 1 was applied to the maximum surface tension and a factor of 0.93 was applied to the minimum surface tension. The latter factor was derived by successive iterations to give the minimum error of predicted versus measured surface tension of GC standards. Using these extreme values for surface tension and weight factors a linear equation was derived to compute a weight factor for each component as a function of their surface tension. An effective or weighted surface tension was thus

computed. The weighted surface tension was then used to compute the mean surface tension of the mixture using Equation 5.2.1.1 below:

$$\sigma_m = \sum_{i=1}^n w_i \sigma_i x_i \quad (5.2.1.1)$$

where

σ_m is the mean surface tension of the mixture (N/m)

σ_i is the surface tension of component i (N/m)

x_i is the mass fraction of component i

w_i is the weight factor for component i

The weight factor w_i is given by Equation 5.2.1.2.

$$w_i = m \sigma_i + c \quad (5.2.1.2)$$

where

m is the slope of the linear weight-function

c is the constant of the linear weight-function

5.3 Atomization Models

Reitz and Bracco (1979) described good atomization in diesel engines to be one which produces a cone shaped spray starting at the nozzle exit. Droplet size is used to characterize the quality of atomization and in diesel engineering the Sauter Mean Diameter is commonly

used to quantify this [Hiroyasu, 1991; Hiroyasu and Kadota, 1974] although there are six different mean diameters which can be used [Marshall, 1954]. The Sauter Mean Diameter is the diameter of a droplet which has the same volume-to-surface ratio as the whole spray and is given by:

$$SMD = \frac{\int N_i d_i^3}{\int N_i d_i^2} \quad (5.3.1)$$

where N_i is the number of droplets with diameter d_i .

Several empirical relations for the Sauter Mean Diameter (SMD) are available. Hiroyasu (1991) and Hiroyasu *et al.* (1989) presented equations in which the Weber number, Reynolds number, nozzle diameter, viscosity, and density ratio were key factors. Nozzle depth-to-diameter ratio (L_j/d_o), or dimensionless nozzle length, and injection pressure were also modeled as key factors in determining the SMD [e.g., Karasawa *et al.*, 1991 and Arai *et al.*, 1984]

Vander Griend *et al.* (1988) determined the Sauter Mean Diameters of neat rape oil and rape oil methyl ester and found that the neat oils had significantly higher diameters than the methyl esters. The viscosity of the neat oil was also much higher than its methyl ester while the surface tension was only slightly higher.

The distribution of the droplet sizes over the spray region can be found by plotting the number of drops at a given diameter versus the diameter. Many authors have investigated various distribution functions to describe the distribution of the droplets. Rosin and

Rammler in 1933 came up with the Rosin-Rammler distribution while Nukiyama and Tanasawa in 1940 came up with the Nukiyama-Tanasawa distribution [Marshall, 1954]. There are also the normal, log-normal and chi-squared distributions. All these models are not truly based on theoretical considerations and thus their merits are based on how well their distribution fits experimental data. Therefore, in selecting a distribution model for wide range applications, as in biodiesels of different make-up, one would have to judge which, if any, of the available models are applicable. The Rosin-Rammler model is commonly used for liquid spray distributions and is given by:

$$R_{over} = \exp\left(-\left(\frac{d}{X}\right)^n\right) \quad (5.3.2)$$

where:

- R_{over} - fraction of droplets over diameter d
- X - a parameter giving a measure of the mean diameter of the distribution
- n - a parameter giving a measure of the spread of the distribution ($n = \infty$ implies a mono size distribution)

The Rosin-Rammler parameters, 'X' and 'n', can also be used to compute the SMD from:

$$SMD = \frac{X}{\Gamma\left(\frac{n-1}{n}\right)} \quad (5.3.3)$$

where Γ is the Euler Gamma Function [Meyer and Chigier, 1986].

6 RESULTS AND DISCUSSION

6.1 Viscosity

6.1.1 Viscosity of Methyl and Ethyl Ester GC Standards

Viscosities of methyl and ethyl ester GC standards were analyzed with a rolling-ball micro-viscometer (“PAAR” model AMV 200). The measured viscosities of fatty acid esters had a complex pattern with respect to the saturation of the fatty acids and the chain length. For saturated fatty acid esters the measured data at 40 °C indicated that the viscosity increased with carbon number (or molecular weight) in a curvilinear trend rather than a linear one. Good correlation was found between the measured data and a second order polynomial function over the range 8:0 to 18:0. Although 20:0 and 22:0 were available, their viscosities could not be measured because they were solid at the test temperature. The test temperature was limited to 40 °C due to the viscometer’s working specifications (50°C maximum). Equations 6.1.1.1 and 6.1.1.2 give the fitted polynomials for saturated methyl and ethyl esters respectively.

$$\mu_{ME-sat} = 1.05E-4 M^2 - 0.0242 M + 2.15 \quad s = 0.0145 \quad (6.1.1.1)$$

$$\mu_{EE-sat} = 1.16E-4 M^2 - 0.0264 M + 2.28 \quad s = 0.0182 \quad (6.1.1.2)$$

where:

- μ - viscosity (mPa.s)
- M - molecular weight (g/mol)
- s - standard error

Figure 6.1.1.1 show a scatter plot of these data and Figure 6.1.1.2 show the data and their trend curves. The viscosities of the saturated ethyl esters were only slightly higher than those for methyl esters; an average of 5.4% higher over the range 8:0 to 18:0.

The viscosity trend for unsaturated esters at 40 °C showed a sharp deviation from the trend of the saturated esters when 18:0 became unsaturated to 18:1. A completely different curve was observed as the degree of unsaturation progressed from 18:1 to 18:3 (Figure 6.1.1.2). As the number of double bonds increased there was a nonlinear decrease in viscosity, with a 21% difference between 18:0 and 18:1, an 18% difference between 18:1 and 18:2, and a 13% difference between 18:2 and 18:3. Although this phenomenon could not be verified at other carbon numbers, it is within reason to believe that the same result would occur at other carbon numbers. This phenomenon could not be verified because 16:1 and 20:1 were very expensive to purchase in the minimum 5 mL quantity required. Although 22:1 was available and measurable, a comparison could not be done because 22:0 was not measurable at the test temperature.

The trend for unsaturated C18 esters also correlated well with second order polynomial functions given in Equations 6.1.1.3 and 6.1.1.4 for methyl and ethyl esters respectively.

$$\mu_{ME-unsat-CN18} = 0.153 NDB^2 - 1.15 NDB + 4.73 \quad s = 0.0112 \quad (6.1.1.3)$$

$$\mu_{EE-unsat-CN18} = 0.147 NDB^2 - 1.09 NDB + 4.82 \quad s = 0.000 \quad (6.1.1.4)$$

where NDB is the number of double bonds at carbon number 18.

At the time the viscosity measurements were carried out linolenic acid ethyl ester (18:3 EE) was not available from the suppliers in the quantity that was required for testing. Only 500 mg sizes were available and it would have required several of those to meet the minimum 5 mL required for all tests, making it very expensive.

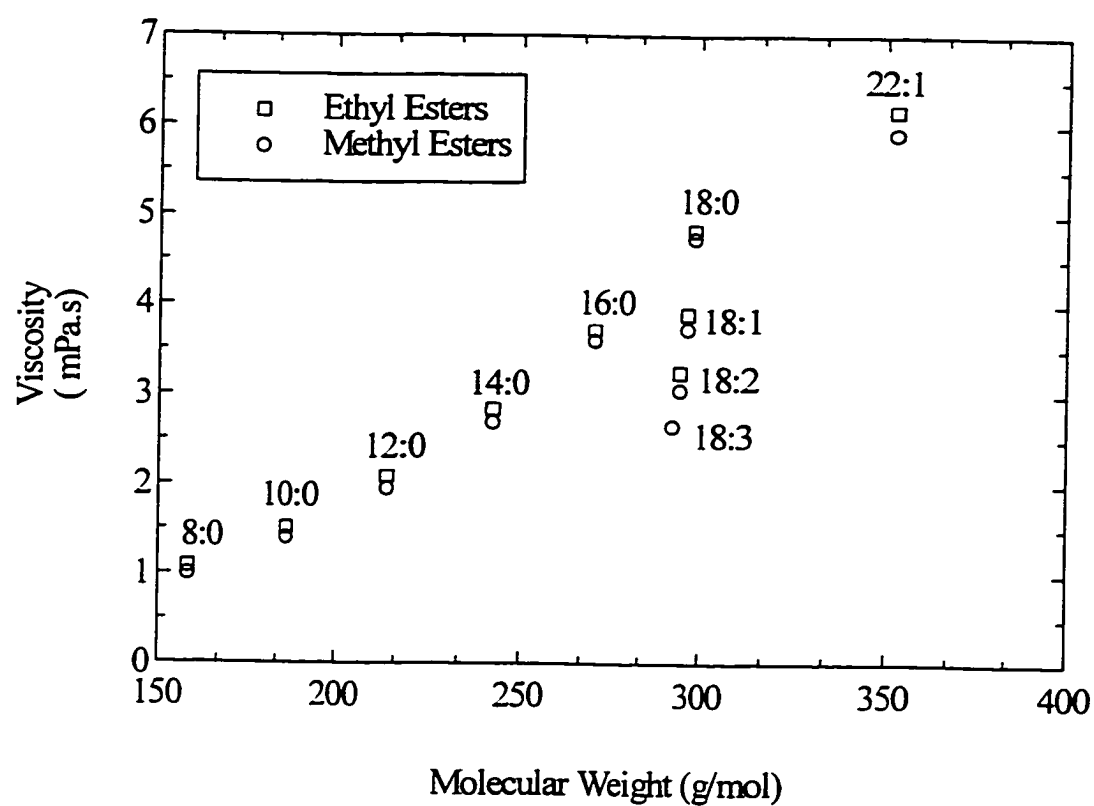


Figure 6.1.1.1 Viscosities of Fatty Acid Methyl and Ethyl Ester GC Standards at 40 °C

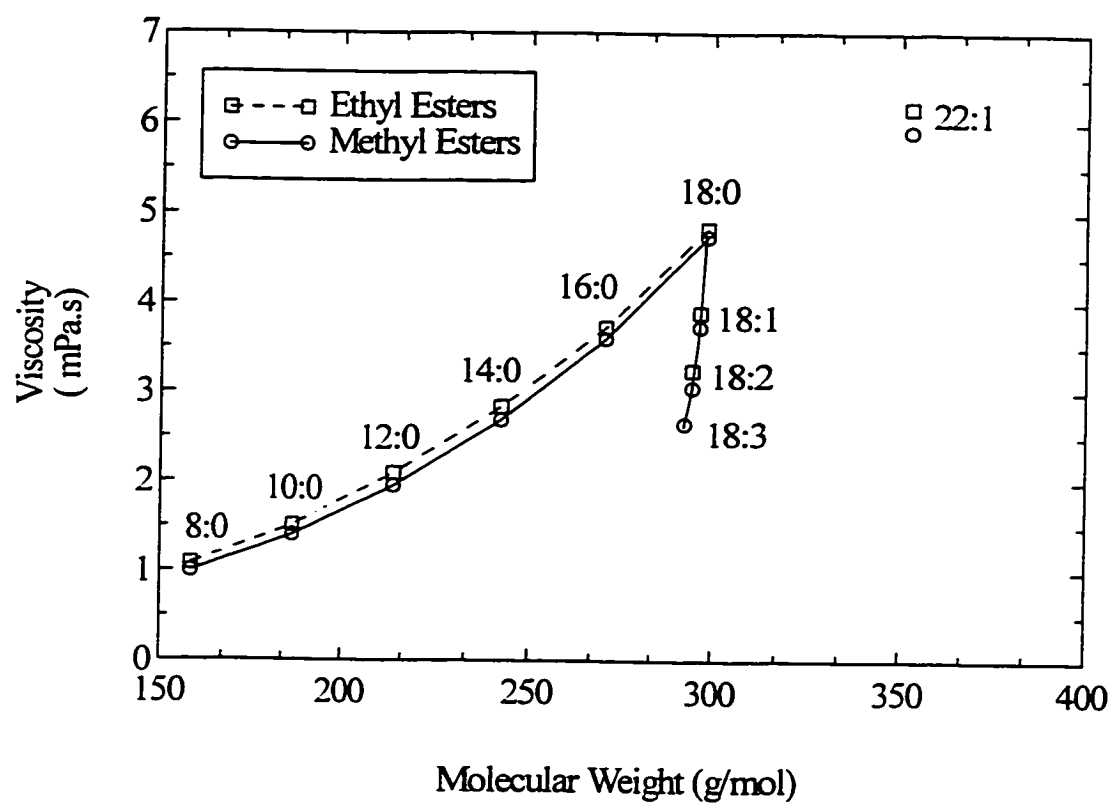


Figure 6.1.1.2 Viscosity Trend Lines for Methyl and Ethyl Ester GC Standards at 40°C

6.1.2 Viscosity of Mixtures of Methyl and Ethyl Ester GC Standards

The logarithmic equation (Equation 5.1.1.1) for predicting the viscosities of multi-component mixtures was tested on fatty acid ester GC standards. Initially the model was tested on binary, ternary, and quaternary mixtures of 8:0, 10:0, 12:0 and 18:1 ethyl ester GC standards at 25 °C. The mixing ratios and results are summarized in Table 6.1.2.1 where it can be seen that the errors in predicting the viscosities are all less than 3.7%. These results were within acceptable limits (maximum of 5%) based on the results of sensitivity analyses. It was thus decided to extend the analyses to more complex mixtures.

Methyl ester GC standards were mixed on a mass basis in proportions to simulate rapeseed, canola, peanut, soybean, palm and coconut oils. Peanut oil required greater than 4% of 20:0 and 22:0 fatty acids combined. These components were not measurable at the test temperature so one of the simulated peanut oil mixes was altered from its typical values to exclude 20:0 and 22:0 for comparison purposes. The other peanut oil mix included 20:0 and 22:0 but these mass fractions were lumped with the values for 18:0 for calculation purposes since no viscosity values were available for them. All other simulations required less than 1% of these fatty acids which had a no effect on the viscosity of the mixture.

Table 6.1.2.2 shows the predicted and measured viscosities along with the mass fractions of the simulated vegetable oil fatty acid methyl esters. The errors on predicting the viscosities of all the simulated oils were less than 2% with the highest absolute error being 0.06 mPa.s. The peanut oil sample with the mass fractions of its 20:0 and 22:0 lumped together with 18:0 had a 1.5% error compared with a 0.3% error for the sample with those two components excluded. Although the error obtained by lumping the three components together is higher than the sample without 20:0 and 22:0, this error is well within an acceptable limit and is comparable with the errors obtained with the other simulations. Since all the errors were within acceptable limits it was concluded that, for practical purposes, the logarithmic equation (Equation 5.1.1.1) was applicable for predicting the viscosities of methyl and ethyl esters of multi-component fatty acid ester mixtures used as biodiesel fuels.

Table 6.1.2.1 Viscosities of Binary, Ternary and Quaternary Mixtures of Fatty Acid Ethyl Ester GC Standards at 25°C

Sample #	Fatty Acid Ethyl Esters Mass Fraction				Measured	Predicted	Error	Percent
	18:1	12:0	10:0	8:0	Viscosity (mPa.s)	Viscosity (mPa.s)	(mPa.s)	Error
1	1.00	5.50
2	...	1.00	2.88
3	1.00	...	1.99
4	1.00	1.37
5	0.52	0.48	1.67	1.66	0.01	0.60%
6	...	0.50	...	0.50	1.91	1.98	-0.07	-3.66%
7	...	0.50	0.50	...	2.39	2.39	0.00	0.00%
8	0.25	0.75	1.51	1.5	0.01	0.66%
9	0.75	0.25	1.82	1.81	0.01	0.55%
10	...	0.25	...	0.75	1.62	1.65	-0.03	-1.85%
11	...	0.75	...	0.25	2.32	2.39	-0.07	-3.02%
12	...	0.25	0.75	...	2.19	2.19	0.00	0.00%
13	...	0.74	0.26	...	2.62	2.62	0.00	0.00%
14	...	0.34	0.33	0.33	1.94	1.99	-0.05	-2.58%
15	...	0.25	0.25	0.51	1.77	1.81	-0.04	-2.26%
16	...	0.19	0.54	0.27	1.91	1.93	-0.02	-1.05%
17	...	0.50	0.25	0.25	2.12	2.18	-0.06	-2.83%
18	0.25	0.25	0.25	0.25	2.51	2.57	-0.06	-2.39%
19	0.52	0.16	0.16	0.16	3.31	3.38	-0.07	-2.11%
20	0.16	0.51	0.16	0.16	2.62	2.67	-0.05	-1.91%
21	0.16	0.16	0.51	0.16	2.32	2.35	-0.03	-1.29%
22	0.16	0.16	0.16	0.51	2.01	2.06	-0.05	-2.49%

Table 6.1.2.2 Viscosities and Mass Fraction of Simulated Vegetable Oil Methyl Esters at 40 °C - (using measured viscosities of pure components)

Fatty Acid ME	Viscosity (mPa.s)	Simulated Vegetable Oil Methyl Esters - Component Mass Fraction						
		Coconut	Palm	Rapeseed	Peanut	Soybean	Canola	*Peanut#2
8:0	0.99	0.078	0.001	0.000	0.000	0.000	0.000	0.000
10:0	1.40	0.070	0.001	0.000	0.000	0.000	0.000	0.000
12:0	1.95	0.466	0.009	0.000	0.000	0.000	0.000	0.000
14:0	2.69	0.182	0.013	0.000	0.000	0.002	0.002	0.000
16:0	3.60	0.092	0.441	0.029	0.106	0.102	0.037	0.104
18:0	4.74	0.028	0.051	0.025	0.010	0.046	0.024	0.033
18:1	3.73	0.068	0.384	0.128	0.499	0.222	0.600	0.529
18:2	3.05	0.017	0.095	0.116	0.334	0.546	0.218	0.327
18:3	2.65	0.000	0.004	0.085	0.005	0.082	0.113	0.005
20:0	...	0.000	0.000	0.000	0.013	0.000	0.000	0.000
22:0	...	0.000	0.000	0.000	0.031	0.000	0.000	0.000
22:1	5.91	0.000	0.000	0.617	0.002	0.000	0.005	0.002
Measured Viscosity (mPa.s)		2.15	3.59	4.70	3.57	3.26	3.45	3.51
Predicted Viscosity (mPa.s)		2.19	3.59	4.72	3.51	3.27	3.45	3.50
Error (mPa.s)		-0.04	0.00	-0.03	0.29	-0.01	0.00	0.01
Percent Error		-2.04%	-0.08%	-0.57%	1.49%	-0.24%	0.11%	0.31%

*Peanut #2 has no 22:0 and 20:0

()⁰ - Mass fraction after being lumped with 18:0

6.1.3 Prediction of the Viscosities of Vegetable Oil Biodiesel Fuels

Five naturally occurring vegetable oils were chosen for viscosity analysis based on their availability and their use as biodiesel fuels. These oils were canola, soya, palm, coconut and peanut. Coconut, palm and peanut oils are not commonly used as biodiesel fuels but are common oils in tropical climates where biodiesel has its highest potential. Rapeseed oil, which is widely used in Europe, was unavailable at the time this study was carried out. Soya and canola oils are used in the USA and Canada. The methyl esters of these oils were produced using the transesterification procedure described in Chapter 4 and their fatty acid composition was determined by gas chromatography analysis after transesterification. A “Perkin-Elmer” model 8420 capillary gas chromatograph was used. The methyl esters were also heated to 100 °C under nitrogen and then filtered through a “Reeve Angel” grade 202 coarse paper filter to remove any sediments in the oil that were carried over from the oil extraction process. At 100 °C all of the oil’s fatty acids would have been very fluid, making it easy for them to pass through the coarse filter.

For the purpose of predicting the viscosities of the vegetable oil biodiesel fuels produced, the relationship between the fatty acid methyl ester GC standards and the naturally occurring fatty acid methyl esters needed to be verified. Verification was required because there were several anomalies with the surface tension of some of the GC standards, as will be discussed in section 6.2.1. Verification also need to be carried out because small variations in the viscosities of the GC standards, with respect to the actual viscosities of the natural components, would accumulate in the mixture equations and result in erroneous predictions. Group contribution methods [Reid *et al.*, 1987] were reported to have wide ranging errors and thus were considered unreliable for predicting the viscosities of the components of the naturally occurring vegetable oil methyl esters. Swern (1979) has a complete listing of kinematic viscosities for 8:0 to 18:0, 18:1 to 18:3, and 22:1 at 40 °C. It was therefore decided

to compare these viscosities with the dynamic viscosities measured in this study. The densities used for the conversion of the kinematic viscosities to dynamic viscosities were the same as those used for the rolling-ball viscometer. A comparison of these two sets of data showed that the values measured in this study were 2-6% lower than that reported by Swern (1979). The two data sets, however, had the same trends for both saturated and unsaturated fatty acids. Since there were anomalies with some of the GC standards and the relationship between the GC standards and the naturally occurring vegetable oil methyl esters could not be verified in any other manner, it was decided to use the values reported by Swern (1979) as an independent data set for the components of the naturally occurring vegetable oil biodiesel fuels. (An independent set was also used for surface tension) Appendix D gives the viscosities of the natural oils predicted using the measured viscosities of the GC standards. This independent data set, however, does not affect the viscosities used in the simulated mixtures since the esters used in those mixes were not from natural sources. Those simulated mixtures were used for the purpose of verifying the applicability of the mixture equation whereby the measured viscosities of the individual components were used in the equations. The individual viscosities of the GC standards used, however, may not be an accurate representation of naturally occurring vegetable oil methyl ester components due to the anomalies found.

The biodiesel fuels produced contained minor quantities of some fatty acid methyl esters whose viscosities were not available. To approximate for these components, their mass fractions were lumped together with a component that had a comparable carbon-number and saturation. The higher saturates 24:0, 22:0, and 20:0, which occurred in minor quantities, were lumped together with 18:0. The unsaturates 20:1 and 16:1 were lumped together with 18:1.

A check was made to ensure that the presence of these higher saturates in the vegetable oil esters did not result in fluids that were significantly non-Newtonian at the test temperature. All of the methyl esters produced were subjected to controlled, variable shear stress viscosity measurements on the rolling-ball viscometer and the effective shear rate was determined as a function of the rolling time. The effective shear rate and effective shear stress for a rolling-ball viscometer [Briscoe *et al.*, 1992] are given in Equations 6.1.3.1 and 6.1.3.2 respectively:

$$\dot{\gamma}_E = \frac{\text{Mean Velocity of Ball}}{\text{Mean Gap (area based)}} = \frac{4 d V}{(D^2 - d^2)} \quad (6.1.3.1)$$

$$\tau_E = d (\Delta\rho) g \sin(\theta) \quad (6.1.3.2)$$

where:

- $\dot{\gamma}_E$ = equivalent shear rate (1/s)
- τ_E = equivalent shear stress (Pa)
- D = capillary diameter (m)
- d = ball diameter (m)
- V = rolling velocity of ball (m/s)
- $\Delta\rho$ = difference in density between ball and fluid (kg/m³)
- θ = angle of inclination of capillary
- g = acceleration due to gravity (m/s²)

The viscometer measures the rolling time of the ball over a fixed distance. This distance was not known for the instrument used in these tests, therefore, the effective shear rate was converted to an effective shear rate per unit rolling distance and is given in Equation 6.1.3.3.

$$\dot{\gamma}_L = \frac{4 d}{(D^2 - d^2) t} \quad (6.1.3.3)$$

where:

$\dot{\gamma}_L$ = equivalent shear rate per unit length (1/m.s)

t = rolling time of ball (s)

For every fuel type tested, a plot of the equivalent shear stress versus the equivalent shear rate per unit length was made (Figure 6.1.3.1). Linear regression lines were then fitted to these points. It can be seen that all the data points fall on their regression line and that these lines pass through a point very close to the origin (Figure 6.1.3.1). These fuels can therefore be considered to behave in a Newtonian manner at 40 °C which means that the higher saturates present in some of the oils did not significantly affect their viscosity characteristic. Apart from their essentially Newtonian behaviour, some of these fuels exhibited a slight “Bingham-plastic” behaviour with a very small shear stress (yield stress) at which no flow occurs. The Bingham-plastic nature was more pronounced for peanut, palm and coconut oils as can be seen from Figure 6.1.3.2 which is a plot of shear stress versus shear rate on a log-log scale. The curves for peanut, palm and coconut deviated from a line which had a slope approximately equal to 1 (0.993) to a curve that tailed off asymptotically parallel to the x-axis. This is typical of Bingham-plastic materials. During the application of these vegetable oil methyl ester fuels, the shear stresses encountered are much higher than the yield stresses observed. Therefore, these fuels can be considered to behave in a Newtonian manner for practical purposes.

The viscosities predicted using the component viscosities taken from Swern (1979) (Figure 6.1.3.3) and with some of the mass fractions lumped were all within 2.8% of the measured viscosities, except for coconut oil which had a 5.7% error (Table 6.1.3.1). The results of the

TLC-FID analysis, given in Table 6.1.3.2, shows that all of the oils contained 98% or more methyl esters except for coconut oil which contained approximately 95% methyl esters with the other 5% being one or a combination of monoglycerides, diglycerides, sterols or polar lipids.

Mono- and di-glycerides were not available for analysis and therefore tests were conducted to establish what were the effects of small amounts of triglycerides on the viscosity of methyl esters. Canola oil, which was readily available, was used in these tests. Canola oil (triglycerides - TG) in mass fraction of 1%, 2%, 4% and 6% were respectively added to canola oil ME. It was found that 1% TG in the ME resulted in a 1.5% increase in viscosity; 2% gave a 3.8% increase; 4% gave a 7.8% increase; and 6% resulted in an 11.8% increase in the viscosity of the mixture. Surface tension was unaffected at all TG levels. The results of these tests, when compared with the error obtained for coconut oil ME, show that mono- and di-glycerides may have similar effects on the viscosity of the fuel. Thus, these results serve to explain why the measured viscosity of coconut oils was 5.8% higher than its predicted viscosity compared with an average 2.1% error for the other oils.

For comparison purposes fatty acid compositions given by Ackman (1996) for coconut, palm, peanut and conola oils were applied to the mixture equation to establish whether or not the viscosities predicted would be in the range of the viscosities measured in this study. Table 6.1.3.3 summarizes these results where it can be seen that all the viscosities were predicted within 3.3% of the measured viscosities.

It is therefore clear from the various results above that the viscosities of biodiesel fuels can be predicted with good accuracy from their fatty acid composition using a logarithmic equation (Equation 5.1.1.1).

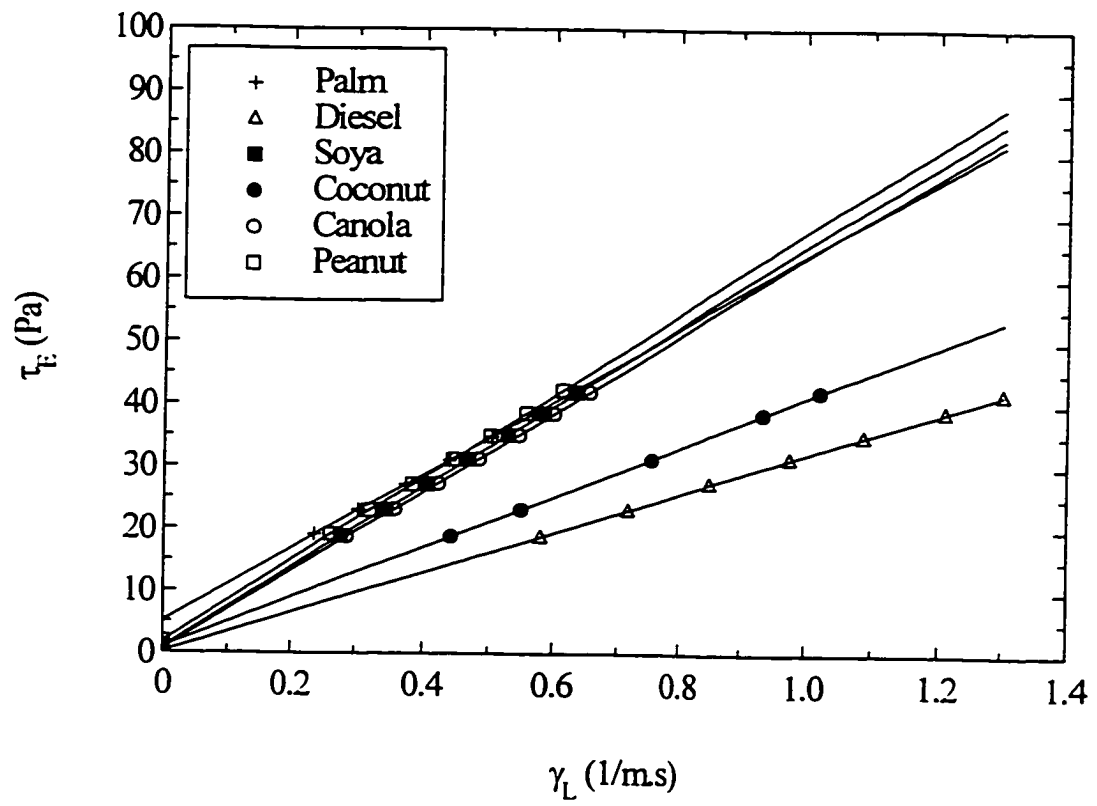


Figure 6.1.3.1 Rheograms for Vegetable Oil Methyl Ester Biodiesel Fuels at 40 °C Plotted on a Linear Scale

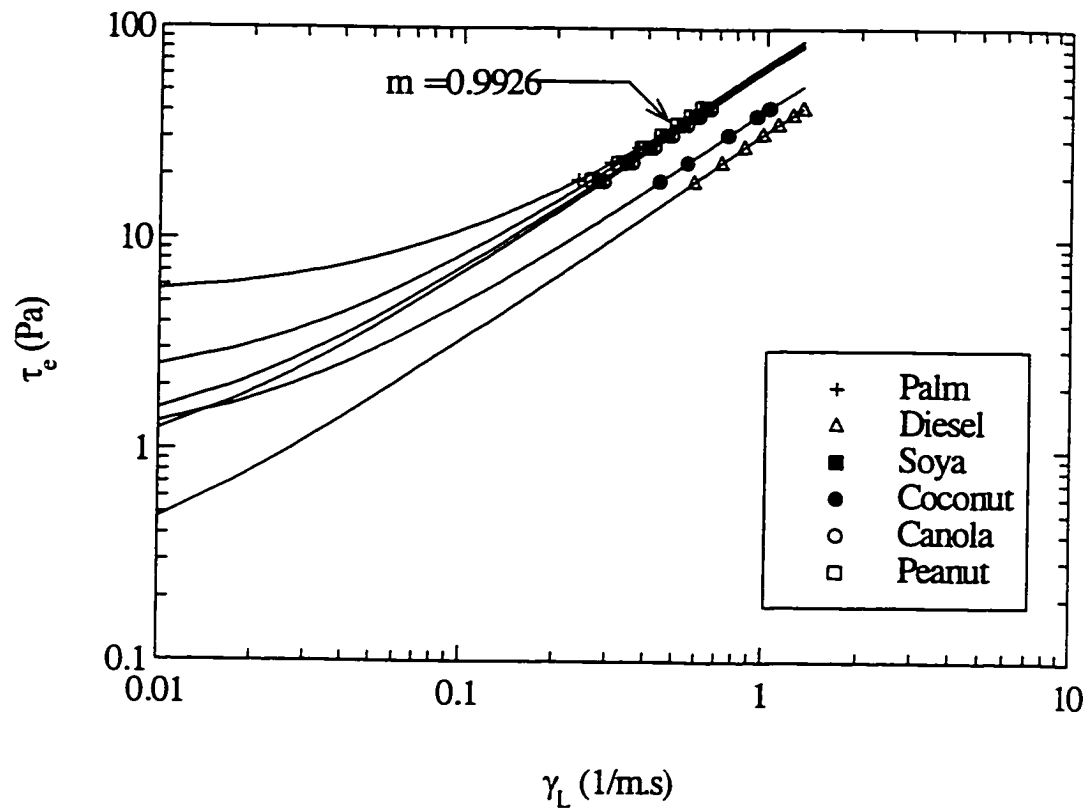


Figure 6.1.3.2 Rheograms for Vegetable Oil Methyl Ester Biodiesel Fuels at 40 °C Plotted on a Log Scale

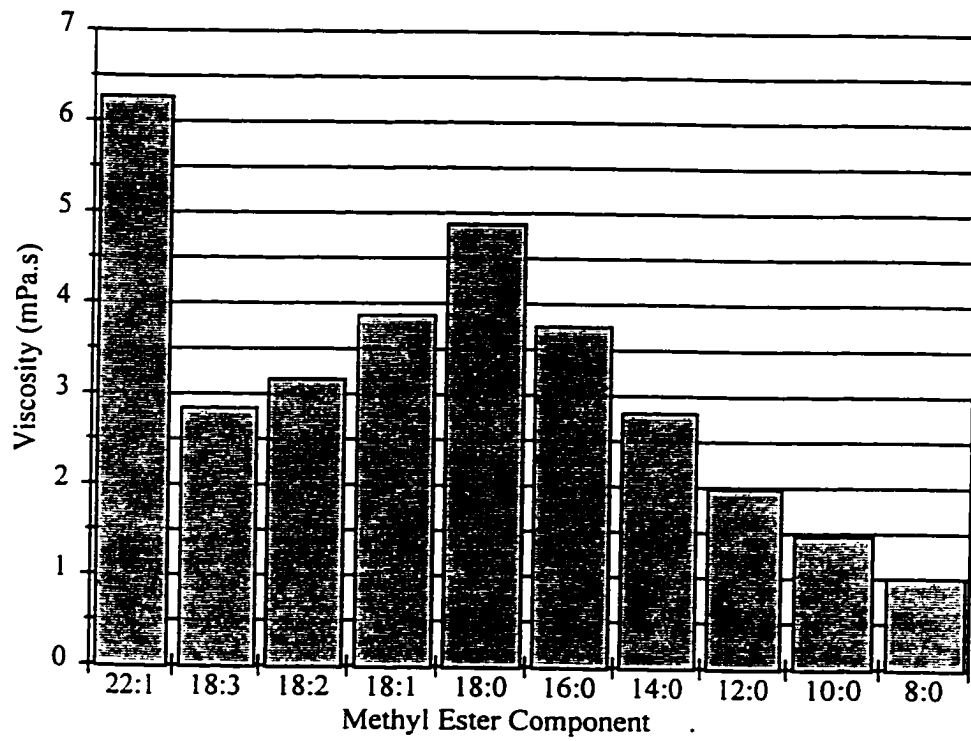


Figure 6.1.3.3 Viscosities of Pure Methyl Ester Biodiesel Fuel Components at 40 °C [Swern, 1979)

Table 6.1.3.1 Viscosities of Methyl Ester Biodiesel Fuels at 40 °C - (using viscosities of pure components taken from Swern (1979) and lumped mass fractions)

Fatty Acid ME	Viscosity (mPa.s)	Methyl Ester Component Mass fraction				
		Coconut	Peanut	Soya	Palm	Canola
24:0	...	0.000	0.035	0.000	0.000	0.000
		...	(0.000) ⁰	(0.000) ⁰
22:1	6.27	0.000	0.000	0.000	0.000	0.000
22:0	...	0.000	0.024	0.000	0.000	0.001
		...	(0.000) ⁰	(0.000) ⁰	...	(0.000) ⁰
20:1	...	0.000	0.014	0.016	0.001	0.021
		...	(0.000) ¹	(0.000) ¹	(0.000) ¹	(0.000) ¹
20:0	...	0.002	0.013	0.007	0.003	0.012
		...	(0.000) ⁰	(0.000) ⁰	(0.000) ⁰	(0.000) ⁰
18:3	2.84	0.000	0.010	0.096	0.002	0.112
18:2	3.17	0.014	0.301	0.199	0.080	0.213
18:1	3.87	0.055	0.466	0.600	0.373	0.574
		...	(0.485)	(0.623)	(0.377)	(0.599)
18:0	4.88	0.019	0.027	0.017	0.040	0.020
		...	(0.099)	(0.023)	(0.042)	(0.033)
16:1	...	0.000	0.004	0.008	0.003	0.004
		...	(0.000) ¹	(0.000) ¹	(0.000) ¹	(0.000) ¹
16:0	3.76	0.073	0.105	0.058	0.481	0.042
14:0	2.81	0.171	0.000	0.000	0.013	0.000
12:0	1.98	0.533	0.000	0.000	0.004	0.000
10:0	1.47	0.060	0.000	0.000	0.000	0.000
8:0	1.01	0.075	0.000	0.000	0.000	0.000
Measured Viscosity (mPa.s)		2.32	3.77	3.67	3.87	3.70
Predicted Viscosity (mPa.s)		2.19	3.71	3.62	3.76	3.61
Error (mPa.s)		0.13	0.06	0.05	0.11	0.09
Percent Error		5.72%	1.71%	1.25%	2.76%	2.50%

()⁰ - mass fraction after being lumped with 18:0

()¹ - mass fraction after being lumped with 18:1

Table 6.1.3.2 Biodiesel Fuel Methyl Ester Composition Obtained by TLD-FID Analysis

Oil Type	Component Type	Percent Composition
Soya	ME	99.76%
	TG&FFA	0.00%
	Others	0.24%
	Total	100.00%
Peanut	ME	99.81%
	TG&FFA	0.00%
	Others	0.19%
	Total	100.00%
Coconut	ME	95.01%
	TG&FFA	0.00%
	Others	4.99%
	Total	100.00%
Canola	ME	100.00%
	TG&FFA	0.00%
	Others	0.00%
	Total	100.00%

Table 6.1.3.3 Viscosities of Methyl Ester Biodiesel Fuels at 40 °C - {using viscosities of pure components taken from Swern (1979) and mass fractions taken from Ackman (1996)}

Fatty Acid ME	Viscosity (mPa.s)	Methyl Ester Component			
		Mass fraction			
		Coconut	Peanut	Palm	Canola
24:0	...	0.000	0.018	0.001	0.002
		...	(0.000) ⁰	(0.000) ⁰	(0.000) ⁰
22:1	6.27	0.000	0.002	0.000	0.005
22:0	...	0.000	0.033	0.001	0.004
		...	(0.000) ⁰	(0.000) ⁰	(0.000) ⁰
20:1	...	0.000	0.015	0.001	0.017
		...	(0.000) ¹	(0.000) ¹	(0.000) ¹
20:0	...	0.002	0.013	0.002	0.007
		...	(0.000) ⁰	(0.000) ⁰	(0.000) ⁰
18:3	2.84	0.000	0.005	0.003	0.111
18:2	3.17	0.017	0.329	0.095	0.210
18:1	3.87	0.069	0.455	0.387	0.583
		...	(0.471)	(0.390)	(0.603)
18:0	4.88	0.029	0.025	0.045	0.018
		...	(0.089)	(0.049)	(0.031)
16:1	...	0.000	0.001	0.002	0.003
		...	(0.000) ¹	(0.000) ¹	(0.000) ¹
16:0	3.76	0.092	0.104	0.439	0.039
14:0	2.81	0.183	0.000	0.013	0.001
12:0	1.98	0.473	0.000	0.009	0.000
10:0	1.47	0.060	0.000	0.001	0.000
8:0	1.01	0.077	0.000	0.001	0.000
Measured Viscosity (mPa.s)		2.32	3.77	3.87	3.7
Predicted Viscosity (mPa.s)		2.27	3.69	3.74	3.62
Error (mPa.s)		0.05	0.08	0.13	0.08
Percent Error		2.36%	2.23%	3.32%	2.27%

()⁰ - mass fraction after being lumped with 18:0

()¹ - mass fraction after being lumped with 18:1

6.2 Surface Tension

6.2.1 Surface Tension of Methyl and Ethyl Ester GC Standards

Samples prepared for viscosity measurements were also used for surface tension measurements. When the surface tension of palmitic acid ethyl ester GC standard (16:0 EE) was measured at 40 °C a sharp deviation from the typical trend for the saturated esters was observed (Figure 6.2.1.1). This, however, did not occur with 16:0 methyl ester. When this irregularity was first observed, a new batch of 16:0 EE GC standard with a different lot number was acquired from the supplier but the same result was obtained when its surface tension was measured. Gas Chromatography (GC) and Thin Layer Chromatography with Flame Ionization Detection (TLC-FID) analyses were carried out to verify the purity of the samples, but all results showed only one sharp peak. A 15 mL sample was then heated at 200 °C under nitrogen for 15 minutes to remove any volatile impurities that may have missed the GC output. The surface tension was re-tested and the same low value was observed. All verification procedures available at the time were exhausted but there was no answer to this problem.

Apart from 16:0 EE, the surface tension of saturated fatty acid esters (Figure 6.2.1.2), like viscosity, increased with increase in carbon number. For methyl esters this trend was curvilinear, however, the data for ethyl esters had more random variation and the trend was more or less a linear one, excluding the effect of 16:0 EE. The surface tension of saturated methyl esters compared well with data given by Swern (1979) as shown in Table 6.2.1.1. No surface tension data for ethyl esters were found for the test temperature. Given the fact that the measured surface tension for methyl esters followed a trend line closely and compared well with data in the literature, it is believed that the ethyl esters GC standards used in these

experiments had some peculiarity which caused a relatively high random variation and in the case of 16:0 a seemingly erroneous result.

Some of the variations in the measured surface tension can be attributed to the lesser degree of control one had over some of the measurement parameters. The temperature at the surface and the vapor pressure above the surface were difficult to maintain and control with the “Du Nouy Ring” Surface Tension Meter used. The point at which the surface broke was subject to judgement and errors and/or variations in ascertaining the exact break point most likely occurred. Taking all these factors into consideration it is estimated that the accuracy of the method for determining the surface tension, the Du Nouy ring method, was within ± 0.5 mN/m.

When the GC standard unsaturated esters were tested a very pronounced deviation from the viscosity trend for saturated esters was observed when 18:0 became unsaturated to 18:1 (Figure 6.2.1.1). As the degree of unsaturation progressed to 18:2 and 18:3 the surface tension increased (Figure 6.2.1.1) rather than continue to decrease as was the case with viscosity. For methyl esters the surface tension of 18:3 was found to be higher than its saturate 18:0. There was also a significant difference between the measured surface tension for erucic acid (22:1) methyl ester compared with 22:1 ethyl ester. No data was found in the literature to confirm the seemingly high value for 18:3 ME, the large drop in surface tension from 18:0 to 18:1, and also the large difference between 22:1 ME and EE.

Evidently, there is a counter effect of the number of double bonds with respect to viscosity compared to surface tension. While increasing the number of double bonds decreased the viscosity, an increase in surface tension was observed.

Table 6.2.1.1 Surface Tension of Saturated Methyl Esters at 40 °C

Carbon Number	Surface Tension Measured (mN/m)	Surface Tension [Swern, 1979] (mN/m)	Difference (mN/m)
8:0	25.4	25.2	0.20
10:	26.3	26.1	0.20
12:0	27.2	27	0.20
14:0	27.9	27.8	0.10
16:0	28.4	28.4	0.00
18:0	29	29.1	-0.10

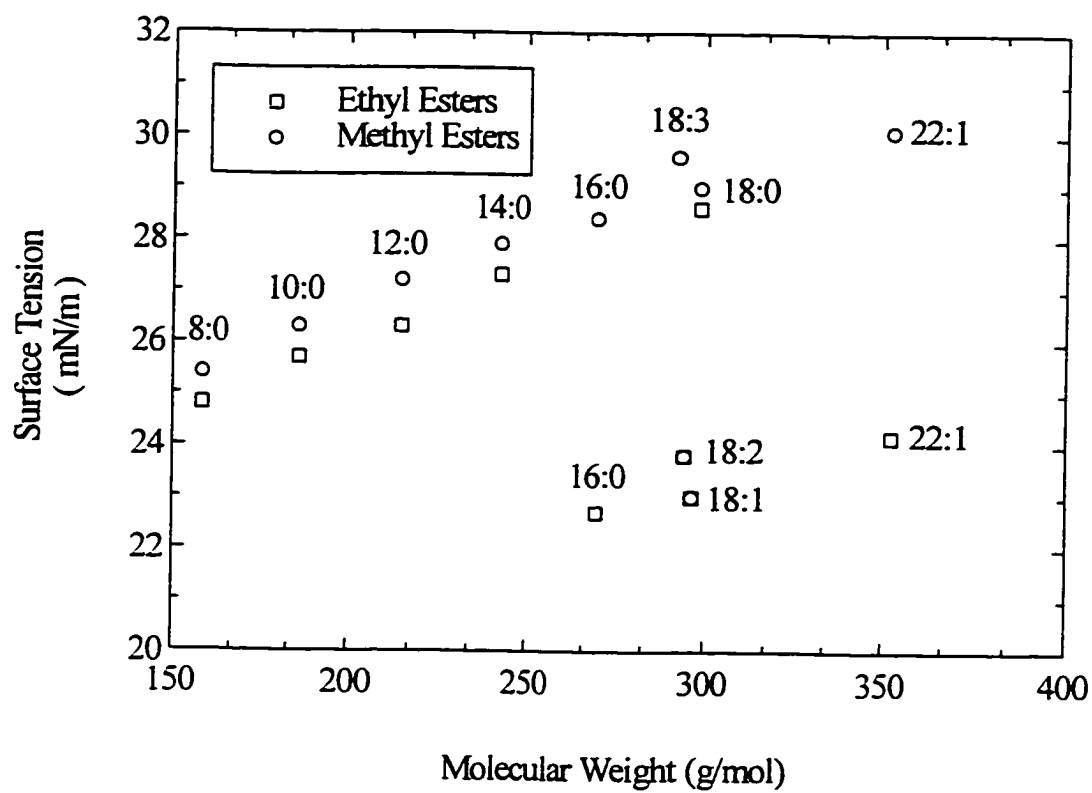


Figure 6.2.1.1 Surface Tension of Fatty Acid Methyl and Ethyl Ester GC Standards at 40°C

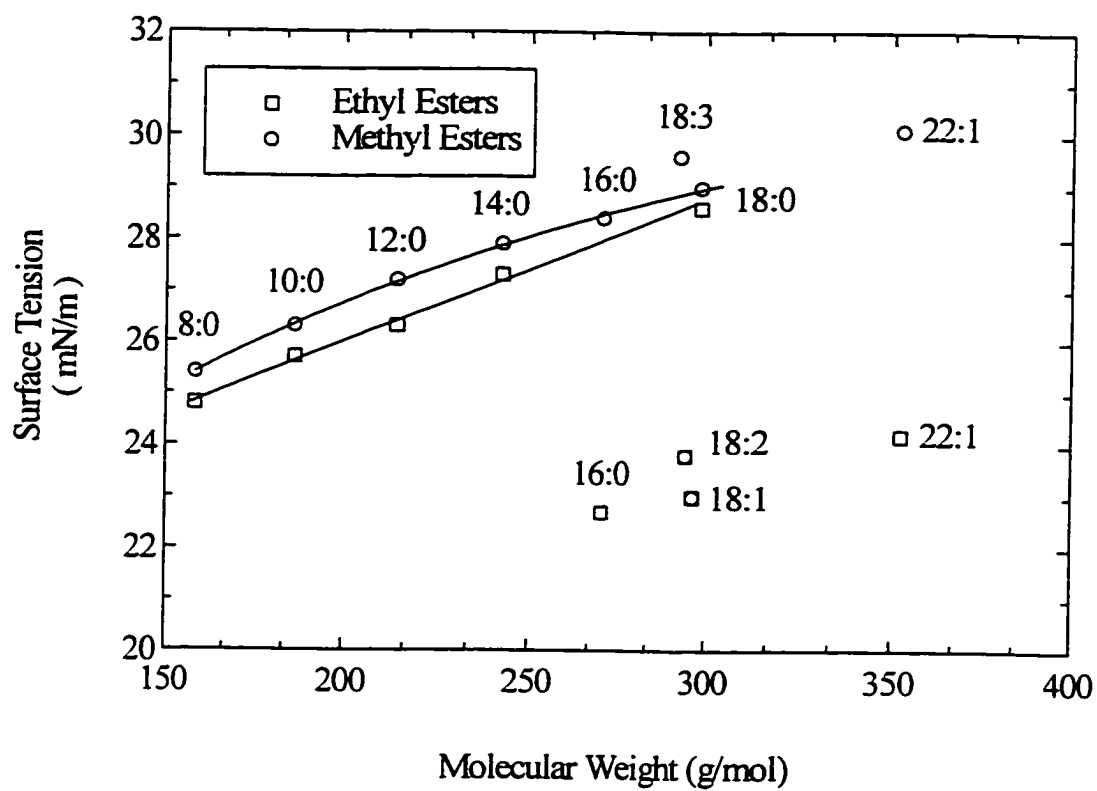


Figure 6.2.1.2 Surface Tension Trend Lines for Saturated Methyl and Ethyl Ester GC Standards at 40 °C

6.2.2 Surface Tension of Mixtures of Methyl and Ethyl Ester GC Standards

Binary, ternary and quaternary mixtures of 18:1, 12:0, 10:0 and 8:0 ethyl ester GC standards in varying proportions were used to test the concept of using a Dalton type mass average equation for predicting the surface tension of mixtures of esters. Table 6.2.2.1 summarizes these results and it can be seen that all errors on predicting the surface tension of these mixtures at 25 °C were less than 3.25%. It was therefore decided to extend the analysis to more complicated mixtures.

The simulated vegetable oils used for viscosity measurements were also used for surface tension measurements. Table 6.2.2.2 shows the results of predicting the surface tension of the simulated rapeseed, palm, canola, peanut, soybean and coconut oil methyl esters at 40 °C. The prediction errors were all negative and ranged from -0.36 to -1.4 mN/m or -1.5 to -5.9%. Due to the fact that all errors were negative, an alternative model was derived (see Chapter 5) based on a weighted mass average method. Errors using this method became more random and were also reduced to 0.04 - 1.01 mN/m or 0.70 - 4.3%. It is thus clear from these results that the weighted mass average method worked better for the mixtures simulating the above mentioned vegetable oil esters.

Table 6.2.2.1 Surface Tension of Binary, Ternary and Quaternary Mixtures of Fatty Acid Ethyl Ester GC Standards at 25°C

Sample	Fatty Acid Mass Fraction				Measured	Predicted	Percent	
	18:1	12:0	10:0	8:0	Surface Tension (mN/m)	Surface Tension (mN/m)	Error (mN/m)	Error
1	1.00	23.6
2	...	1.00	27.0
3	1.00	...	27.0
4	1.00	26.2
5	0.52	0.48	26.5	26.6	-0.12	-0.43%
6	...	0.54	...	0.46	27.0	26.6	0.32	1.18%
7	...	0.50	0.50	...	27.0	27.0	0.00	0.00%
8	0.25	0.75	26.5	26.4	0.10	0.38%
9	0.75	0.25	27.0	26.8	0.20	0.74%
10	...	0.25	...	0.75	26.7	26.4	0.30	1.12%
11	...	0.75	...	0.25	27.7	26.8	0.90	3.25%
12	...	0.25	0.75	...	27.6	27.0	0.55	2.00%
13	...	0.74	0.26	...	27.9	27.0	0.90	3.23%
14	...	0.34	0.33	0.33	27.3	26.7	0.57	2.08%
15	...	0.25	0.25	0.51	27.0	26.6	0.40	1.50%
16	...	0.19	0.54	0.27	27.3	26.8	0.51	1.88%
17	...	0.50	0.25	0.25	27.4	26.8	0.60	2.19%
18	0.25	0.25	0.25	0.25	25.4	25.9	-0.54	-2.11%
19	0.52	0.16	0.16	0.16	25.1	25.1	0.00	0.02%
20	0.16	0.51	0.16	0.16	26.0	26.3	-0.31	-1.18%
21	0.16	0.16	0.51	0.16	26.1	26.3	-0.21	-0.82%
22	0.16	0.16	0.16	0.51	25.4	26.0	-0.64	-2.51%

Table 6.2.2.2 Surface Tension of Simulated Vegetable Oil Methyl Esters at 40 °C

Fatty Acid ME	Measured	Weight Factor	Weighted	<u>Simulated Vegetable Oil Methyl Esters</u>						
	Surface Tension (mN/m)		Surface Tension (mN/m)	<u>Component Mass Fraction</u>						
				Coconut	Palm	Rape	Peanut	Soybean	Canola	Peanut#2
8:0	25.40	0.955	24.26	0.078	0.001	0.000	0.000	0.000	0.000	0.000
10:0	26.30	0.964	25.34	0.070	0.001	0.000	0.000	0.000	0.000	0.000
12:0	27.20	0.972	26.44	0.466	0.009	0.000	0.000	0.000	0.000	0.000
14:0	27.90	0.979	27.31	0.182	0.013	0.000	0.000	0.002	0.002	0.000
16:0	28.40	0.984	27.94	0.092	0.441	0.061	0.106	0.102	0.037	0.104
18:0	29.00	0.989	28.69	0.028	0.051	0.023	0.010	0.046	0.024	0.033
18:1	22.80	0.930	21.20	0.068	0.384	0.189	0.499	0.222	0.600	0.529
18:2	23.80	0.940	23.36	0.017	0.095	0.175	0.334	0.546	0.218	0.327
18:3	29.60	0.995	29.46	0.000	0.004	0.133	0.005	0.082	0.113	0.005
20:0	0.000	0.000	0.000	0.013	0.000	0.000	0.000
22:0	0.000	0.000	0.000	0.031	0.000	0.000	0.000
22:1	30.1	1.000	30.1	0.000	0.000	0.420	0.002	0.000	0.005	0.002
Measured Surface Tension (mN/m)				26.5	24.4	26.4	23.00	23.40	23.60	23.6
Predicted Using Mass Average (MA) (mN/m)				26.93	25.81	27.42	24.11	24.78	2.17	23.96
Error (mN/m)				-0.43	-1.41	-1.02	-1.11	-1.38	-0.57	-0.36
Percent Error				-1.61%	-5.76%	-3.88%	-4.84%	-5.88%	-2.41%	-1.55%
Predicted Using MA & Weighted Surface Tension (mN/m)				26.13	24.82	26.82	22.7	23.56	22.86	22.59
Error (mN/m)				0.37	-0.42	-0.42	0.23	-0.16	0.74	1.01
Percent Error				1.40%	-1.72%	-1.58%	1.00%	-0.70%	3.16%	4.27%

Peanut#2 has no 22:0 and 20:0

()^o - Mass fraction after being lumped with 18:0

6.2.3 Prediction of the Surface Tension of Vegetable Oil Biodiesel Fuels

Methyl ester biodiesel fuels made from coconut, peanut, soya, palm and canola oils were also used for surface tension measurements. It may be recalled that the surface tension of 18:1 ME GC standard decreased by a significant amount compared with its saturate 18:0 and that there were other anomalies. It was very unlikely that the addition of just one double bond to the 18:0 chain would cause such a drastic change to that component's surface tension and, since no values were found in the literature for the surface tension for 18:1, 18:2, 18:3 and 22:1, it was decided to use an independent method of predicting the surface tension of the individual components of the biodiesel fuels.

The Sugden's Parachor method described in Chapter 5 which has been used by many authors [Reid *et al.*, 1987; Meissner and Michaels, 1949; among others] with some degree of success was selected to predict the surface tension of the individual components of the methyl ester biodiesel fuels. Table 6.2.3.1 compares the calculated surface tension using the Sugden's Parachor method with the measured values. It can be seen that 8:0 to 18:0 compared well with both the calculated and measured values giving a maximum error of only 0.16 mN/m or 0.6%. Linolenic (18:3) and erucic (22:1) also compared well with errors of 0.41 mN/m (1.4%) and 0.24 mN/m (0.8%) respectively. Oleic (18:1) and linoleic (18:2) however had errors of 5.88 mN/m (20%) and 5.57 mN/m (19%) respectively. These results show clearly that there were peculiarities with the 18:1 and 18:2 methyl ester GC standards. It was thus decided to use the surface tension calculated by the Parachor method as an independent data set for the mixture equation. This independent data set (Figure 6.2.3.1) was used to compute the surface tension of the methyl esters of the naturally occurring vegetable oils. Appendix E gives the predicted surface tension of the natural oils using the measured surface tension of the GC standards.

Table 6.2.3.2 summarizes results obtained for predicting surface tension of vegetable oil methyl ester biodiesel fuels using component viscosities calculated with the Parachor method. The errors obtained using the mixture equation and the weighted surface tension parameter ranged from 0.04 - 0.87 mN/m or 0.2 - 3.3%.

For comparison purposes, fatty acid compositions given by Ackman (1996) for coconut, palm, peanut and conola oils were applied to the mixture equation to establish whether or not the surface tension predicted would be in the range of the surface tension measured in this study. Table 6.2.3.3 summarizes these results where it can be seen that the surface tension was predicted within 3.3% of the measured surface tension for all the vegetable oil methyl ester types.

It is therefore clear from the results of the various surface tension tests that the Sudgen's Parachor and the weighted surface tension methods provided an acceptable procedure for predicting the surface tension of the biodiesel fuels based on their fatty acid composition.

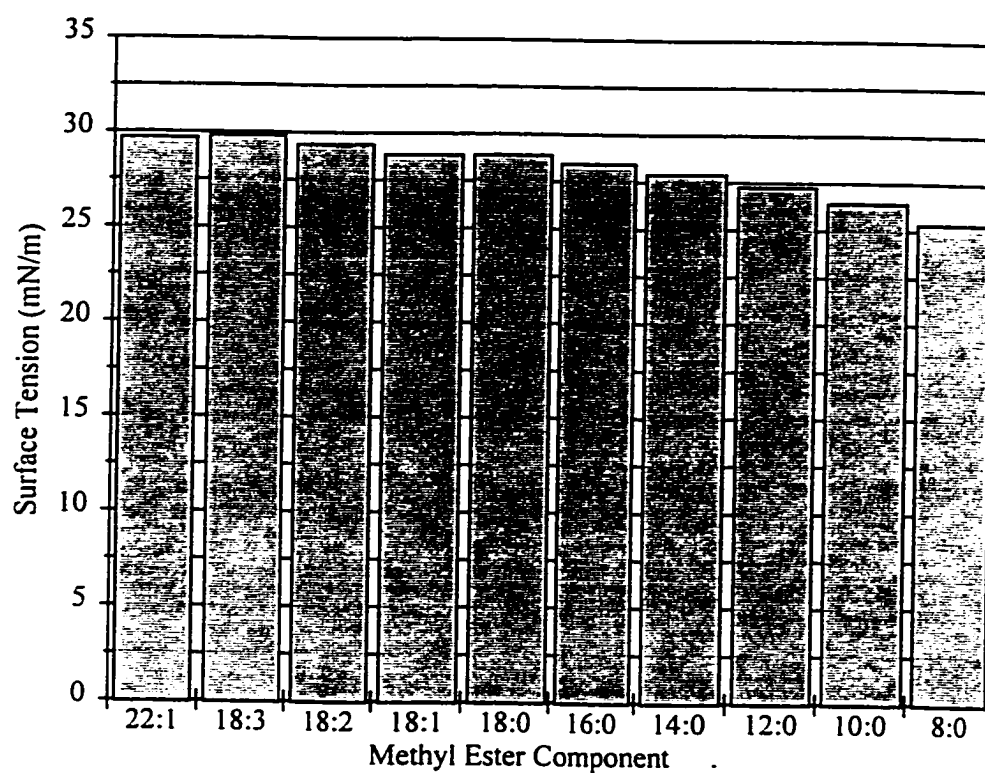


Figure 6.2.3.1 Surface Tension of Pure Methyl Ester Biodiesel Fuel Components at 40 °C
Calculated using Sugden's Parachors

Table 6.2.3.1 Surface Tension of Pure Methyl Esters Calculated Using the Sugden's Parachor

Saturates							Double Bond	Molecular		Surface Tension	Surface Tension	
CN	CH ₂	C	H	O ₂	DB	Parachor [P]	Weight g/mol	Density g/ml	Calculated mN/m	Measured mN/m	Difference mN/m	
8	6	3	6	1	0	411	158.2	0.86	25.37	25.4	0.03	
10	8	3	6	1	0	489	186.3	0.86	26.46	26.3	-0.16	
12	10	3	6	1	0	567	214.3	0.86	27.29	27.2	-0.09	
14	12	3	6	1	0	645	242.4	0.86	27.94	27.9	-0.04	
16	14	3	6	1	0	723	270.4	0.86	28.47	28.4	-0.07	
18	16	3	6	1	0	801	298.5	0.86	28.89	29.0	0.11	
20	18	3	6	1	0	879	326.6	0.86	29.26	
22	20	3	6	1	0	957	354.6	0.86	29.56	
24	22	3	6	1	0	1035	382.7	0.86	29.83	
Mono-Unsaturates												
CN	CH ₂	C	H	O ₂	DB	[P]						
16	12	5	8	1	1	712	268.4	0.87	28.36	
18	14	5	8	1	1	790	296.5	0.87	28.88	23.0	-5.88	
20	16	5	8	1	1	868	324.6	0.87	29.31	
22	18	5	8	1	1	946	352.6	0.87	29.69	30.1	0.41	
Di-Unsaturates												
CN	CH ₂	C	H	O ₂	DB	[P]						
18	12	7	10	1	2	779	294.5	0.88	29.37	23.8	-5.57	
Tri-Unsaturates												
CN	CH ₂	C	H	O ₂	DB	[P]						
18	10	9	12	1	3	768	292.5	0.89	29.84	29.6	-0.24	

Table 6.2.3.2 Surface Tension of Methyl Ester Biodiesel Fuels at 40 °C (using component surface tension calculated by the Sugden's Parachor method)

Fatty Acid ME	Calculated Surface Tension (mN/m)	Weight Factor	Weighted Surface Tension (mN/m)	Methyl Ester Component Mass Fraction				
				Coconut	Peanut	Soya	Palm	Canola
8:0	25.37	0.955	25.38	0.075	0.000	0.000	0.000	0.000
10:0	26.46	0.965	26.16	0.060	0.000	0.000	0.000	0.000
12:0	27.29	0.973	26.74	0.533	0.000	0.000	0.004	0.000
14:0	27.94	0.979	27.19	0.171	0.000	0.000	0.013	0.000
16:0	28.47	0.984	27.54	0.073	0.105	0.058	0.481	0.046
16:1	0.000	0.004	0.008	0.003	0.005
				...	(0.000) ¹	(0.000) ¹	(0.000) ¹	...
18:0	28.89	0.988	27.82	0.019	0.027	0.017	0.040	0.021
				...	(0.099)	(0.023)	(0.042)	
18:1	28.88	0.988	27.81	0.055	0.466	0.600	0.373	0.618
				...	(0.485)	(0.623)	(0.377)	...
18:2	29.37	0.993	28.13	0.014	0.301	0.199	0.080	0.189
18:3	29.84	0.998	28.43	0.000	0.010	0.096	0.002	0.097
20:0	0.002	0.013	0.007	0.003	0.007
				(0.000) ⁰	(0.000) ⁰	(0.000) ⁰	(0.000) ⁰	(0.000) ⁰
20:1	0.000	0.014	0.016	0.001	0.017
				...	(0.000) ¹	(0.000) ¹	(0.000) ¹	(0.000) ¹
22:0	0.000	0.024	0.000	0.000	0.000
				...	(0.000) ⁰	(0.000) ⁰
22:1	29.69	0.996	28.33	0.000	0.000	0.000	0.000	0.000
24:0	0.000	0.035	0.000	0.000	0.000
				...	(0.000) ⁰	(0.000) ⁰
Measured Surface Tension (mN/m)				26.11	28.79	28.2	28.5	27.88
Predicted ST (Mass Average) (mN/m)				27.44	28.99	29.05	28.71	29.07
Error (mN/m)				-1.33	-0.2	-0.85	-0.21	-1.19
Percent Error				5.09%	-0.69%	-3.01%	-0.74%	-4.27%
Predicted ST (Weighted Mass Average)				26.75	28.69	28.75	28.32	28.79
Error (mN/m)				-0.64	0.1	-0.55	0.18	-0.91
Percent Error				-2.45%	0.35%	-1.95%	0.63%	-3.26%

Table 6.2.3.3 Surface Tension of Methyl Ester Biodiesel Fuels at 40 °C (using mass fractions given by Ackman (1996) and component surface tension calculated by the Sugden's Parachor method)

Fatty Acid ME	Calculated Surface Tension (mN/m)	Weight Factor	Weighted Surface Tension (mN/m)	Methyl Ester Component Mass Fraction			
				Coconut	Peanut	Palm	Canola
8:0	25.37	0.955	25.38	0.077	0.000	0.001	0.000
10:0	26.46	0.965	26.16	0.06	0.000	0.001	0.000
12:0	27.29	0.973	26.74	0.473	0.000	0.009	0.000
14:0	27.94	0.979	27.19	0.183	0.000	0.013	0.001
16:0	28.47	0.984	27.54	0.092	0.104	0.439	0.039
16:1	0.000	0.001	0.002	0.003
				...	(0.000) ¹	(0.000) ¹	(0.000) ¹
18:0	28.89	0.988	27.82	0.029	0.025	0.045	0.018
				...	(0.089)	(0.049)	(0.031)
18:1	28.88	0.988	27.81	0.069	0.455	0.387	0.583
				...	(0.471)	(0.390)	(0.603)
18:2	29.37	0.993	28.13	0.017	0.329	0.095	0.21
18:3	29.84	0.998	28.43	0.000	0.005	0.003	0.111
20:0	0.002	0.013	0.002	0.007
				(0.000) ⁰	(0.000) ⁰	(0.000) ⁰	(0.000) ⁰
20:1	0.000	0.015	0.001	0.017
				...	(0.000) ¹	(0.000) ¹	(0.000) ¹
22:0	0.000	0.033	0.001	0.004
				...	(0.000) ⁰	(0.000) ⁰	(0.000) ⁰
22:1	29.69	0.996	28.33	0.000	0.002	0.000	0.005
24:0	0.000	0.018	0.001	0.002
				...	(0.000) ⁰	(0.000) ⁰	(0.000) ⁰
Measured Surface Tension (mN/m)				26.11	28.79	28.5	27.88
Predicted ST (Mass Average) (mN/m)				27.51	29.01	28.72	29.08
Error (mN/m)				-1.4	-0.22	-0.22	-1.2
Percent Error				5.37%	-0.75%	-0.76%	-4.29%
Predicted ST (Weighted Mass Average)				26.84	28.7	28.34	28.79
Error (mN/m)				-0.73	0.09	0.16	-0.91
Percent Error				-2.78%	0.30%	0.57%	-3.27%

6.3 Atomization

6.3.1 Spray System Preliminary Results

The diesel pump used to produce the high pressure spray had an inherent problem which led to several setbacks during the initial setup period. When the pump was operated several air bubbles were seen emerging from the pump inlet through the transparent inlet hose. These bubbles were present with both diesel and biodiesel fuels whose temperatures were controlled at low levels (25 °C) to reduce their vapor pressure. It was first thought that the pump element was worn and therefore a new element was acquired. However, the same problem persisted even with thorough bleeding of the system. After attempting to debug this problem for in excess of two months using several techniques, including submerging the pump in diesel fuel during operation, applying a 35 kPa (5 psi) pressure to the supply tank, and thoroughly debugging the Malvern analyzer and electronic system, the problem persisted. The main result of this problem was that, for the same rack position, an unsteady spray was produced that caused inconsistent results from the Malvern analyzer. The distribution pattern and SMD varied from run to run with no change of settings. Measurements had to be taken at the spray tip taken because of multiple scattering effects and the problem was more pronounced there.

However, a suitable solution to the spray variation problem was found when the rack position was reduced to give a low flow. At this setting no multiple scattering effect occurred when the spray was sampled midway along its length where the spray was stable. Using this spray setting, a sequence of ten runs were done and good repeatability of the measurements were obtained. Figures 6.3.1.1, 6.3.1.2, 6.3.1.3, 6.3.1.4, 6.3.1.5 and 6.3.1.6 show the ten runs for diesel, canola ME, coconut ME, soya ME, peanut ME and palm ME respectively. Diesel

fuel, which was used as a standard, was measured before and after each biodiesel test. Procedures previously discussed in Chapter 4 were followed for all tests.

The selection of the distribution function to represent the droplet distribution of the fuels was done by comparing the three models available from the Malvern data analysis system with the 15 parameter “model independent” distribution. Figures 6.3.1.7 and 6.3.1.8 show these comparisons for diesel fuel and neat canola oil respectively. Diesel fuel is the best case scenario in terms of atomization while neat vegetable oil is the worst case scenario. The Malvern software system fits these models to the energy distribution obtained from the receiver diodes and a least square analysis is carried out to establish the goodness of fit. The model independent distribution is normally used as a first approximation since it is a 15 parameter polynomial equation which is capable of following complex data patterns. Having established the pattern of the energy distribution a two or three parameter model that suits the data best can be selected. Two or three parameter models can be readily incorporated into complex models such as combustion models. The log-difference (Equation 6.3.1.1) is used as a guide to the selection of a model and the lower the log-difference the better the model fits the data. Ideally the log-difference of a model should be below 5.5, but as a “rule-of-thumb” a log-difference with a similar or better value than the log-difference of the model independent distribution is desired [Meyer and Chigier, 1986].

$$\text{log-difference} = \log \sum (\text{light calculated} - \text{light measured})^2 \quad (6.3.1.1)$$

It can be seen that with both diesel fuel and neat canola oil the Rosin-Rammler model [Meyer and Chigier, 1986] compared well with the model independent distribution. Table 6.3.1.1 shows the log-difference and the SMD computed by the Malvern software system for each model using diesel fuel. Of the three two-parameter models, the Rosin-Rammler had the best

log-difference which was comparable with the log-difference for the model independent distribution; thus, this model was selected to represent the droplet distribution of all the tests carried out in these studies. To verify the suitability of the Rosin-Rammler model, the log of the computed distribution versus the droplet diameter were plotted on a log-log scale. This plot is shown in Figure 6.3.1.9 where it can be seen that a linear line was achieved for both diesel fuel and canola oil ME. This verifies the suitability of the Rosin-Rammler distribution for modeling the distribution of biodiesel and diesel fuels. As noted previously, the Rosin-Rammler model is conventionally used for droplets [Meyer and Chigier, 1986].

Table 6.3.1.1 Comparison of Log-Differences for Four Droplet Distribution Models (taken at spray tip for medium flow pump rack position)

<u>Diesel Fuel</u>			
<u>Model</u>	<u>SMD</u>	<u>Log-Diff</u>	<u>Obscuration</u>
Model Independent	18.19	3.7	0.27
Rosin- Rammler	17.13	3.88	0.27
Normal	17.08	5.72	0.27
Log-Normal	19.58	4.42	0.27
<u>Canola Oil Fuel</u>			
<u>Model</u>	<u>SMD</u>	<u>Log-Diff</u>	<u>Obscuration</u>
Model Independent	34.38	3.75	0.16
Rosin- Rammler	35.57	4.52	0.16
Normal	31.17	5.96	0.16
Log-Normal	41.50	5.19	0.16

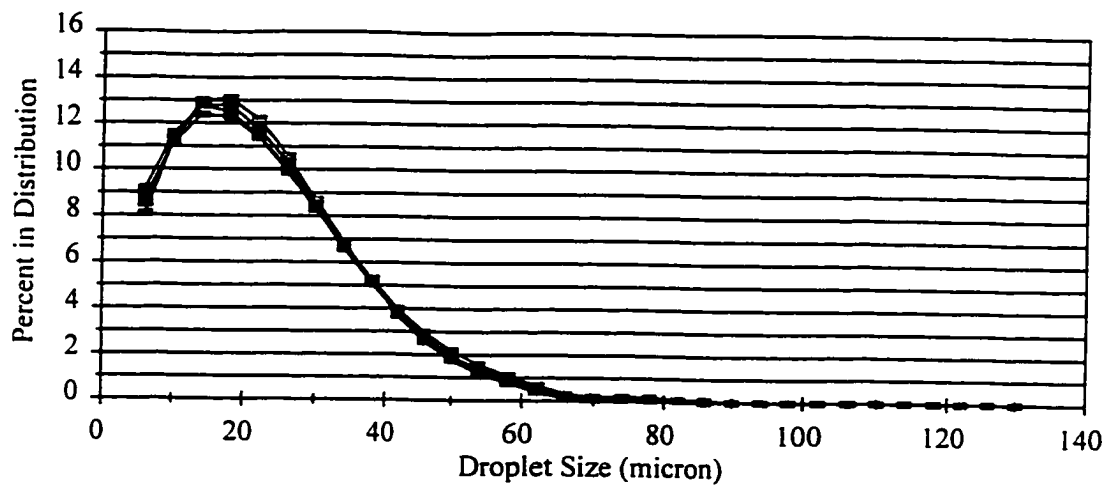


Figure 6.3.1.1 Diesel Fuel Droplet Distribution for Ten Runs

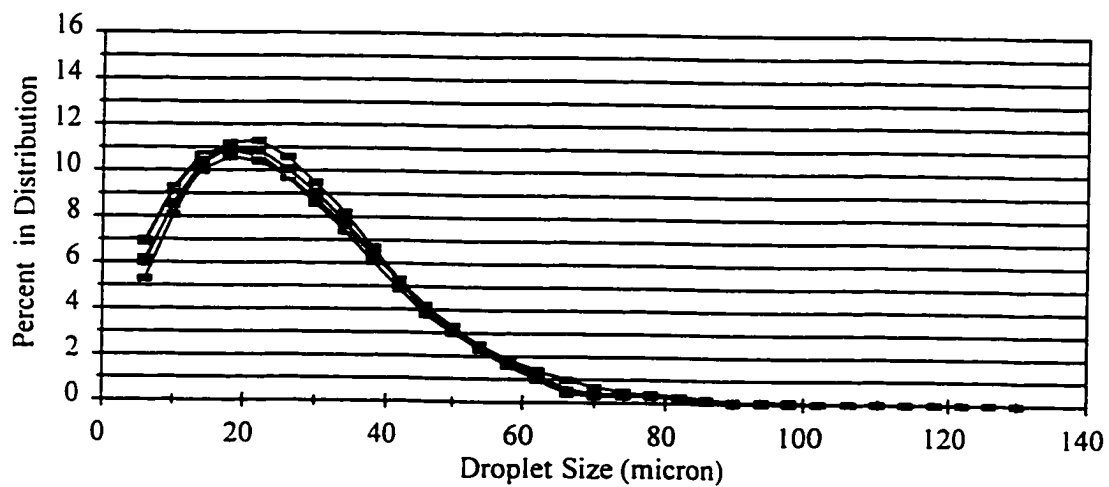


Figure 6.3.1.2 Canola ME Biodiesel Fuel Droplet Distribution for Ten Runs

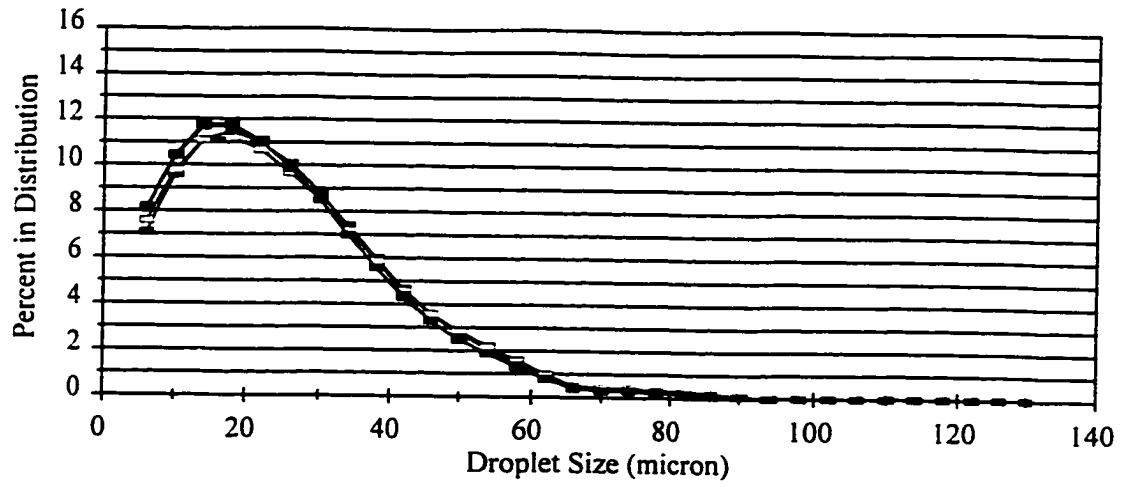


Figure 6.3.1.3 Coconut ME Biodiesel Fuel Droplet Distribution for Ten Runs

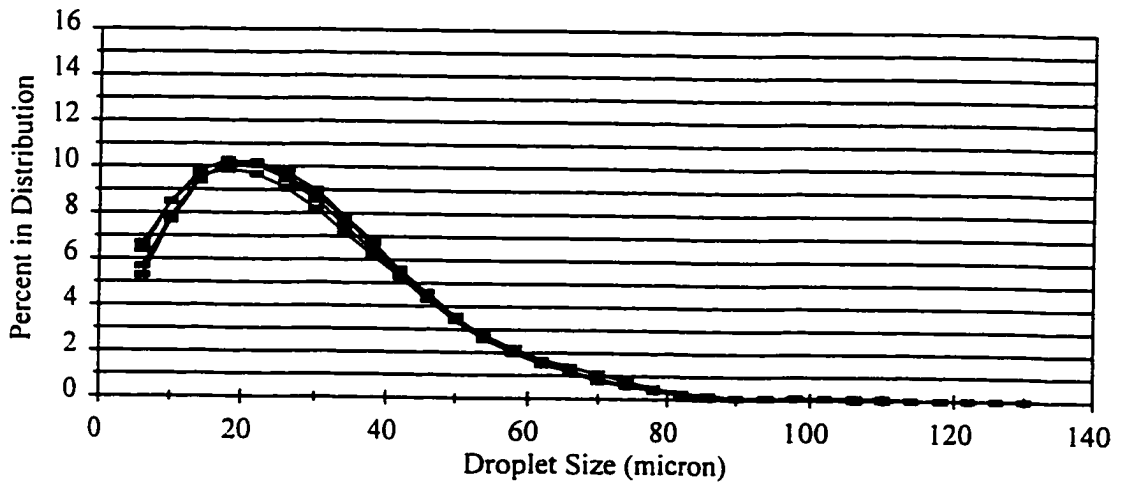


Figure 6.3.1.4 Soya ME Biodiesel Fuel Droplet Distribution for Ten Runs

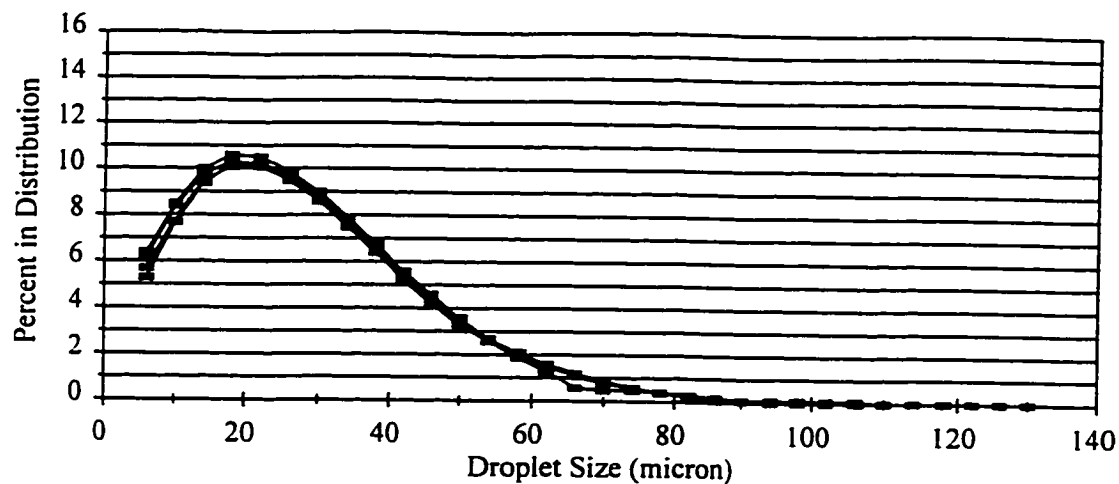


Figure 6.3.1.5 Peanut ME Biodiesel Fuel Droplet Distribution for Ten Runs

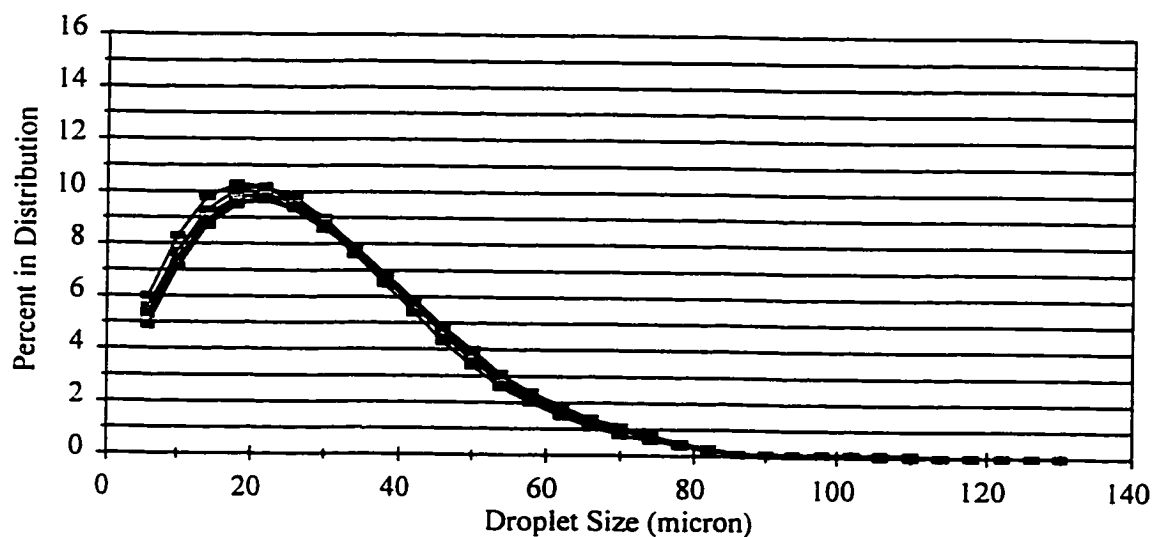


Figure 6.3.1.6 Palm ME Biodiesel Fuel Droplet Distribution for Ten Runs

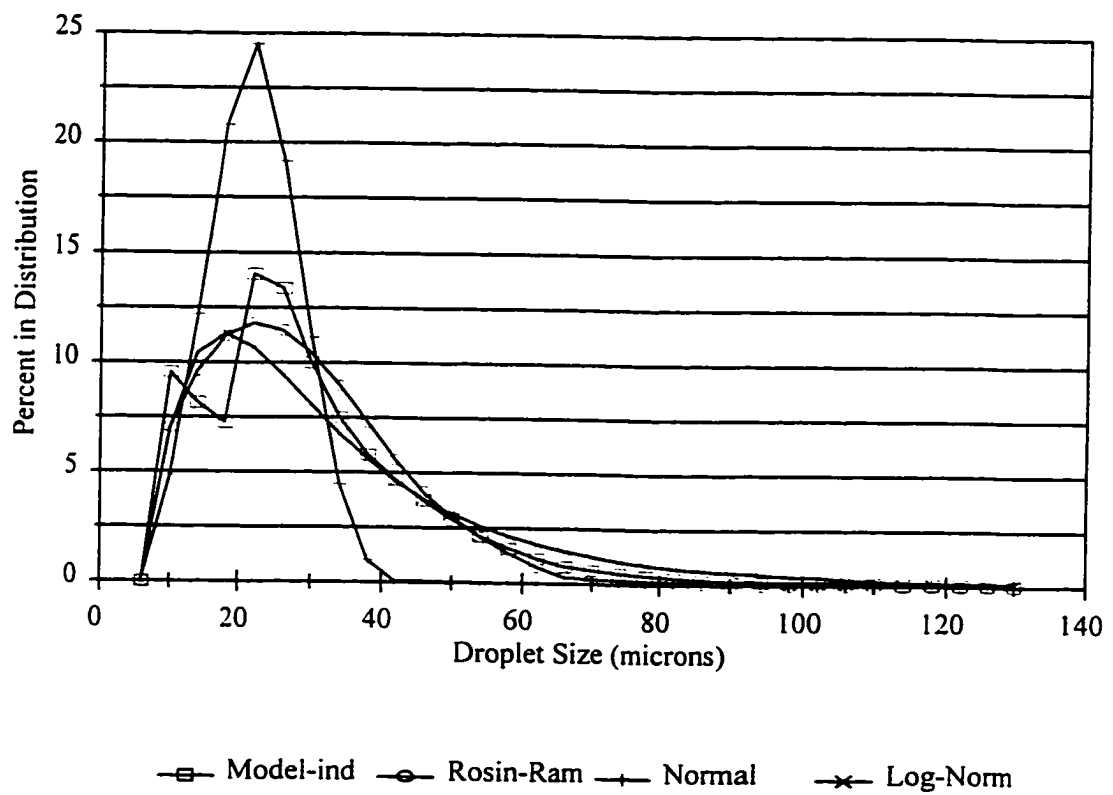


Figure 6.3.1.7 Diesel Fuel Droplet Distribution Using Different Models

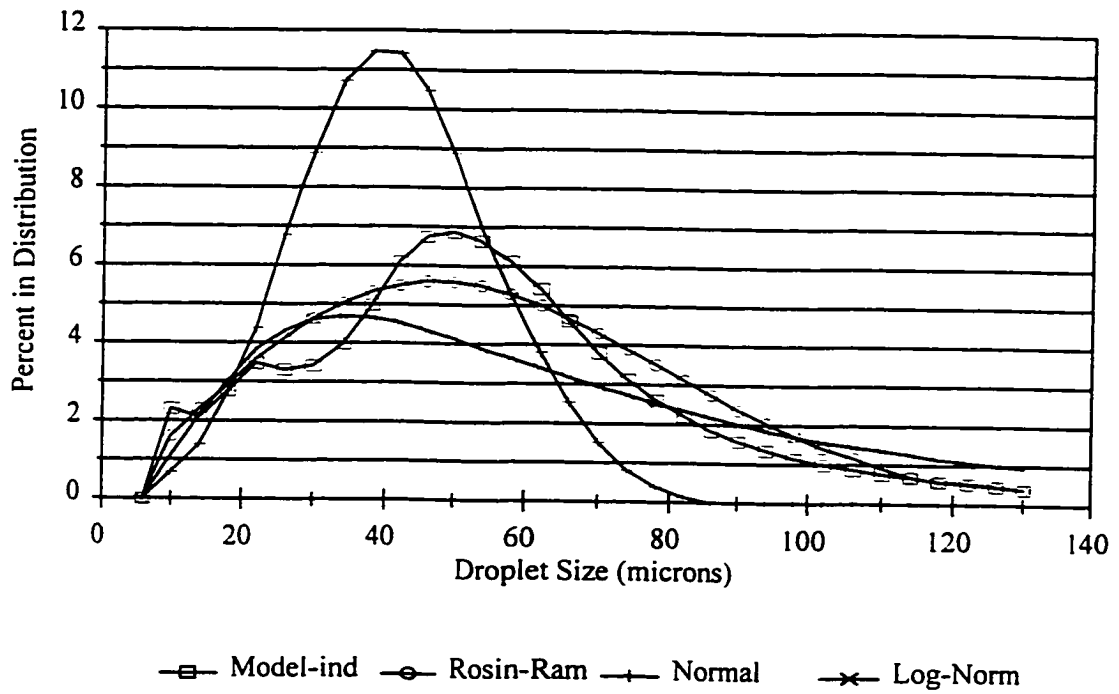


Figure 6.3.1.8 Canola Oil Droplet Distribution Using Different Models

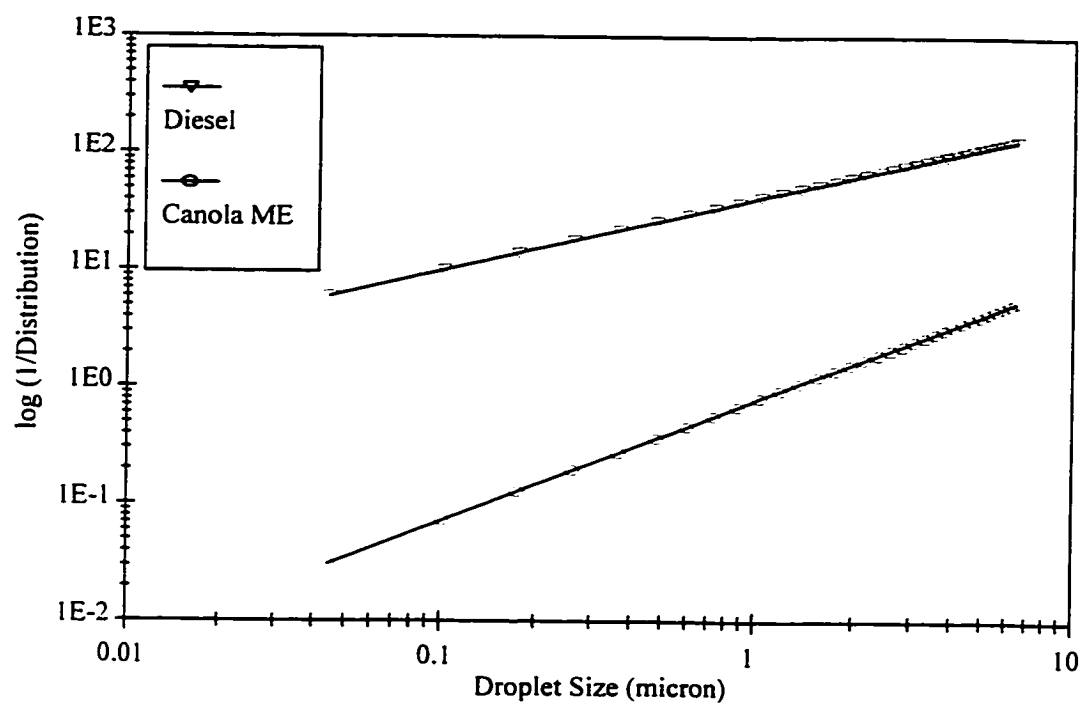


Figure 6.3.1.9 Verification of the Rosin-Rammler Distribution

6.3.2 Atomization of Biodiesel Fuels

Tests were carried out to establish if there were any differences between typical diesel, vegetable oil methyl ester, and neat vegetable oil fuels. The droplet distribution of these three sample types, using canola oil as a reference, are shown in Figure 6.3.2.1 where it can be seen that there are distinct differences between the three. It should be noted that these tests were done with the pump rack in a higher flow position compared with the general tests which were done with the rack in the low flow position, thus the shape of the diesel and ME distributions are different. The medium flow tests could not be repeated at the low flow rack position because the neat vegetable oil required a high pumping power and the first electrical motor used was burned out after a few sequences of runs with the neat oil. The droplet distribution for the neat vegetable oil was flat and wide indicating the existence of several large-size droplets. These would contribute to poor combustion in a diesel engine.

The Rosin-Rammler distribution parameters and the calculated SMDs for coconut, canola, peanut, soya and palm oil methyl ester biodiesel fuels produced were compared with each other and with diesel using the Duncan Mean Range Test¹ (DMRT) at a 95% confidence level. The droplet distributions for these fuels are compared in Figure 6.3.2.2

Figures 6.3.2.3 shows the SMDs of the various fuels and 6.3.2.4 shows how the SMD for the biodiesel fuels compare with diesel fuels. An analysis of these SMDs using the DMRT showed that all were significantly different at the 95% level except for canola compared with soya, canola compared with peanut, and coconut compared with diesel. Diesel fuel had an SMD of 10.88 μm ; coconut oil ME 11.16 μm , 2.60% higher than diesel; canola oil ME 13.58 μm , 24.78% higher than diesel; soya oil ME 13.37 μm , 22.92% higher than diesel;

¹ DMRT software written by Dr. Ken Wilkie - DalTech

peanut oil ME 13.99 μm , 28.55% higher than diesel; and palm oil ME 14.51 μm , 33.36% higher than diesel. These results are summarized in Table 6.3.2.1.

The Rosin-Rammler distribution function parameters 'X' and 'n' are summarized in Table 6.3.2.2 and 6.3.2.3 respectively. The DMRT demonstrated that all the 'X' parameters were significantly different at the 95% level except for soya compared with peanut. The 'n' parameters showed a high degree of variation and several of them were found to be similar. At the 95% level, soya and diesel; soya and coconut; canola and peanut; peanut and palm; canola and palm; and coconut and diesel were found to be NOT significantly different.

Table 6.3.2.1 SMD of Biodiesel and Diesel Fuels

Test Number	Canola SMD (μm)	Coconut SMD (μm)	Soya SMD (μm)	Peanut SMD (μm)	Palm SMD (μm)	Diesel SMD (μm)
1	14.25	11.10	11.91	15.16	14.05	10.51
2	12.14	11.10	14.25	14.75	14.33	11.04
3	12.03	11.10	14.25	14.75	14.78	10.80
4	12.77	11.10	12.31	14.25	15.16	10.51
5	12.03	10.85	11.67	12.31	14.75	10.51
6	12.19	10.85	11.93	14.25	15.16	10.51
7	12.77	10.80	11.34	13.33	15.16	11.49
8	12.77	12.61	11.99	14.25	15.16	11.04
9	11.81	11.30	14.25	14.25	14.69	10.51
10	12.77	11.04	12.03	14.25	14.78	10.51
11	13.44	10.46	14.25	14.25	12.93	11.10
12	14.65	11.49	12.58	13.33	15.19	11.10
13	12.57	10.11	14.25	14.75	15.19	11.35
14	14.65	10.80	11.91	14.25	15.83	11.10
15	12.45	10.80	11.40	14.25	16.19	11.10
16	13.78	11.10	14.25	13.44	14.75	11.10
17	14.65	11.35	13.44	14.25	14.25	11.10
18	14.65	10.80	14.25	13.44	12.70	11.10
19	14.65	10.51	13.44	13.63	12.27	11.10
20	14.65	10.80	14.25	14.75	12.84	11.10
21	13.33	12.43	12.87	14.75	14.51	11.04
22	14.25	11.37	14.25	14.05	14.53	10.51
23	14.25	11.37	14.25	14.75	14.54	10.51
24	14.25	11.78	14.25	11.92	14.53	10.80
25	14.25	11.37	14.25	14.75	14.50	10.51
26	14.25	11.29	14.25	13.33	14.49	10.80
27	14.25	11.29	14.75	12.58	14.45	10.75
28	14.25	11.29	14.25	13.05	14.42	10.51
29	14.25	11.29	13.33	14.25	14.38	11.49
30	14.25	11.29	14.75	14.25	14.36	10.75
Average	13.58	11.16	13.37	13.99	14.51	10.88
Std. Dev.	0.97	0.5	1.12	0.78	1.03	0.31
%Difference from Diesel	24.78%	2.60%	22.92%	28.55%	33.36%	...

Table 6.3.2.2 Rosin-Rammler 'X' Parameters for Biodiesel ME and Diesel Fuels

Test Number	Canola X	Coconut X	Soya X	Peanut X	Palm X	Diesel X
1	30.6	25.37	29.89	31.54	30.68	24.01
2	28.86	25.37	30.6	30.68	30.78	24.11
3	28.59	25.37	30.6	30.68	32.27	24.68
4	27.42	25.37	29.27	30.6	31.54	24.01
5	28.6	24.78	29.27	29.27	30.68	24.01
6	29.27	24.78	28.36	30.6	31.54	24.01
7	27.42	24.68	28.46	29.89	31.54	23.89
8	27.42	24.01	29.11	30.6	31.54	24.11
9	28.06	24.68	30.6	30.6	33.88	24.01
10	27.42	24.11	28.59	30.6	32.27	24.01
11	29.34	22.85	30.6	30.6	31.38	25.37
12	28.6	23.89	29.89	29.89	33.18	25.37
13	28.2	23.33	30.6	30.68	33.18	24.78
14	28.6	24.68	29.89	30.6	34	25.37
15	27.93	24.68	28.6	30.6	34.76	25.37
16	28.67	25.37	30.6	29.87	30.68	25.37
17	28.6	24.78	29.87	30.6	30.6	25.37
18	28.6	24.68	30.6	29.87	28.48	25.37
19	28.6	24.01	29.87	29.27	29.16	25.37
20	28.6	24.68	30.6	30.68	28.8	25.37
21	29.89	27.15	30.6	30.68	31.55	24.11
22	30.6	25.97	30.6	30.68	31.59	24.01
23	30.6	25.97	30.6	30.68	31.63	24.01
24	30.6	27.18	30.6	28.32	31.6	24.68
25	30.6	25.97	30.6	30.68	31.6	24.01
26	30.6	25.79	30.6	29.89	31.65	24.68
27	30.6	25.79	30.68	29.89	31.65	24.57
28	30.6	25.79	30.6	29.27	31.66	24.01
29	30.6	25.79	29.89	30.6	31.66	23.89
30	30.6	25.79	30.68	30.6	31.55	24.57
Average	29.16	25.09	30.04	30.3	31.55	24.55
Std. Dev.	1.15	0.96	0.76	0.63	1.65	0.59

Table 6.3.2.3 Rosin-Rammler 'n' Parameters for Biodiesel ME and Diesel Fuels

Test Number	Canola n	Coconut n	Soya n	Peanut n	Palm n	Diesel n
1	1.68	1.61	1.52	1.72	1.66	1.61
2	1.57	1.61	1.68	1.72	1.68	1.66
3	1.57	1.61	1.68	1.72	1.66	1.61
4	1.68	1.61	1.57	1.68	1.72	1.61
5	1.57	1.61	1.52	1.57	1.72	1.61
6	1.56	1.61	1.57	1.68	1.72	1.61
7	1.68	1.61	1.52	1.63	1.72	1.72
8	1.68	1.85	1.55	1.68	1.72	1.66
9	1.57	1.66	1.68	1.68	1.6	1.61
10	1.68	1.66	1.57	1.68	1.66	1.61
11	1.66	1.66	1.68	1.68	1.55	1.61
12	1.81	1.72	1.57	1.63	1.66	1.61
13	1.63	1.6	1.68	1.72	1.66	1.66
14	1.81	1.61	1.52	1.68	1.68	1.61
15	1.63	1.61	1.52	1.68	1.68	1.61
16	1.72	1.61	1.68	1.64	1.72	1.61
17	1.81	1.66	1.64	1.68	1.68	1.61
18	1.81	1.61	1.68	1.64	1.63	1.61
19	1.81	1.61	1.64	1.68	1.57	1.61
20	1.81	1.61	1.68	1.72	1.63	1.61
21	1.63	1.66	1.57	1.72	1.67	1.66
22	1.68	1.61	1.68	1.66	1.67	1.61
23	1.68	1.61	1.68	1.72	1.67	1.61
24	1.68	1.6	1.68	1.57	1.67	1.61
25	1.68	1.61	1.68	1.72	1.66	1.61
26	1.68	1.61	1.68	1.63	1.66	1.61
27	1.68	1.61	1.72	1.57	1.66	1.61
28	1.68	1.61	1.68	1.63	1.65	1.61
29	1.68	1.61	1.63	1.68	1.65	1.72
30	1.68	1.61	1.72	1.68	1.65	1.61
Average	1.68	1.63	1.63	1.67	1.67	1.62
Std. Dev.	0.08	0.05	0.07	0.04	0.05	0.03

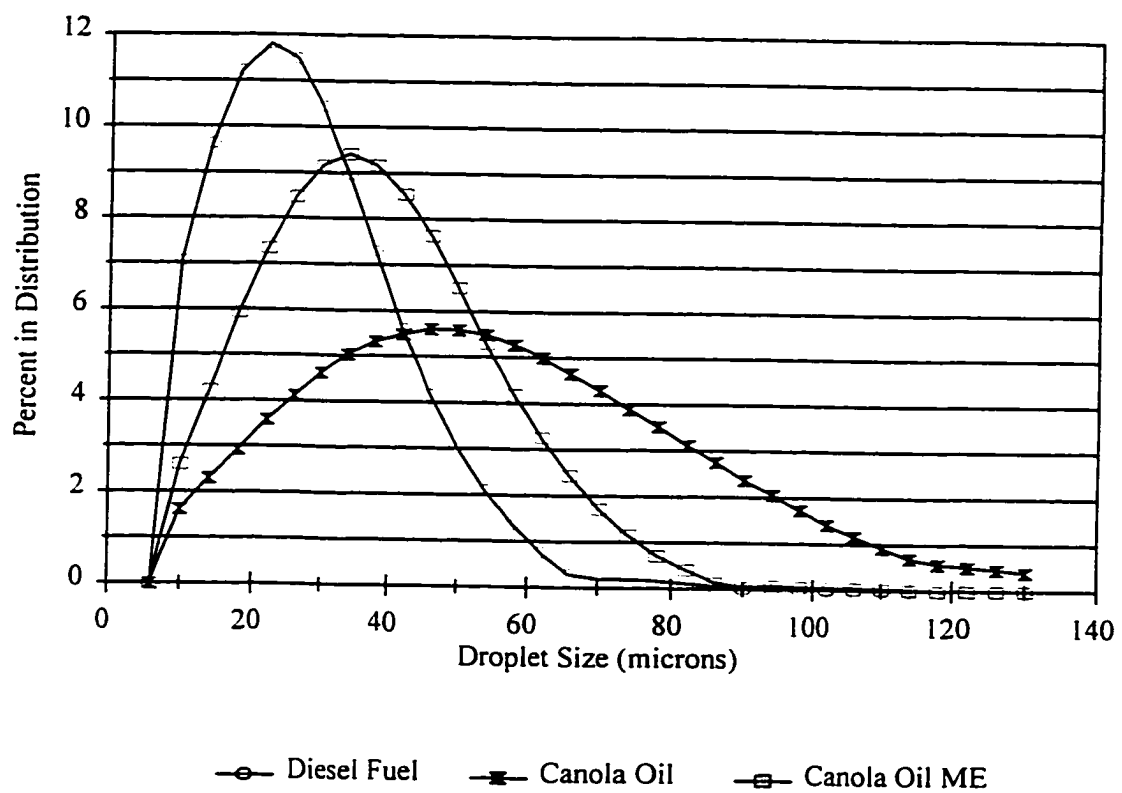


Figure 6.3.2.1 Droplet Distribution of Diesel Fuel, Neat Canola Oil and Canola Oil Methyl Ester

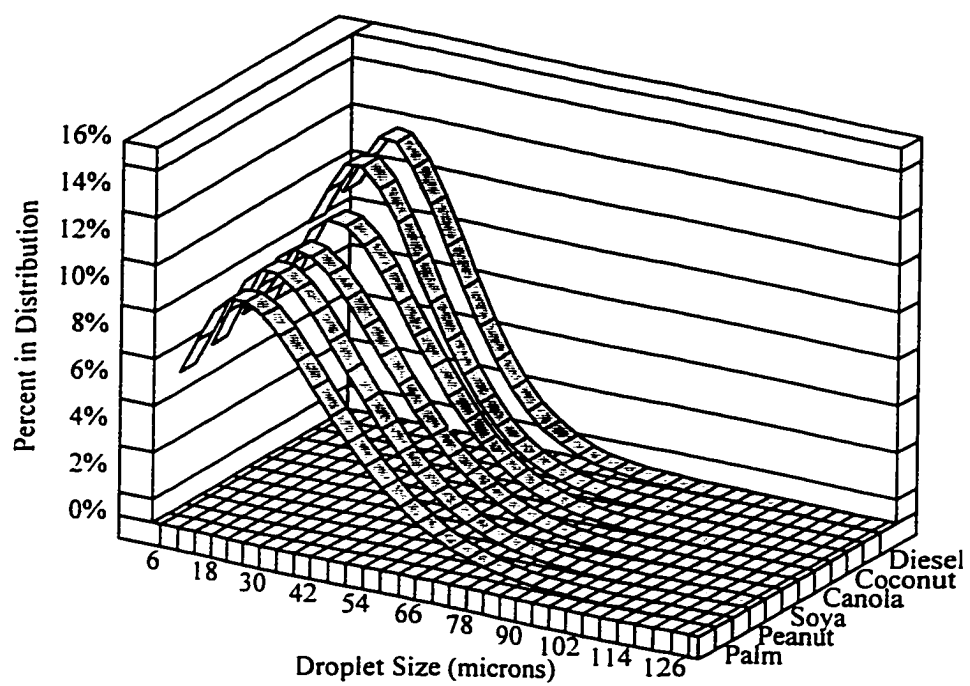


Figure 6.3.2.2 Droplet Distributions of Biodiesel ME and Diesel Fuels

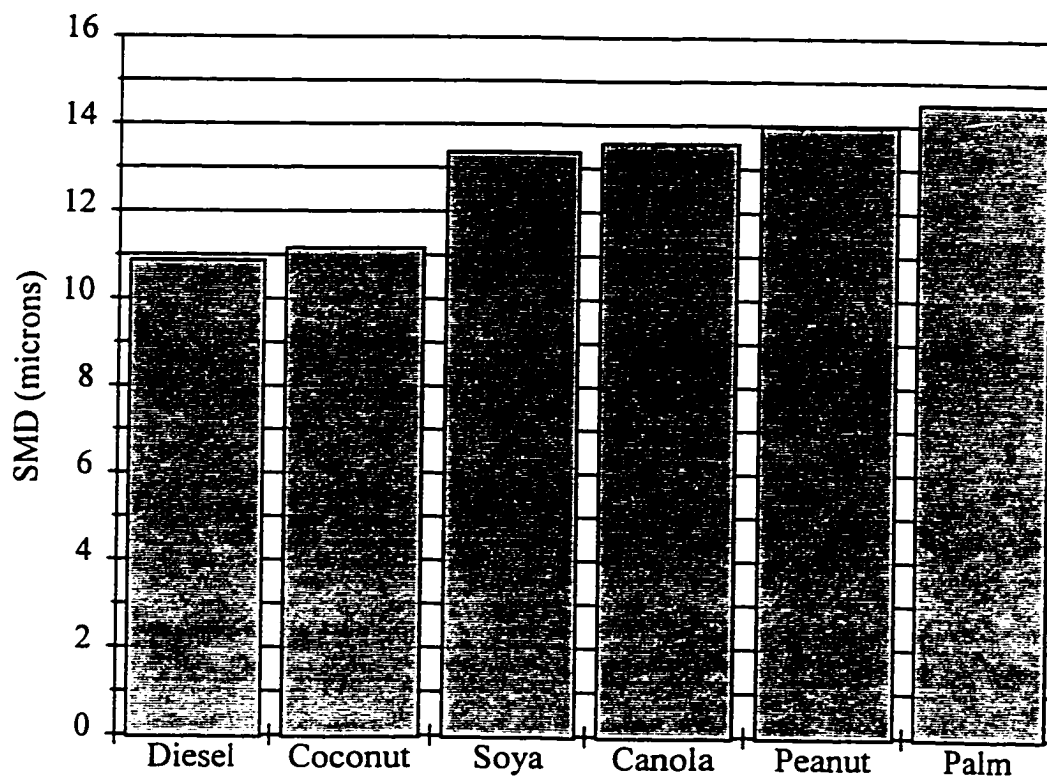


Figure 6.3.2.3 Measured SMD of Methyl Ester Biodiesel Fuels

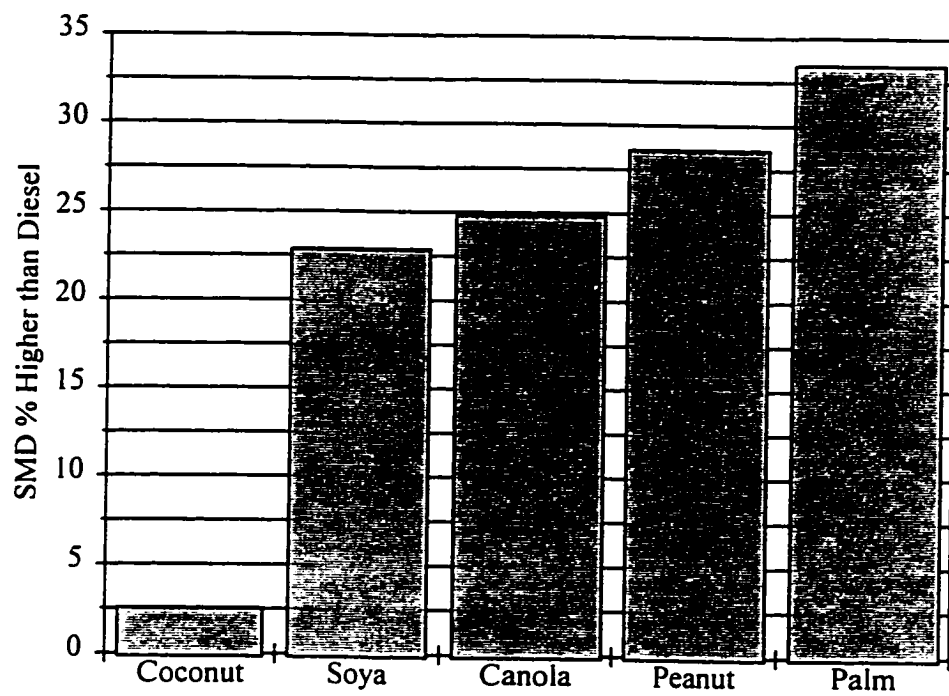


Figure 6.3.2.4 Percent Difference of the Measured SMD of Methyl Ester Biodiesel Fuels Compared with Diesel Fuel

6.3.3 Predicting the Rosin-Rammler Parameters and SMD using Regression Models

Regression models were generated using experimental data for the Rosin-Rammler ‘X’ parameters, ‘n’ parameters and the SMDs obtained from atomization tests carried out on five naturally occurring vegetable oil methyl ester biodiesel fuels and diesel #2 fuel. These models incorporated two independent variables, viscosity and surface tension. All other parameters including nozzle characteristics, injector pump rack position, motor speed, fuel temperature and sampling position in the spray were kept constant. Density was assumed constant for all practical purposes since the range of densities that were likely to be encountered was found to have little effect on SMD in the sensitivity analyses previously discussed.

The regression models were generated with and without a constant term. The statistical significance of the coefficients of the independent variables were analyzed using the P-values generated by the regression analysis. The P-value gives the probability of the coefficient of the independent variable being equal to 0; i.e, it tells whether that independent variable has any significant effect on the dependent variable. Equations 6.3.3.1 to 6.3.3.8 give the models tested in the regression analyses for the dependent variables SMD, ‘X’ and ‘n’.

$$\text{Dependent-Variable} = K_1 + K_2 \mu + K_3 \sigma^{\pm 1} + K_4 \mu \sigma^{\pm 1} \quad (6.3.3.1)$$

$$\text{Dependent-Variable} = K_1 \mu + K_2 \sigma^{\pm 1} + K_3 \mu \sigma^{\pm 1} \quad (6.3.3.2)$$

$$\text{Dependent-Variable} = K_1 + K_2 \mu + K_3 \sigma^{\pm 1} \quad (6.3.3.3)$$

$$\text{Dependent-Variable} = K_1 \mu + K_2 \sigma^{\pm 1} \quad (6.3.3.4)$$

$$\text{Dependent-Variable} = K_1 + K_2 \mu + K_3 \mu \sigma^{\pm 1} \quad (6.3.3.5)$$

$$\text{Dependent-Variable} = K_1 \mu + K_2 \mu \sigma^{\pm 1} \quad (6.3.3.6)$$

$$\text{Dependent-Variable} = K_1 + K_2 \mu \sigma^{\pm 1} \quad (6.3.3.7)$$

$$\text{Dependent-Variable} = K_1 \mu \sigma^{\pm 1} \quad (6.3.3.8)$$

A complete listing of the regression analyses are given in Appendix F. The best-fit regression model obtained for the SMD is given in Table 6.3.3.1. The P-values for all the coefficients of the independent variables were well within the acceptable range (P-value less than 0.05) indicating that all the coefficients and the constant term were significant. The F-test and P-value for the regression model also showed that there was a good fit of the model to the data. There was also a perfect correlation coefficient (r^2) of 100%. The standard deviation of the regression equation was only 0.03 μm . There was, however, some concern with respect to the interpretation of some of the coefficients and the constant term of the model. The regression equation indicated that as the surface tension and the viscosity tend to zero, the SMD tends to a finite value of 168 μm . This is a very high value and is not practical. Also the negative coefficients of the surface tension and the viscosity were somewhat contrary to the physical process. This means that the coefficients are included solely for the purpose of generating a best fit to the data which implies that this model will

give realistic values for SMD only when the independent variables are within the range over which the model was developed. It can be seen in Chapter 7 that, unless the surface tension and viscosity of a fuel are paired in an exact manner as those used in the model development, this model with a perfect correlation coefficient (r^2) failed a sensitivity analysis due to the complex relationship between the coefficients of μ , σ , $\mu\sigma$, and the constant term.

Table 6.3.3.2 gives a second model for SMD which also had an adequate fit to the data. This model had no constant term and only two coefficients, one for surface tension and the other for viscosity. Both of these coefficients were positive which indicated that an increase in either surface tension or viscosity, all things being equal, leads to an increase in SMD which is probably the case for jet breakup. The standard deviation of this model was $0.3 \mu\text{m}$ and both coefficients had low P-values indicating that they were significant. The fitted data, standard deviation of the fitted points and the 95% confidence limits are given in Table 6.3.3.3 for both of the SMD models. Unlike the first 4-parameter model, the second 2-parameter model did not fail a sensitivity analysis (Chapter 7) and thus was selected as the model of choice.

Table 6.3.3.4 gives the selected regression models for the 'X' parameter and Table 6.3.3.5 gives the 95% confidence intervals. This model excluded the constant term which was found to be insignificant at the 95% level in the other models (Appendix F). All of the regression parameters of this model were acceptable and the standard deviation was $0.6 \mu\text{m}$. The physical significance of the regression coefficients were similar to the SMD 2-parameter regression model.

Regression analysis of the 'n' parameter (Table 6.3.3.6) resulted in a model similar to the model for the 'X' parameter, that is, no constant term and coefficients of surface tension and viscosity only. The standard deviation of this model was 0.03. The 95% confidence intervals

are given in Table 6.3.3.7. The coefficients of the regression model imply that a decrease in viscosity leads to an increase in 'n'. This is physically acceptable since a larger 'n' implies a narrower distribution with most of the droplets having similar diameters to the mean diameter. The coefficient of surface tension implies that an increase in surface tension leads to an increase in 'n' which is probably the case for droplet breakdown after the initial jet breakup.

Equations 6.3.3.9, 6.3.3.10 give the regression models for SMD and Equations 6.3.3.11 and 6.3.3.12 give the selected regression models for the 'X' and 'n' respectively.

$$SMD_1 = 1.6837E-4 - 0.04165 \mu - 0.00618 \sigma + 1.66314 \mu \sigma \quad (6.3.3.9)$$

$$SMD_2 = 0.002103 \mu + 0.000330 \sigma \quad (6.3.3.10)$$

$$X = 2.0993E-3 \mu + 7.8852E-4 \sigma \quad (6.3.3.11)$$

$$n = -67.32 \mu + 67.63 \sigma \quad (6.3.3.12)$$

where:

- SMD - Sauter Mean Diameter (m)
- μ - dynamic viscosity (Pa.s)
- σ - surface tension (N/m)
- X - Rosin-Rammler mean diameter parameter (m)
- n - Rosin-Rammler distribution spread parameter

Table 6.3.3.1 Regression Analysis for SMD of Methyl Ester Biodiesel Fuels using Three Coefficients and a Constant

Regression Analysis for SMD

The regression equation is

$$\text{SMD} = 0.000168 - 0.0417 \mu - 0.00618 \sigma + 1.66 \mu.\sigma$$

Predictor	Coef	StDev	T	P
Constant	0.00016837	0.00000751	22.42	0.002
μ	-0.041654	0.001810	-23.01	0.002
σ	-0.0061782	0.0002919	-21.16	0.002
$\mu.\sigma$	1.66314	0.07084	23.48	0.002

S = 0.000000027 R-Sq = 100.0% R-Sq(adj) = 100.0%

Analysis of Variance

Source	DF	SS	MS	F	P
Regression	3	1.15687E-11	3.85625E-12	5455.18	0.000
Error	2	1.41379E-15	7.06896E-16		
Total	5	1.15702-11			

Table 6.3.3.2 Regression Analysis for SMD of Methyl Ester Biodiesel Fuels using Two Coefficients and No Constant

Regression Analysis for SMD					
The regression equation is					
SMD = 0.00120 μ + 0.000330 σ					
Predictor	Coef	StDev	T	P	
No constant					
μ	0.0012037	0.0001931	6.23	0.003	
σ	0.00032950	0.00002302	14.31	0.000	
S = 0.000000328 R-Sq = 99.96% R-Sq(adj) = 99.95%					
Analysis of Variance					
Source	DF	SS	MS	F	P
Regression	2	1.01192E-09	5.05962E-10	4712.47	0.000
Error	4	4.29467E-13	1.07367E-13		
Total	6	1.01235E-09			

Table 6.3.3.3 Fitted Data and Confidence Limits for SMD

Biodiesel Type	Measured SMD	Fitted SMD	Standard Deviation of Fit	95% Confidence Lower Limit	95% Confidence Upper Limit
<u>Model 1 - Three Coefficients and a Constant (Equation 3.3.3.1)</u>					
Diesel #2	1.09e-05	1.09e-05	0.00e+00	1.08e-05	1.10e-05
Coconut	1.12e-05	1.12e-05	0.00e+00	1.11e-05	1.12e-05
Canola	1.36e-05	1.36e-05	0.00e+00	1.35e-05	1.36e-05
Soya	1.34e-05	1.34e-05	0.00e+00	1.33e-05	1.35e-05
Peanut	1.40e-05	1.40e-05	0.00e+00	1.39e-05	1.41e-05
Palm	1.45e-05	1.45e-05	0.00e+00	1.44e-05	1.46e-05
<u>Model 2 - Two Coefficients and No Constant (Equation 3.3.3.2)</u>					
Diesel #2	1.09e-05	1.07e-05	3.00e-07	9.90e-06	1.14e-05
Coconut	1.12e-05	1.14e-05	2.00e-07	1.09e-05	1.19e-05
Canola	1.36e-05	1.36e-05	2.00e-07	1.32e-05	1.41e-05
Soya	1.34e-05	1.37e-05	2.00e-07	1.33e-05	1.41e-05
Peanut	1.40e-05	1.40e-05	2.00e-07	1.36e-05	1.45e-05
Palm	1.45e-05	1.40e-05	2.00e-07	1.36e-05	1.45e-05

Table 6.3.3.4 Regression Analysis for the 'X' Parameter of Methyl Ester Biodiesel Fuels

Regression Analysis for the Rosin-Rammler 'X' Parameter

The regression equation is

$$X = 0.00210 \mu + 0.000789 \sigma$$

Predictor	Coef	StDev	T	P
No constant				
μ	0.0020993	0.0003873	5.42	0.006
σ	0.00078852	0.00004618	17.08	0.000

S = 0.000000657 R-Sq = 99.96% R-Sq(adj) = 99.96%

Analysis of Variance

Source	DF	SS	MS	F	P
Regression	2	4.88694E-09	2.44347E-09	5656.40	0.000
Error	4	1.72793E-12	4.31983E-13		
Total	6	4.88867E-09			

Table 6.3.3.5 Fitted Data and Confidence Limits for 'X'

Biodiesel Type	Measured 'X'	Fitted 'X'	Standard Deviation of Fit	95% Confidence Lower Limit	95% Confidence Upper Limit
Diesel #2	2.45e-05	2.42e-05	5.00e-07	2.27e-05	2.57e-05
Coconut	2.51e-05	2.55e-05	4.00e-07	2.44e-05	2.65e-05
Canola	2.91e-05	2.98e-05	3.00e-07	2.89e-05	3.06e-05
Soya	3.00e-05	2.99e-05	3.00e-07	2.91e-05	3.08e-05
Peanut	3.03e-05	3.06e-05	3.00e-07	2.97e-05	3.15e-05
Palm	3.16e-05	3.06e-05	3.00e-07	2.96e-05	3.16e-05

Table 6.3.3.6 Regression Analysis for the 'n' Parameter for Methyl Ester Biodiesel Fuels

Regression Analysis for the Rosin-Rammler 'n' Parameter

The regression equation is

$$n = -67.3 \mu + 67.63 \sigma$$

Predictor	Coef	StDev	T	P
No constant				
μ	-67.32	18.42	-3.65	0.022
σ	67.632	2.196	30.80	0.000

S = 0.03126 R-Sq = 99.98% R-Sq(adj) = 99.97%

Analysis of Variance

Source	DF	SS	MS	F	P
Regression	2	16.3345	8.1672	8359.25	0.000
Error	4	0.0039	0.0010		
Total	6	16.3384			

Table 6.3.3.7 Fitted Data and Confidence Limits for 'n'

Biodiesel Type	Measured 'n'	Fitted 'n'	Standard Deviation of Fit	95% Confidence Lower Limit	95% Confidence Upper Limit
Diesel #2	1.62	1.62	0.0185	1.56	1.68
Coconut	1.63	1.63	0.0154	1.58	1.68
Canola	1.68	1.66	0.0155	1.61	1.71
Soya	1.63	1.66	0.0101	1.62	1.69
Peanut	1.67	1.66	0.0172	1.61	1.72
Palm	1.67	1.67	0.0113	1.63	1.70

6.3.4 Dimensional Analysis of SMD Regression Model

The two regression models for SMD contained coefficients of surface tension (σ), viscosity (μ), and the product of these two ($\sigma\mu$). However, the coefficients of regression models may or may not relate to physical parameters of the mechanism which it models. One way of testing the physical significance of the coefficients of a regression model is by means of dimensional analysis. The analysis used here was similar to the Buckingham PI theorem with matrix analysis.

The variables considered for the dimensional groups were:

$$\text{SMD} = \mathcal{F} \{P_L, P_g, \sigma_f, \mu_f, Q_f, \rho_f, \rho_g, d_o, L_o\} \quad (6.3.4.1)$$

where

P_L	-	fuel injection line pressure (N/m ²) {ML ⁻¹ T ⁻² }
P_g	-	pressure of gas atmosphere (N/m ²) {ML ⁻¹ T ⁻² }
σ_f	-	surface tension of fuel (N/m) {MT ⁻² }
μ_f	-	dynamic viscosity of fuel (Pa.s) {ML ⁻¹ T ⁻¹ }
Q_f	-	volume flow of fuel (m ³ /s) {L ³ T ⁻¹ }
ρ_f	-	fuel density (kg/m ³) {ML ⁻³ }
ρ_g	-	density of gas atmosphere (kg/m ³) {ML ⁻³ }
d_o	-	nozzle orifice diameter (m) {L}
L_o	-	nozzle sac characteristic length (m) {L}

Some of the above variables were further simplified by using the following groups.

$$\Delta P = (P_L - P_g) \quad (6.3.4.2)$$

$$\Delta \rho = (\rho_f - \rho_g) \quad (6.3.4.3)$$

$$Q_f = \frac{\pi d_o^2}{4} \sqrt{2} \frac{\sqrt{\Delta P}}{\sqrt{\rho_f}} \quad (6.3.4.4)$$

$$\psi = \frac{\rho_f}{\rho_g} \quad (6.3.4.5)$$

$$\phi = \frac{L_o}{d_o} \quad (6.3.4.6)$$

Following extensive analysis of the above variables it was found that the only dimensional groups that represented the coefficients of the regression model were:

Group 1

$$\frac{1}{(\Delta P)} \phi^n \psi^m \sigma_f \quad (6.3.4.7)$$

dimensions = $N^{-1}m^2 \ N.m^{-1}$ = m

Group 2

$$\frac{d_o^2}{\rho_f Q_f} \phi^p \psi^q \mu_f \quad (6.3.4.8)$$

dimensions = $m^2 \ kg.m^{-1}.s^{-1} \ kg^{-1}.m^3 \ m^{-3}.s$ = m

Applying Equation 6.3.4.4, Group 2 can be rewritten as:

$$\frac{1}{\sqrt{\rho_f \Delta P}} \phi^r \psi^s \mu_f \quad (6.3.4.9)$$

$$\text{dimensions} = \text{kg.m}^{-1}.\text{s}^{-1} \text{ kg}^{-1/2}.\text{m}^{3/2} \text{ kg}^{-1/2}.\text{m}^{1/2}.\text{s} = \text{m}$$

Group 3

$$\frac{1}{d_o \rho_f^{1/2} \Delta P^{3/2}} \phi^t \psi^u \sigma_f \mu_f \quad (6.3.4.10)$$

$$\text{dimensions} = \text{m}^{-1} \text{ kg}^{-1/2}.\text{m}^{3/2} \text{ kg}^{-3/2}.\text{m}^{3/2}.\text{s}^3 \text{ kg}.\text{s}^{-2} \text{ kg}.\text{m}^{-1}.\text{s}^{-1} = \text{m}$$

Equation 6.3.4.11 give the dimensional form of the SMD regression model given by Equation 6.3.3.9 and Equation 6.3.4.12 give the dimensional form of the SMD regression model in Equation 6.3.3.10.

$$MD = K_1 - \frac{1}{\Delta P} \phi^m \psi^n \sigma_f - \frac{1}{\sqrt{\rho_f \Delta P}} \phi^r \psi^s \mu_f + \frac{1}{d_o \rho_f^{1/2} \Delta P^{3/2}} \phi^t \psi^u \sigma_f \quad (6.3.4.11)$$

$$SMD = \frac{1}{\Delta P} \phi^{m'} \psi^{n'} \sigma_f + \frac{1}{\sqrt{\rho_f \Delta P}} \phi^{r'} \psi^{s'} \mu_f \quad (6.3.4.12)$$

The regression models give the numeric values of the dimensional groups of the dimensional models. The exact values for the injection pressure, nozzle diameter and nozzle sac length were not known for the atomization setup used. Therefore, it was not possible to ascertain the exact values of indices m , n , p , q , r , s , t and u which were dependent on experimental data.

Although the numeric values given by the regression models were very specific to the atomization systems they can be used with average parameter-values from the literature to determine the order of magnitude of the indices. These indices were determined for the second regression model for SMD only, since the first model failed a sensitivity analysis as mentioned earlier. The data used to determine the magnitude of the indices is given in Table 6.3.4.1. Following extensive analysis using the numeric values of the coefficients of the regression model and the average parameters taken from the literature the indices given in Equation 6.3.4.13 were derived.

$$SMD = \frac{1}{\Delta P} \phi^{1.50} \psi^{1.255} \sigma_f + \frac{1}{\sqrt{\rho_f \Delta P}} \phi^{3.88} \mu_f \quad (6.3.4.13)$$

As can be seen from Equation 6.3.4.13 the magnitude of all the indices were of order (1) and not order (10) or higher. This indicated that the dimensional parameters were representative of the actual system. This model, however, cannot be further tested on the experimental data since some of the experimental parameters, although constant, were unknown.

Table 6.3.4.1 Typical Values for Atomization Parameters

Parameter	Value
Nozzle Diameter d_o (m)	0.0004
Nozzle Sac Length L_o (m)	0.0015
Injection Pressure P_L (MPa)	23
Atmospheric Pressure P_g (kPa)	101

6.4 Review of Experimental Results

The initial phase of this research showed that the viscosity and surface tension of mixtures of methyl esters can be predicted with two relatively simple mixture equations. The average error for both of these prediction equations was 3% when mixtures of GC standards were used.

Using an independent data set for the viscosity and surface tension of pure methyl ester components, the mixture equations were applied to five natural vegetable oil methyl ester complexes and their measured viscosity and surface tension were also predicted within 2.5% on average.

The droplet mean diameter and distribution of the five vegetable oil methyl ester biodiesel fuels were determined experimentally by holding all parameters constant except for the fuel's surface tension and viscosity. The Duncan Mean Range Test was carried out to establish significant similarities and/or differences between fuel types where it was found that only coconut oil ME had a statistically similar SMD to diesel fuel. Regression models were also developed to correlate the atomization parameters to viscosity and surface tension. Good correlation was found between the experimental data and the data predicted by the models.

If the fatty acid composition of a biodiesel methyl ester fuel is known, then its viscosity and surface tension can be predicted using the mixture models developed in this study. These values can then be used to compute the fuel's droplet mean diameter and distribution using the regression models. Although the droplet mean diameters and distributions are specific to the experimental apparatus used, they can be used in a qualitative and /or comparative analysis of the fuels.

7 APPLICATION OF PREDICTION MODELS TO BIODIESEL FUELS

The fatty acid composition of 15 fat and oils are given by Ackman (1996). For the purpose of applying the mixture equations to predict the viscosity and surface tension of these oils, some minor quantities of their fatty acids were lumped together in a manner previously described in Chapter 6. Table 7.1 gives a listing of the oils/fats and the fatty acid composition used in the analyses to follow.

Equation 5.1.1.1 was applied to predict the viscosity of the methyl esters (ME) of the 15 oils. These results are summarized in Table 7.2 along with the upper and lower prediction limits. These limits were based on the average error of the model. Figure 7.1 shows the predicted viscosities graphically along with prediction error bars. It can be seen that rapeseed oil ME had the highest predicted viscosity (4.72 mPa.s) while coconut oil ME had the lowest (2.25 mPa.s). Most of the other oils had similar viscosities ranging from 3.31 to 3.94 mPa.s.

Equations 5.2.1.1 and 5.2.1.2 were applied to predict the surface tension of the 15 methyl ester biodiesel fuels. The predicted values, along with the upper and lower prediction limits, are given in Table 7.3 while Figure 7.2 gives a graphical representation of the data. Rapeseed ME had the highest surface tension (29.24 mN/m) while coconut ME had the lowest (26.82 mN/m). The others ranged from 27.69 to 28.98 mN/m.

In order to decide which regression model for SMD was most suitable, a sensitivity analysis was done. The viscosity was first held constant at the lowest value used in the model development while the surface tension was varied from the lowest to the highest value used in the model development. When the model containing a constant term and coefficients for μ , σ , and $\mu\sigma$ (Equation 6.3.3.9) was tested it was found that an increase in surface tension led to a sharp decrease in SMD which was out of the region over which the model was

developed (Table 7.4). Although this model was capable of predicting the SMD with 100% correlation when the exact paired viscosity and surface tension from the experimental data were used (Table 6.3.3.3), it failed when it was applied in a general manner. The sensitivity analysis for the second model given by Equation 6.3.3.10, however, passed the sensitivity analysis (Table 7.5) for both varying surface tension and viscosity. The manner in which the SMD varied and the range over which it varied were both practical. This model was thus selected for predicting the SMD of the 15 biodiesel fuel types.

Using the predicted viscosity and surface tension for the 15 fuel types, the Sauter Mean Diameter was predicted using Equation 6.3.3.10. The SMD error bands were also computed using the error bands of the viscosity and surface tension. These error bands were further increased to accommodate the standard error of the SMD regression model. Table 7.6 summarized the predicted SMD and the lower and upper prediction limits. Figure 7.3 shows this data graphically and Figure 7.4 shows the SMDs compared with diesel fuel. As expected, rapeseed oil ME had the highest SMD (15.31 μm) while coconut oil ME had the lowest (11.55 μm). The others ranged from 13.17 to 14.10 μm . Compared with diesel most of the oils had SMDs that were 20 - 30% higher than diesel while coconut oil ME was approximately 6% higher than diesel and rapeseed oil ME 40% higher.

The droplet distributions for the 15 fuels were also predicted using the Rosin-Rammler distribution. The two parameters of the distribution, 'X' and 'n', were computed using the regression models given in Equations 6.3.3.11 and 6.3.3.12 respectively. Figure 7.5 shows the distributions graphically where it can be seen that all of the fuel types had similar droplet distribution patterns.

The data above showed that the surface tension of the fifteen biodiesel types varied by 9%. This variation is relatively small and indicates that the SMD may be estimated using

viscosity alone. A regression model (Table 7.7) which incorporated viscosity as the only independent variable was thus derived from the measured atomization data. The standard error of this model was 15% higher than the original regression model that included both viscosity and surface tension as independent variables. When this model (Table 7.7) was tested on the 15 biodiesel types, the predicted SMDs were only 1.35% higher than the SMDs predicted using the original model that included both viscosity and surface tension. Therefore, the regression model in Table 7.7 may be very useful for atomization analyses providing the surface tension of the fuel being evaluated is within the range of the experimental data (28.5 ± 2 mN/m). For analyses requiring a higher degree of precision, Equation 6.3.3.10 is the preferred equation.

Table 7.1 Fatty Acid Composition of 15 Fats and Oils (Ackman, 1996)

Oil Type	Fatty Acid Composition									
	Caprylic 8:0	Capric 10:0	Lauric 12:0	Myristic 14:0	Palmitic 16:0	Stearic 18:0	Oleic 18:1	Linoleic 18:2	Linolenic 18:3	Erucic 22:1
Peanut	0.0	0.0	0.0	0.0	10.4	8.9	47.1	32.9	0.5	0.2
Rapeseed	0.0	0.0	0.0	0.0	2.7	2.8	21.9	13.1	8.6	50.9
Canola	0.0	0.0	0.0	0.1	3.9	3.1	60.2	21.1	11.1	0.5
Olive	0.0	0.0	0.0	0.0	11.0	3.6	75.3	9.5	0.6	0.0
Coconut	8.3	6.0	46.7	18.3	9.2	2.9	6.9	1.7	0.0	0.0
Corn	0.0	0.0	0.0	0.0	9.9	3.1	29.1	56.8	1.1	0.0
Palm	0.1	0.1	0.9	1.3	43.9	4.9	39.0	9.5	0.3	0.0
Safflower	0.0	0.0	0.0	0.1	6.6	3.3	14.4	75.5	0.1	0.0
Sunflower	0.0	0.0	0.0	0.1	6.0	5.9	16.0	71.4	0.6	0.0
Soybean	0.0	0.0	0.0	0.1	10.3	4.7	22.5	54.1	8.3	0.0
Sunola	0.0	0.0	0.0	0.0	3.0	4.4	88.2	4.3	0.1	0.0
Cottonseed	0.0	0.0	0.0	0.8	22.9	3.1	18.5	54.2	0.5	0.0
Beef Tallow	0.0	0.1	0.1	3.3	25.2	19.2	48.9	2.7	0.5	0.0
Butterfat	5.5	3.0	3.6	11.6	33.4	11.4	27.8	3.1	0.6	0.0
Lard	0.0	0.1	0.1	1.4	25.5	15.8	47.1	8.9	1.1	0.0

Table 7.2 Predicted Viscosities for 15 Biodiesel Fuel Types (40 °C)

Oil Type	Viscosity (mPa.s)		
	Predicted	Lower Prediction Limit	Upper Prediction Limit
Peanut	3.69	3.58	3.79
Rapeseed	4.72	4.59	4.85
Canola	3.61	3.51	3.72
Olive	3.81	3.70	3.92
Coconut	2.25	2.19	2.32
Corn	3.46	3.36	3.56
Palm	3.74	3.64	3.85
Safflower	3.35	3.25	3.44
Sunflower	3.39	3.29	3.48
Soybean	3.41	3.32	3.51
Sunola	3.87	3.76	3.98
Cottonseed	3.46	3.36	3.56
Beef Tallow	3.94	3.83	4.05
Butterfat	3.31	3.22	3.41
Lard	3.74	3.63	3.84

Table 7.3 Predicted Surface Tension for 15 Biodiesel Fuel Types (40 °C)

	Surface Tension (mN/m)		
	Predicted	Lower Prediction Limit	Upper Prediction Limit
Peanut	28.70	27.84	29.56
Rapeseed	29.24	28.36	30.12
Canola	28.79	27.93	29.66
Olive	28.55	27.70	29.41
Coconut	26.82	26.02	27.63
Corn	28.86	27.99	29.72
Palm	28.34	27.49	29.19
Safflower	28.98	28.11	29.85
Sunflower	28.96	28.09	29.83
Soybean	28.93	28.06	29.79
Sunola	28.56	27.70	29.41
Cottonseed	28.76	27.90	29.62
Beef Tallow	28.39	27.54	29.24
Butterfat	27.86	27.03	28.70
Lard	27.69	26.86	28.52

Table 7.4 Sensitivity Analysis of SMD Regression Model #1 (Equation 6.3.3.9)

Viscosity (mPa.s)	Surface Tension (mN/m)	SMD (μm)
2.25	26.50	10.09
2.25	27.00	8.87
2.25	27.50	7.65
2.25	28.00	6.44
2.25	28.50	5.22
2.25	29.00	4.00
2.25	29.50	2.78

Table 7.5 Sensitivity Analysis of SMD Regression Model #2 (Equation 6.3.3.10)

Viscosity (mPa.s)	Surface Tension (mN/m)	SMD (μm)
2.25	26.50	11.44
2.25	27.00	11.60
2.25	27.50	11.77
2.25	28.00	11.93
2.25	28.50	12.10
2.25	29.00	12.26
2.25	29.50	12.43
2.25	26.50	11.44
2.50	26.50	11.74
2.75	26.50	12.04
3.00	26.50	12.34
3.25	26.50	12.64
3.50	26.50	12.94
3.75	26.50	13.25
4.00	26.50	13.55
4.25	26.50	13.85
4.50	26.50	14.15
4.75	26.50	14.45

Table 7.6 SMD Predicted for 15 Biodiesel Fuel Types Based on Specific Atomization Parameters

Oil Type	Sauter Mean Diameter - SMD (μm)		
	Predicted	Lower Prediction Limit	Upper Prediction Limit
Peanut	13.89	13.49	14.30
Rapeseed	15.31	14.87	15.76
Canola	13.84	13.43	14.24
Olive	13.99	13.58	14.40
Coconut	11.55	11.21	11.89
Corn	13.67	13.27	14.07
Palm	13.84	13.44	14.25
Safflower	13.58	13.18	13.98
Sunflower	13.62	13.22	14.02
Soybean	13.64	13.24	14.04
Sunola	14.07	13.66	14.48
Cottonseed	13.64	13.24	14.04
Beef Tallow	14.10	13.69	14.51
Butterfat	13.17	12.78	13.56
Lard	13.62	13.22	14.02

Table 7.7 Regression Analysis for SMD of Methyl Ester Biodiesel Fuels using Viscosity as the only Independent Variable

Regression Analysis for SMD

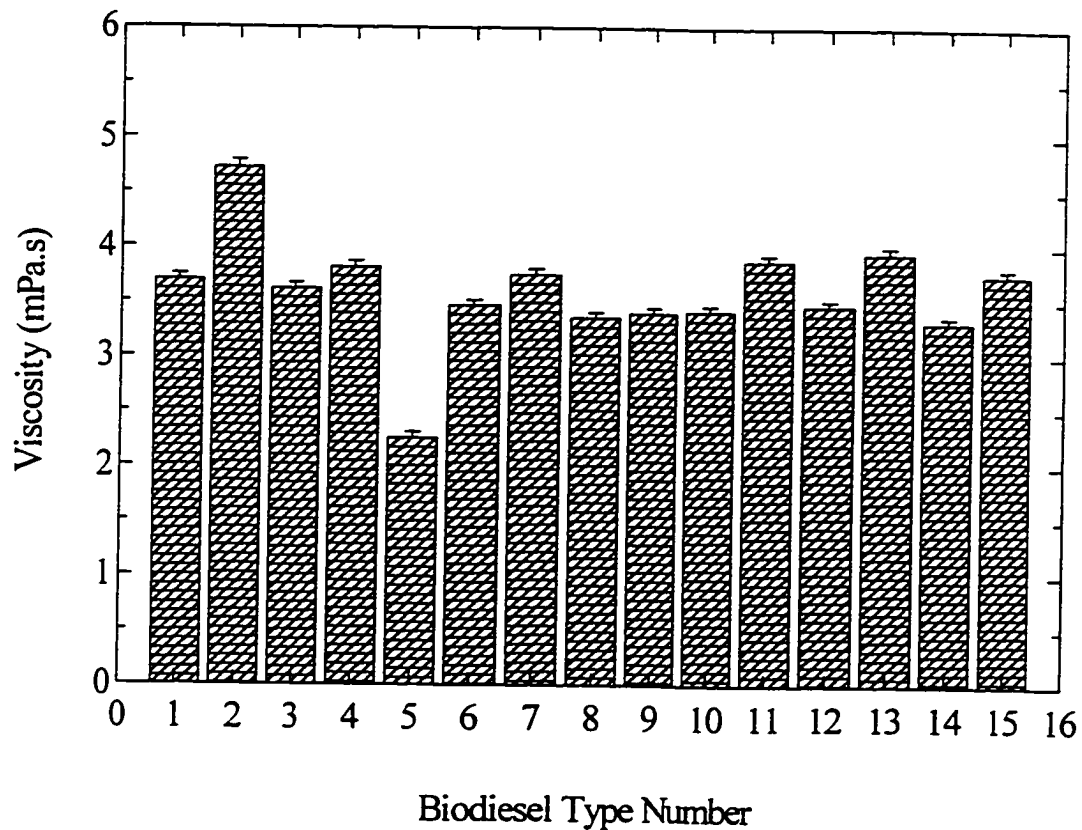
The regression equation is
 $SMD = 0.000008 + 0.00165 \mu$

Predictor	Coef	StDev	T	P
Constant	0.00000766	0.00000062	12.40	0.000
μ	0.0016514	0.0001878	8.79	0.001

S = 0.000000377 R-Sq = 95.1% R-Sq(adj) = 93.9%

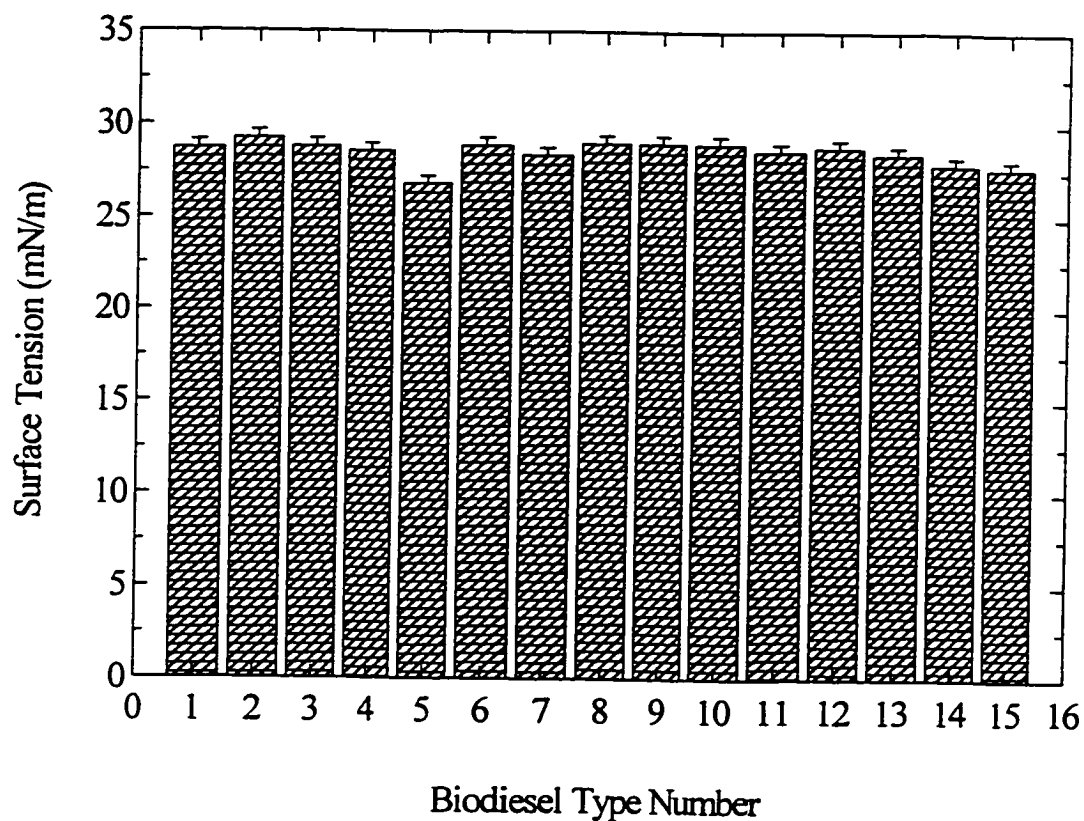
Analysis of Variance

Source	DF	SS	MS	F	P
Regression	1	1.10011E-11	1.10011E-11	77.34	0.001
Error	4	5.69011E-13	1.42253E-13		
Total	5	1.15702E-11			



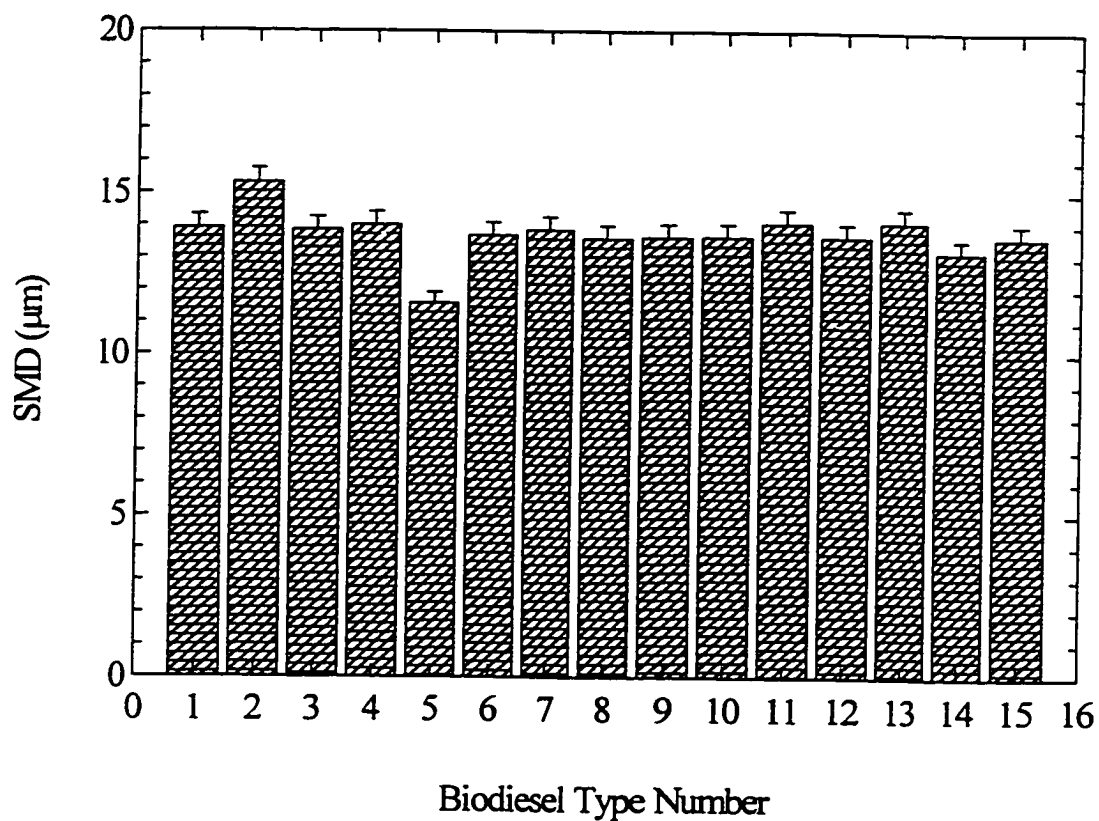
1-peanut, 2-rapeseed, 3-canola, 4-olive, 5-coconut, 6-corn, 7-palm, 8-safflower, 9-sunflower, 10-soybean, 11-sunola, 12-cottonseed, 13-beef tallow, 14-butterfat, 15-lard

Figure 7.1 Predicted Viscosities at 40 °C for 15 Methyl Ester Biodiesel Fuels



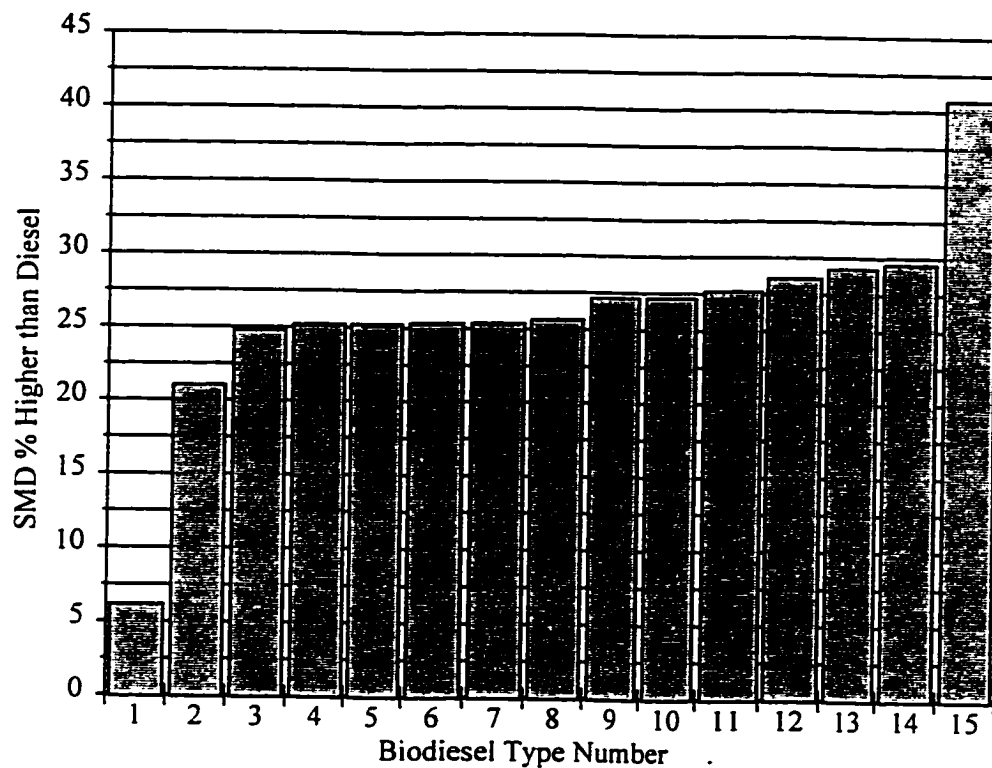
1-peanut, 2-rapeseed, 3-canola, 4-olive, 5-coconut, 6-corn, 7-palm, 8-safflower, 9-sunflower, 10-soybean, 11-sunola, 12-cottonseed, 13-beef tallow, 14-butterfat, 15-lard

Figure 7.2 Predicted Surface Tension at 40 °C for 15 Methyl Ester Biodiesel Fuels



1-peanut, 2-rapeseed, 3-canola, 4-olive, 5-coconut, 6-corn, 7-palm, 8-safflower, 9-sunflower, 10-soybean, 11-sunola, 12-cottonseed, 13-beef tallow, 14-butterfat, 15-lard

Figure 7.3 Predicted SMD for 15 Methyl Ester Biodiesel Fuels



1-coconut, 2-butterfat, 3-safflower, 4-sunflower, 5-lard, 6-soybean, 7-cottonseed, 8-corn, 9-canola, 10-palm, 11-peanut, 12-olive, 13-sunola, 14-beef tallow, 15-rapeseed

Figure 7.4 Predicted SMD for 15 Biodiesel Types Compared with Diesel Fuel

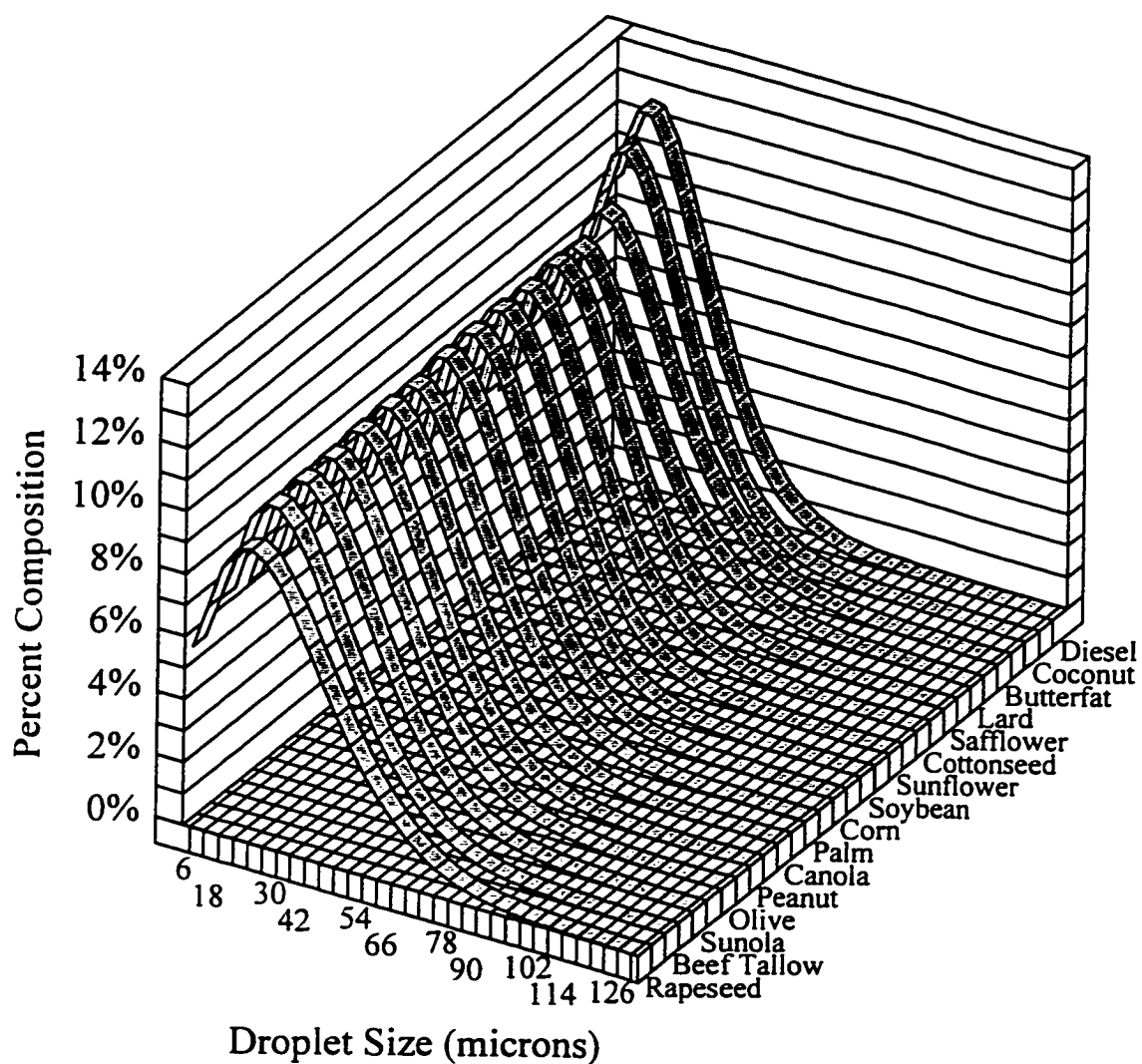


Figure 7.5 Predicted Droplet Distribution for 15 Methyl Ester Biodiesel Fuels

7.1 Inferences on Biodiesel Fuel Atomization Based on Predicted Parameters

Based on the results obtained in the previous section, the following inferences can be made about the atomization properties of the 15 methyl ester biodiesel fuel types investigated:

- The methyl esters of the fats and oils investigated have similar surface tensions, all being within 1.5 mN/m of each other. This represents a 5% difference only, thus one could conclude that any major differences in the atomization performance of these biodiesel fuels most likely will not be as a result of their surface tension.
- The viscosity of methyl ester biodiesel fuels varied by as much as 100% between different types. Therefore, unlike surface tension, major differences in the atomization performance of these biodiesel fuel types can be as a result of their viscosity.
- The SMD, which can be considered to be influenced mainly by the fuel's viscosity, is similar for most biodiesel fuels containing mainly 18:1, 18:2 and 18:3 fatty acid methyl esters. The exception to these are rapeseed oil ME and coconut oil ME which contain mainly 22:1 and 12:0 respectively; and other saturated oils e.g., butterfat, lard, beef tallow etc.
- Even though the differences in SMD for very different biodiesel fuel types can be up to 32%, the spread of the droplet distributions of all the fuel types are similar.
- In general, most biodiesel fuel types should have acceptable atomization characteristics provided they are at a temperature well above their pour point (some fats and oils are solid at room temperature).

8 CONCLUSIONS

The atomization characteristics of biodiesel fuels were investigated through experimental and analytical analyses. Viscosity and surface tension, which are two main properties affecting atomization, were also investigated. Based on the results of various analyses carried out, the following conclusions are made.

1. For the C18 biodiesel fuel component, increasing the unsaturation of the chain leads to significant decreases in its viscosity as the degree of unsaturation increases. This may also be the case at other carbon numbers.
2. Increasing the unsaturation of C18 biodiesel fuel component leads to only slight increases in the surface tension.
3. The viscosity of mixtures of fatty acid methyl esters used as biodiesel fuels can be predicted within 3% on average using a logarithmic equation which incorporates the viscosities of the pure components of the mixture.
4. The surface tension of mixtures of fatty acid methyl esters can be predicted within 2.5% on average using a mass average equation and weighted surface tension of the pure components of the mixture.
5. Viscosities of the methyl esters of typical oils may vary by as much as 100%. This variation is the major contributing factor to differences of the atomization characteristics between some biodiesel fuels.

6. Surface tension has little influence on differences of atomization characteristics between some biodiesel fuels since there is only a 5% difference on average in the surface tension of 15 fats and oil investigated.
7. Experimental results and regression analyses show that, all things being equal, the SMD of biodiesel fuels can be predicted with 5-6% accuracy using their viscosities and surface tension.
8. The difference in the SMD between some biodiesel fuels is as high as 32%. The SMD is however similar for oils containing mainly C18 unsaturated fatty acids. Oils with mainly low carbon numbers (\leq C14 saturates) fatty acids have lower SMDs, those with high carbon numbers (\geq C16 saturates) fatty acids have higher SMDs, and those with mainly C18 unsaturates have moderate SMDs.
9. The SMD of biodiesel fuels are from 5 to 40% higher than diesel fuel. The atomization characteristics of coconut oil ME biodiesel fuel was not significantly different from diesel fuel at a 95% confidence level. All other biodiesel types investigated were significantly different from diesel fuel.

9 RECOMMENDATIONS

1. The anomalies found with respect to the surface tension of some of the GC standards are of concern. It is recommended that C16 and C18 saturated and unsaturated fatty acids be acquired from natural oils by a suitable separation procedure. These acids should then be esterified into methyl esters and measurements of their surface tension and viscosity should be carried out. Other analytical methods should also be used to establish the differences between the GC standards used in these studies and samples obtained from natural sources.
2. The temperature used in these studies is below the temperature of the fuel in the injectors just before injection. Typical values of the temperature of the fuel in the injector sac should be ascertained and the atomization characteristics should be re-evaluated at these temperatures for combustion modeling applications.
3. Using a hot, pressurized, inert atmosphere, droplet evaporation characteristics should be analyzed using the Malvern system. This can be done by measuring the obscuration of the spray at sequential intervals during the spray period. The electronic system devised in this study is capable of such time sequencing. These results can be correlated with thermal properties which can be determined using differential scanning calorimetry (DSC).
4. It was observed that some of the biodiesel fuel types attacked the surface of rubberized materials causing them to become sticky. This was especially prevalent with coconut oil methyl ester. This phenomena should be thoroughly investigated using component-wise analysis to ascertain if there are particular components of the biodiesel fuels that are responsible for the deterioration of the rubberized parts.

5. The production of ethyl esters was very difficult to control during the washing phase of the process. Hard to break emulsions formed which reduced the yields of ethyl esters. Studies should be carried out to ascertain the effects, if any, of small percentages of catalyst on combustion and emissions. If no significant effects are observed, the washing process can be eliminated and high yields of ethyl esters can be achieved with catalyst deactivation only. Ethyl alcohol and vegetable oils are both from renewable sources and thus this alcohol type should be favoured over methyl alcohol.

6. The equations derived in this study for the prediction of atomization characteristics based on the fatty acid composition of the vegetable oil can be used by genetics engineers to develop a crop that would be an optimum biodiesel feedstock. This crop does not need to have high nutritional values.

REFERENCES

- Ackman, R.G., 1996. Fatty Acids in Newer Fats and Oils. In: Bailey's Industrial Oil and Fat Products. Edited by Hui, Y.H. vol. 1. John Wiley and Sons, New York. pp. 427-439
- Ali, Y., Eskiridge, K.M., and Hanna, M.A., 1995. Testing of Alternative Diesel Fuel from Tallow and Soybean Oil in Cummins N14-410 Diesel Engine. *Bioresource Technology*. vol. 53, pp. 243-254
- Ali, Y., Hanna, M.A., and Borg, J.E., 1996. In-Cylinder Pressure Characteristics of a CI Engine Using Blends of Diesel Fuel and Methyl Ester of Beef Tallow. *Trans ASAE*. vol. 39(3), pp. 799-804
- Allen, C.A.W. and Watts, K.C., 1996. A Batch Type Transesterification Unit for Biodiesel Fuels. CSAE paper 96404. CSAE, Saskatoon, SK.
- Allen, C.A.W., Watts, K.C., and Ackman, R.G., 1996. Properties of Methyl Esters of Interesterified Triacylglycerols. In: Liquid Fuels and Industrial Products from Renewable Resources. Proceeding of the Third Liquid Fuel Conference. ASAE, St. Joseph, MI. pp 73-82
- Amsden, A.A., 1993. KIVA 3: A KIVA Program with Block-Structured Mesh for Complex Geometries. Los Almos National Laboratory. Report LA-12503-MS
- Amsden, A.A., O'Rourke, P.J., and Butler, T.D., 1989. KIVA II: A Computer Program for Chemically Reactive Flows with Sprays. Los Almos National Laboratory. Report LA-11560-MS
- Arai, M., Tabata, M., Hiroyasu, H., and Shimizu, M., 1984. Disintegrating Process and Spray Characterization of Fuel Jet Injected by a Diesel Nozzle. SAE paper 840275. SAE, Warrendale, PA.
- Arnold, A.C., 1990. A Comparative Study of Drop Sizing Equipment for Agricultural Fan-Spray Atomizers. *Aerosol Science and Technology*. vol. 12, pp 431-445
- Bailer, J., Hodl, P., de Hueber, K, Mettelbach, M., Plank, C., and Schindlbauer, H., 1994. Handbook of Analytical Methods for Fatty Acid Methyl Esters Used as Diesel Fuel Substitutes. Fichte University of Technology, Vienna

- Barhey, E.A., 1992. Palm Tree Oil: Petrol Blends for IC Engines. *Agricultural Engineering*. (Winter), pp. 119-121
- Belland, J. and Harstad, K., 1990. The Dynamics of Dense and Dilute Clusters of Drops Evaporating in Large, Coherent Vortices. *Twenty-Third Symposium (International) on Combustion*. The Combustion Institute. pp. 1375-1380
- Benson, R.S. and Whitehouse, N.D., 1979. Internal Combustion Engines: A Detailed Introduction to the Thermodynamics of Spark and Compression Ignition Engines, their Design and Development. Pergamon Press, Oxford
- Bhattacharyya, S. and Reddy, C.S., 1994. Vegetable Oils as Fuels for Internal Combustion Engines: A Review. *JAER*. vol. 57(3), pp. 157-166
- Borgelt, S.C. and Harris, F.D., 1982. Endurance Test Using Soybean Oil-Diesel Fuel Mixture to Fuel Small Pre-Combustion Chamber Engines. In: Vegetable Oil Fuels. ASAE International Conference Proceedings. ASAE, St. Joseph MI. pp. 364-366
- Briscoe, B.J., Luckham, P.F., and Ren, S.R., 1992. An Assessment of a Rolling-Ball Viscometer for Studying Non-Newtonian Fluids. *Colloids and Surfaces*. vol. 62, pp. 153-162
- Buckley-Golder, D. and Langley, K., 1985. Fuel Sources for Field Machines. *Agricultural Engineering*. (Spring), pp. 28-34
- Chella, G., Tognotti, L., and Zanelli, S., 1986. A High-speed Photographic System and its Application in Spray Diagnosis. *Atomization and Spray Technology*. vol. 2, pp. 187-200
- Chigier, N.A., 1991. The Physics of Atomization. *ICLASS-91*. pp. 1-10
- Clarke, S.J., Wagner, L., Schrock, M.D., and Piennaar, P.G., 1984. Methyl and Ethyl Soybean Esters as a Renewable Fuel for Diesel Engines. *JAOCS*. vol. 61(10), pp. 1632-1638
- Cvengros, J. and Povazenec, F., 1996. Production and Treatment of Rapeseed Oil Methyl Esters as Alternative Fuels for Diesel Engines. *Bioresource Technology*. vol. 55, pp 145-150
- De Filippis, P., Giavarrini, C., Scarsella, M., and Sorrentino, M., 1995. Transesterification Process for Vegetable Oils: A Simple Control Method of Methyl Ester Content. *JAOCS*. vol. 72(11), pp.1399-1404

- Dobbins, R.A., Crocco, L., and Glassman, I., 1963. Measurement of Mean Particle Size of Sprays from Diffractively Scattered Light. *AIAA Journal*. vol. 1(8), pp 1882-1886.
- Dodge, L.G. and Cerwin, S.A., 1984. Extending the Applicability of Diffraction-Based Drop Sizing Instruments. In: Liquid Particle Size Measurement Techniques. ASTM STP 848. pp. 72-81
- Dodge, L.G., 1984. Calibration of the Malvern Particle Sizer. *Applied Optics*. vol. 23(14), pp. 2415-2419
- Dodge, L.G., Rhodes, D.J., and Reitz, R.D., 1987. Drop-size Measurement Techniques for Sprays: Comparison of Malvern Laser-Diffraction and Aerometrics Phase/Doppler. *Applied Optics*. vol. 26(11), pp 2144-2154
- Engler, C.R., Lepori, W.A., Johnson, L.A., and Yarbrough, C.M., 1992. Process Requirements for Plant Oils as Alternative Diesel Fuels. In: Liquid Fuels from Renewable Resources. Proceedings on Alternative Energy Conference. ASAE, St. Joseph MI. pp. 79-83
- Faeth, G.M., 1996. Spray Combustion Phenomena. Twenty-Sixth Symposium (International) on Combustion. The Combustion Institute. pp. 1593-1612
- Ferguson, C.R. 1986. Internal Combustion Engines: Applied Thermosciences. John Wiley and Sons, New York
- Fichot, F., Harstad, K., and Bellan, J., 1994. Unsteady Evaporation and Combustion of a Drop Cluster Inside a Vortex. *Combustion and Flame*. vol. 98, pp. 5-8
- Fisher, C.H., 1988. Evaluating and Predicting n-Fatty Acid Properties. *JAOCS*. vol. 65(10), pp. 1647-1651
- Freedman, B., Pryde, E.H., and Kwolek, W.F., 1984a. Variables Affecting the Yields of Fatty Acids from Transesterified Oil. *JAOCS*. vol. 61(10), pp. 1638-1642
- Freedman, B., Pryde, E.H., and Kwolek, W.F., 1984b. Thin layer Chromatography / Flame Ionization Analysis of Transesterified Vegetable Oils. *JAOCS*. vol. 61(7), pp.1215-1220
- Fuls, J., Hawkins, C.S., and Hugo, F.J.C., 1984. Tractor Engine Performance on Sunflower Oil Fuel. *JAER*. vol. 30, pp. 29-33

- Goering, C.E., Schwab, A.W., Daugherty, M.J., Pryde, E.H., and Heakins, A.J., 1987. Evaluation of Vegetable Oil Fuels in Engines. ASAE paper 87-1586. ASAE, St. Joseph MI.
- Goodrum, J.W., Patel, V.C., and McClendon, R.W., 1996. Diesel Injector Carbonization by Three Alternative Fuels. Trans. ASAE. vol. 39(3), pp. 817-821
- Griffiths, J.F., Halford-Maw, P.A., and Rose, D.J., 1993. Fundamental Features of Hydrocarbon Autoignition in a Rapid Compression Machine. Combustion and Flame. vol. 95, pp. 291-296
- Grunberg, L. and Nissan, A.H., 1949. Mixture Law for Viscosity. Nature. vol. 164, pp. 799-800
- Gulder, O.L., 1990. Multiple Scattering Effects in Dense Spray Sizing by Laser Diffraction. Aerosol Science and Technology. vol. 12, pp. 570-577
- Gutsche, B., 1997. Technology of Methyl Esters Production and its Application to Biofuels. Lipid. vol. 99, pp. 418-427
- Hammond Jr., D.C., 1981. Deconvolution Technique for Line-of-Sight optical scattering Measurements in Axisymmetric Sprays. Applied Optics. vol. 20(3), pp. 493-498
- Hassett, D.J. and Hasan, R.A., 1982. Sunflower Oil Methyl Ester as a Diesel Fuel. In: Vegetable Oil Fuels. ASAE International Conference Proceedings. ASAE, St. Joseph MI. pp. 123-128
- Hawkins, C.S. and Fuls, J., 1982. Comparative Combustion Studies on Various Plant Oil Esters and the Long Term Effects of an Ethyl Ester on Compression Ignition Engine. In: Vegetable Oil Fuels. ASAE International Conference Proceedings. ASAE, St. Joseph MI. pp. 184-189
- Hildebrand, J.H., 1971. Motions of Molecules in Liquids: Viscosity and Diffusivity. Science. vol.174, pp. 490-493
- Hirleman, E.D. and Dellenback, P.A., 1989. Adaptive Fraunhofer Diffraction Particle Sizing Instrument using a Spatial Light Modulator. Applied Optics. vol. 28(22), pp. 4870-4878
- Hirleman, E.D., 1984. Particle Sizing by Optical, Non-Imaging Techniques. In: Liquid Particle Size Measurement Techniques. ASTM STP 848. pp. 35-60

- Hiroyasu, H. and Kadota, T., 1974. Fuel Droplet Size Distribution on Diesel Combustion Chamber. SAE paper 740715. SAE, Warrendale, PA.
- Hiroyasu, H., 1991. Experimental and Theoretical Studies on the Structure of Fuel Sprays in Diesel Engines. ICLASS-91. pp. 17-21
- Hiroyasu, H., Arai, M., and Tabata, M., 1989. Empirical Equations for the Sauter Mean Diameter of a Diesel Spray. SAE paper 890464. SAE, Warrendale, PA.
- Irving, J.B., 1977. Viscosity of Binary Liquid Mixtures: A Survey of Mixture Equations. NEL Report 630. National Engineering Laboratory. Department of Industry, London, England
- Karasawa, T., Tanaka, M., Abe, K., Shiga, S., and Kurabayashi, T., 1991. Effects of Nozzle Configuration on the Atomization of Steady Spray. ICLASS-91. pp. 571-574
- Kihm, K.D. and Caton, J.A., 1992. Synchronization of a Laser Diffraction Drop Sizing Technique with Intermittent Spray Systems. Applied Optics. vol. 31(12), pp. 1914-1916
- Knothe, G., Dunn, R.O., and Bagby, M.O., 1996. Technical Aspects of Biodiesel Standards. INFORM. vol. 7(8), pp. 827-829
- Korus, R.A. and Jo, J., 1985. A Rapid Engine Test to Measure Injector Fouling in Diesel Engines Using Vegetable Oil Fuels. JAOCS. vol. 61(10), pp. 1563-1572
- Krawczyk, T., 1996. Biodiesel Alternative Fuel Makes Inroads but Hurdles Remain. INFORM. vol. 7(8), pp. 801-815
- Krisnngkura, K. and Simamharnop, R., 1992. Continuous Transmethylation of Palm Oil in an Organic Solvent. JAOCS. vol. 69(2), pp. 166-169
- Kusy, P.F., 1982. Transesterification of Vegetable Oils for Fuels. In: Vegetable Oil Fuels. ASAE International Conference Proceedings. ASAE, St. Joseph MI. pp. 127-131
- Lague, C.M., Lo, V. and Staley, L.M., 1987. Waste Vegetable Oil as a Diesel Fuel Extender. CAE. vol. 1, pp 27-30
- Law, C.K., 1978. Theory of Thermal Ignition in Fuel Droplet Burning. Combustion and Flame. vol. 31, pp. 285-292

- Lechner, M., Bauer-Plank, C., and Lorbeer, E., 1997. Determination of Acylglycerols in Vegetable Oil Methyl Esters by On-Line Normal Phase LC-GC. *Journal of High Resolution Chromatography*. vol. 20, pp. 581-585
- Liew, K.Y., Seng, C.E., and Lau, E.K., 1991. Viscosities of some Long-Chain Fatty Acids and their Relationship with Chain-Length. *JAOCS*. vol. 68(7), pp. 488-492
- Markley, K.S., 1960. Fatty Acids - Their Chemistry, Properties, Production, and Uses. Part 1. Interscience Publishing Inc., New York
- Marshall Jr., W.R., 1954. Atomization and Spray Drying. *Chemical Engineering Progress Monographs Series*; no. 2. American Institute of Chemical Engineers, New York
- Mazed, M.A., Summers, J.D., and Batchelder, D.G., 1985. Diesel Engine Diesel/Vegetable Oil Short Term Performance Tests. ASAE paper 851058. ASAE, St. Joseph, MI.
- Megaridis, C.M. and Sirignano, W.A., 1990. Numerical Modelling of a Vaporizing Multicomponent Droplet. Twenty-Third Symposium (International) on Combustion. The Combustion Institute. pp. 1413-1419
- Meissner, H.P. and Michaels, A.S., 1949. Surface Tension of Pure Liquids and Liquid Mixtures. *Industrial and Engineering Chemistry*. vol. 41(12), pp. 2782-2787
- Meyer, P. and Chigier, N., 1986. Dropsize Measurement Using a Malvern 2200 Particle Sizer. *Atomization and Spray Technology*. vol. 2, pp. 261-298
- Mittelbach, M. and Trillhart, P., 1988 Diesel Fuels Derived From Vegetable Oils, III. Emission Test Using Methyl Esters of Used Frying Oil. *JAOCS*. vol. 65(10), pp. 1185-1190
- Mittelbach, M., 1996. Diesel Fuels Derived from Vegetable Oils, VI: Specifications and Quality Control of Biodiesel. *Bioresource Technology*. vol. 56(1), pp. 7-11
- Mittelbach, M., Roth, G., and Bergmann, A., 1996. Simultaneous Gas Chromatographic Determination of Methanol and Free Glycerol in Biodiesel. *Chromatographia*. vol. 42(7/8), pp. 43-434
- Monnery, W.D., Svrcek, W.Y., and Mehrotra, A.K., 1995. Viscosity: A Critical Review of Practical Predictive and Correlative Methods. *Canadian Journal of Chemical Engineering*. vol. 73, pp. 3-40
- Morrison, R.T. and Boyd, R.N., 1971. Organic Chemistry. Allyn and Bacon Inc., Boston

- Msipa, C., Goering, C., and Karcher, T., 1983. Vegetable Oil Atomization in a DI Diesel Engine. *Trans ASAE*. vol. 26(6), pp.1669-1672
- Noureddini, H., Harkey, D., and Medikonduru, V., 1996. A Continuous Process for the Conversion of Vegetable oils into Biodiesel. In: Liquid Fuels and Industrial Products from Renewable Resources. Proceedings of the Third Liquid Fuel Conference. ASAE, St. Joseph, MI. pp. 83-94
- Noureddini, H. and Zhu, D., 1997. Kinetics of Transesterification of Soybean Oil. *JAOCS*. vol. 74(11), pp. 1457-1463
- Noureddini, H., Teoh, B.C., and Clemens, L.D., 1992. Viscosities of Vegetable Oils and Fatty Acids. *JAOCS*. vol. 66(12), pp. 1189-1191
- O'Rourke, P.J. and Amsden, A.A., 1987. The Tab Method for Numerical Calculation of Spray Droplet Breakup. SAE paper 872089. SAE, Warrendale, PA.
- Peterson, C. and Reece, D., 1996. Emission Characteristics of Ethyl and Methyl Ester of Rapeseed Oil Compared With Low Sulphur Diesel Control Fuel in a Chassis Dynamometer Test of a Pickup Truck. *Trans ASAE*. vol. 39(3), pp. 805-816
- Peterson, C.L. and Mora, P., 1985. The Effect of Fumigation and Transesterification on Injector Coking. ASAE paper 85-3572. ASAE, St. Joseph, MI.
- Peterson, C.L., 1986. Vegetable Oil as Diesel Fuel: Status and Research Priorities. *Trans ASAE*. vol. 29(5), pp. 1413-1417
- Peterson, C.L., Reece, D.L., Cruz, R., and Thompson, J., 1992. A Comparison of Methyl and Ethyl Esters of Vegetable Oils as Diesel Fuel Substitutes. In: Liquid Fuels from Renewable Resources. Proceedings on Alternative Energy Conference. ASAE, St. Joseph, MI. pp. 99-105
- Peterson, C.L., Kordus, R.A., Mora, J.P., and Madsen, J.P., 1987. Fumigation with Propane and Transesterification Effects on Injector Coking with Vegetable Oil Fuels. *Trans ASAE*. vol. 31(1), pp. 28-35
- Pischinger, G.H., Falcon, A.M., Siekmann, R.W., and Fernandes, F.R., 1982. Methyl Esters of Plant Oil as Diesel Fuels, Either Straight or in Blends. In: Vegetable Oil Fuels. ASAE International Conference Proceedings. ASAE, St. Joseph, MI. pp. 198-204

- Plank, C. and Lorbeer, E., 1994. On-Line Liquid Chromatography - Gas Chromatography for the Analysis of Free and Esterified Sterols in Vegetable Oil Methyl Esters used as Diesel Fuel Substitutes. *Journal of Chromatography A*. vol. 683(1), pp. 95-104
- Pryde, E.H., 1983. Vegetable Oils as Diesel Fuels: Overview. *JAOCS*. vol. 60(8), pp. 1557-1562
- Quale, O.R., 1953. The Parachors of Organic Compounds: An Interpretation and Catalogue. *Chemical Reviews*. vol.53, pp. 439-475
- Quick, G.R., 1980. Developments in the Uses of Vegetable Oils as Fuel for Diesel Engines. ASAE paper 801525. ASAE, St. Joseph, MI.
- Ralston, A.W., 1948. Fatty Acids and Their Derivatives. John Wiley & Sons, New York
- Reid, J.F., Hansen, A.C., and Goering, C. E., 1989. Quantifying Diesel Injection Coking with Computer Vision. *Trans ASAE*. vol. 35(2), pp. 1503-1511
- Reid, R.C., Prausnitz, J.M., and Poling, B.E., 1987. The Properties of Gases and Liquids. McGraw-Hill, New York
- Reitz, R.D. and Bracco, R.B., 1979. On the Dependence of Spray Angle and Other Spray Parameters on Nozzle Design and Operating Conditions. SAE paper 790494. SAE, Warrendale, PA.
- Reitz, R.D. and Diwakar, R., 1987. Structure of High-Pressure Fuel Sprays. SAE paper 870598. SAE, Warrendale, PA.
- Rizk, N.K. and Lefebvre, A.H., 1984. Measurement of Drop-Size Distribution by a light-Scattering Technique. In: Liquid Particle Size Measurement Techniques. ASTM STP 848. pp. 61-71
- Ryan III, T.W., Dodge, L.G., and Callahan, T.J., 1984. The Effects of Oil Properties on Combustion in Two Different Diesel Engines. *JAOCS*. vol. 61(10), pp. 1610-1617
- Schumacher, L.G., 1994. The Use of Strata-Fuel in Blends of Soydiesel. ASAE paper 946533. ASAE, St. Joseph, MI.
- Sidahmed, M.M., 1996a. A Theory for Predicting the Size and Velocity of Droplets from Pressure Nozzles. *Trans ASAE*. vol. 39(2), pp. 385-391

Sidahmed, M.M., 1996b. A Model for Predicting the Droplet Size from Liquid Sheets in Airstreams. *Trans ASAE*. vol. 39(5), pp. 1651-1655

Siekman, R.W., Pischinger, G.H., Blackman, D., and Cavalho, L.D., 1982. The Influence of Lubricant Contamination by Methyl Esters of Plant Oils and Oxidant Stability and Life. In: Vegetable Oil Fuels. ASAE International Conference Proceedings. ASAE, St. Joseph, MI. pp. 209-214

Stambuleanu, A., 1976. Flame Combustion Processes in Industry. Abacus Press, Tunbridge Wells, England

Strahle, W.C., 1993. An Introduction to Combustion. Gordon and Breach Science Publishers, Langhorne, PA.

Swern, D., 1979. Bailey's Industrial Oil and Fat Products. 1, John Wiley and Sons, New York. pp. 177-232

Swithenbank, J., Beer, J.M., Taylor, D.S., Abbot, D., and McCreath, G.C., 1977. A Laser Diagnostic Technique for the Measurement of Droplet and Particle Size Distribution. In: Experimental Diagnostics in Gas Phase Combustion Systems. Progress in Astronautics and Aeronautics. Edited by B.T. Zinn. vol.53. pp. 421-477

Tahir, A.R., Lapp, H.M., and Buchanan, L.C., 1982. Sunflower Oil as Fuel for Compression Ignition Engines. In: Vegetable Oil Fuels. ASAE International Conference Proceedings. ASAE, St. Joseph, MI. pp 82-89

Taylor, C.F., 1985a. The Internal Combustion Engine in Theory and Practice - Thermodynamics, Fluid Flow, Performance. vol. 1. MIT Press, Cambridge, MA.

Taylor, C.F., 1985b. The Internal Combustion Engine in Theory and Practice - Combustion, Fuels, Materials, Design. vol. 2. MIT Press, Cambridge, MA.

Van Gerpin, J., 1996. Cetane Testing of Biodiesel. In: Liquid Fuels and Industrial Products from Renewable Resources. Proceeding of the Third Liquid Fuel Conference. ASAE, St. Joseph, MI. pp. 197-206

Vander Griend, L., Feldman, M., and Peterson, C.L., 1988. Properties of Rape Oil and its Methyl Esters Relevant to Combustion Modeling. ASAE paper 886507. ASAE, St. Joseph, MI.

Vinyard, S., Renoll, E.S., Goodling, J.S., Hawkins, L., and Bunt, R.C., 1982. Properties and Performance Testing With Blends of Biomass Alcohols, Vegetable Oils and Diesel Fuels. In: Vegetable Oil Fuels. ASAE International Conference Proceedings. ASAE, St. Joseph MI. pp. 287-292

Wagner, L.E., Clarke, S.J. and Schrock, M.D., 1984. Effects of Soybean Oils Esters on the Performance, Lubricating Oil, and Water of Diesel Engines. International Conference on Combustion in Engineering, paper 841385. The Institute of Mechanical Engineers.

Wakisaka, T., Shimamoto, Y., Isshiki, Y., Akamatsu, S., and Ibaraki, K., 1997. Improvement in a Droplet Breakup Model for Numerical Analysis of Fuel Sprays. Japan Society of Automotive Engineers. vol. 18(1), pp. 3-10

Williams, A., 1973. Combustion of droplets of Liquid Fuels: A Review. Combustion and Flame. vol. 21, pp. 1-31

Wong, S., Chang, J., and Yang, J, 1993. Autoignition of Droplets in Nondilute Monodisperse Clouds. Combustion and Flame. vol. 94, pp. 397-402

Zubik, J., Sorenson, S.C., and Goering, C.E., 1984. Diesel Engine Combustion of Sunflower Oil Fuels. Trans ASAE. vol. 27(3), pp. 1252-1259

APPENDIX A

Design of an Engine Test Facility for Biodiesel Fuels

Engines

Two, virtually identical, single cylinder, air-cooled engines were obtained differing only in the combustion chamber design. One was direct injection, Kubota AC 60-DQ1, and the other was indirect injection, Kubota OC 60-DQ1. Both have a continuous rating of 4.2 kW (5.6 HP at 3600 RPM with an intermittent power up to 4.6 kW at the same speed. Both have the same displacement of 276 cm³ with the same bore and stroke, 72 mm and 68 mm respectively. Their speed range is 1300 to 3800 RPM. The direct injection system uses a MD type mini pump with injection time in the range of 17-19 degrees BTDC giving an injection pressure of 22.4-23.4 MPa (3250-3400 psi). Its compression ratio is 20.5:1. The indirect injection system is a three - vortex combustion system using an NC type (DENSO) fuel pump with injection 15-17 degrees BTDC at a pressure of 13.9-14.7 MPa (2020-2130) psi. Its compression ratio is 24.5:1.

In order to change the injection angle, extensions to the cam driver for the pumps have been designed so that the pump can be rotated around the cam. No provision has been made for varying the injection pressure as yet.

Fuel System

Two fuel tanks for each engine are in place at all times, one for diesel fuel and one for the biodiesel, so that the engines can be started and stopped on diesel fuel. Only the biodiesel tanks are supported on a strain-gauged cantilever for monitoring fuel consumption.

Dynamometers

Two D.C. electric motors made by ECK Dynamo and Motor Co. were used as generators. Each is rated at 10 HP at 1210 RPM. A gear down ratio of 3:1 is necessary because of the different rated speeds for engines and dynamometers.

In order to have the generators supply adequate torque at low speeds, a special electrical load system was implemented. The generators were rated at 10 HP at 1210 RPM. However, as the engines were loaded the generated EMF was reduced as well as the armature current due to the decrease in rpm with engine load. This, in turn, resulted in a reduced torque which was insufficient to further load down the engines. To conquer this problem the field strength was maintained at maximum by way of a separate power supply. Then, as the RPM and generated EMF reduced, the armature current was increased by switching in specially selected load resistors in parallel with a permanent load. By this means, the total effective load resistance decreased and thus armature current increased even though a lower EMF was being generated. With higher armature current the torque increased and the engines were further loaded. With this system the generators were capable of loading the engines at full throttle throughout their speed ranges.

One advantage of using the electric motors is that they can be used to start the diesels by connecting their armature to the electric mains and then disconnecting them to run as generators when the engines are started. This has the distinct advantage of avoiding the need of a clutch system with its attendant mechanical inefficiencies. The circuit diagram is shown in Figure A.1.

The D.C machines were mounted on bearings to allow them to rotate around their axes. The torque developed was measured by a "Cardinal" Z50, S-type load cells with a capacity of 50 lb, and an overload up to 75 lb. Guards were also built to prevent the load cells from being

overloaded. Considerable variations in the output from the load was caused by the transmission of engine vibration through the frame. This was alleviated by floating the frames between 2.5 cm thick shock rubbers which were pinned to the ground. The load cells were also mounted through small rubber mounts at each end. Electrical filters were also designed and installed to filter the electrical noise picked up by the load cells.

The speed measurement is obtained using an optical pick-up system shown in Figure A.2. The shaft of the D.C machine has one half of its circumference painted in flat black while the other half is painted with a highly reflective aluminium paint. As the shaft rotates high and low voltage levels are sent out by the optical sensors as the dark and bright portion of the shaft alternate. The result is a square wave being formed. This signal is passed through an op-amp and then a comparator to condition it to a perfect square wave of fixed amplitude. This square wave signal is then passed to a monostable oscillator which produces a pulse of a fixed duration whenever it receives a positive going edge of the square wave. The duration of the pulse from the monostable is set equal to the period of the frequency corresponding to the highest expected engine rpm. The fixed duration pulse is then fed to an integrator which outputs an analog voltage corresponding linearly to the speed of the engine. A magnetic pickup was much more expensive.

The power is transferred between the electric motor and diesel engines via a gear belt drive system. This was chosen since it has little power loss due to friction, quiet operation, high speed capability, is less dangerous if it breaks during operation, has a reasonably low cost and no unusual maintenance is required. Figure A.3 shows a schematic outline of the layout of the test units and Figure A.4 shown an overall view of the engine and D.C motor setup.

Exhaust System

The exhaust from both engines are ducted to a common pipe. Thermocouple wells situated right after each engine so as to get a true exhaust temperature are constructed in the exhaust pipes. An MPSI's PGA 9000 gas analyzer was purchased to obtain the CO₂, the O₂, the CO and the hydrocarbons. This analyzer was chosen for its low price and its capability of interface with a computer. When it was first connected to the computer, it was found that the manufacturer's advertised "computer interface" meant that, if the computer had VT100 emulation capability, then the screen could be visualized on and controlled by the computer. This was inadequate for our purposes. However, it was found by trial and error that the serial printer interface was capable of being used as a data send/receive port. In this mode, commands to print a "snap-shot" of the exhaust gas composition were sent from a PC's RS232 interface along a null modem cable to the gas analyzer and the response from the gas analyzer was in turn recorded by the PC along that same line.

The exhaust from diesel engines can contain considerable unburned carbon. At this point, no carbon filter is built into the system.

Data Acquisition System

A Hewlett Packard 3497A data acquisition system is used and controlled by a HP 87 computer. The acquisition system is very accurate (5 ½ digits) and has cards for temperature, analog input and digital output. Because of its high accuracy, it cannot sample at high speeds (above 80 Hz) on more than one channel at a time. The thermocouple card had to be modified for the cold junction reference temperature for Chromel Alumel type K thermocouples that are required in this study.

The data is later transferred via the serial interface to a remote PC for further analysis and storage.

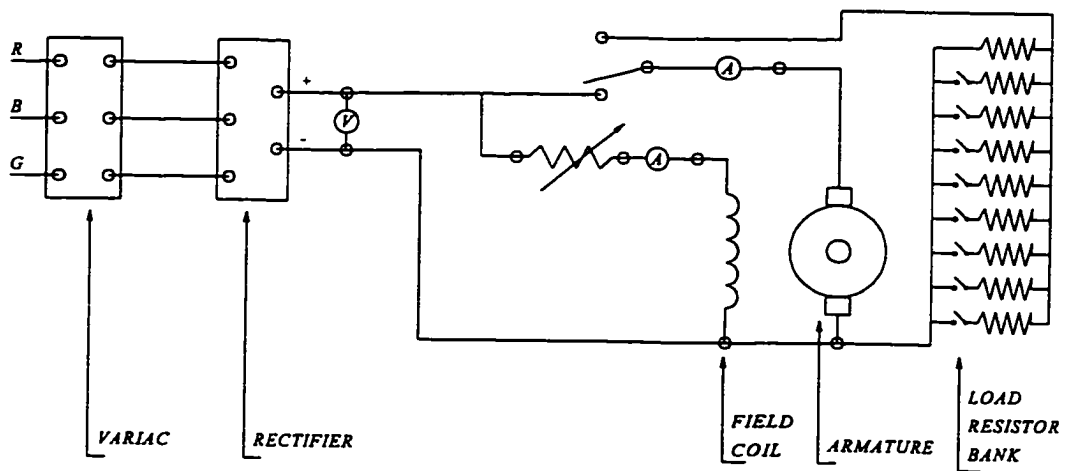


Figure A.1 Schematic of Circuit Diagram for D.C. Machines

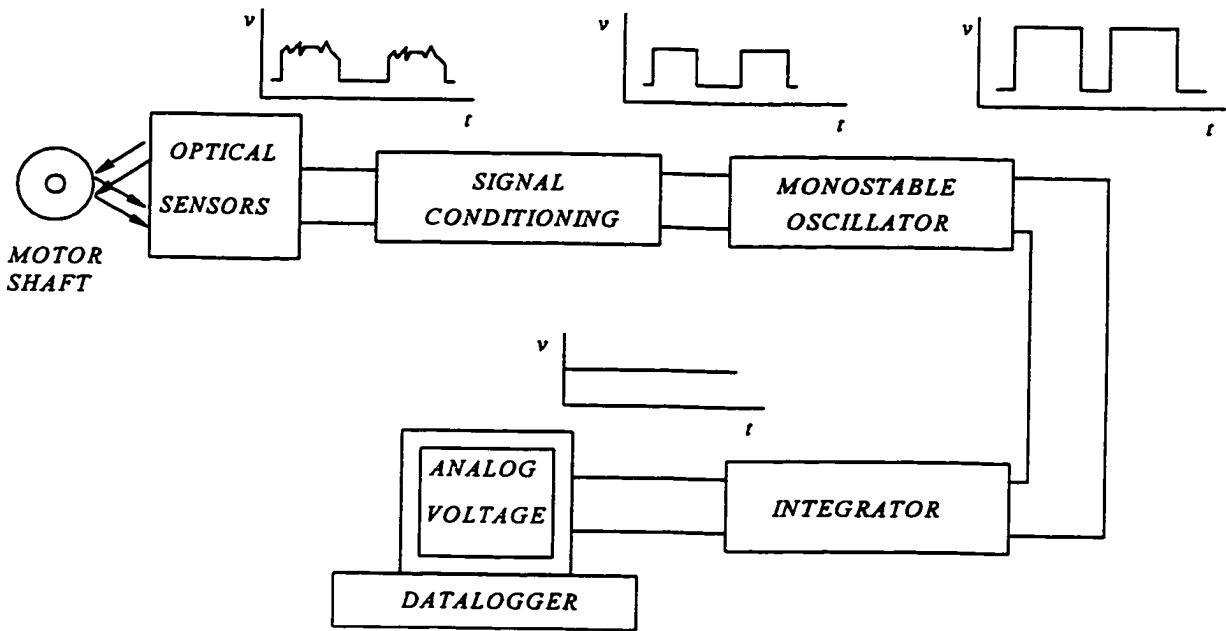


Figure A.2 Schematic of Optical Speed Sensor

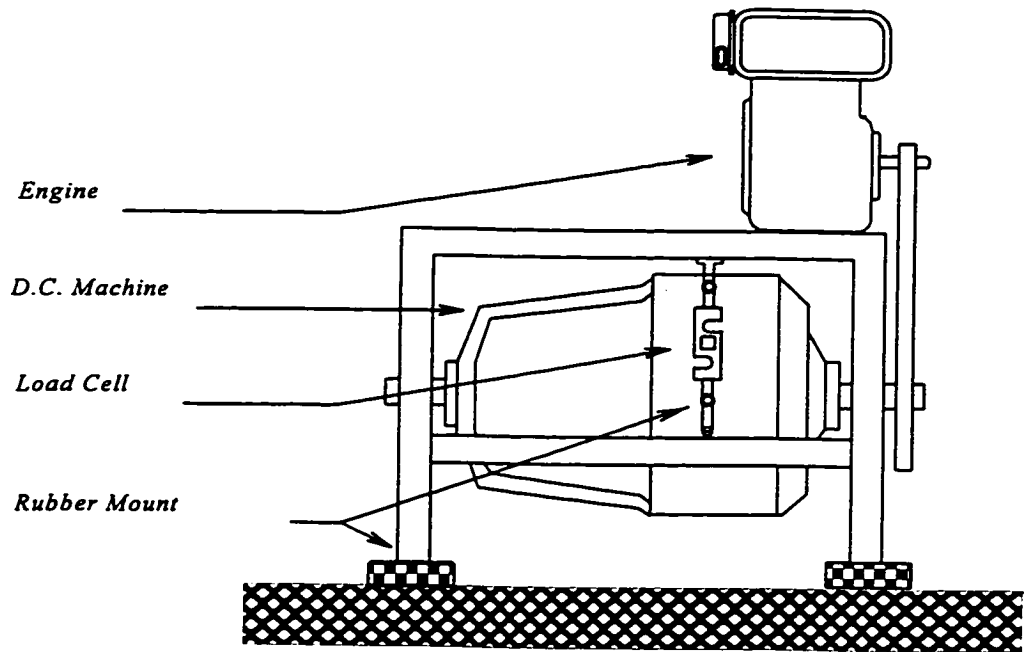
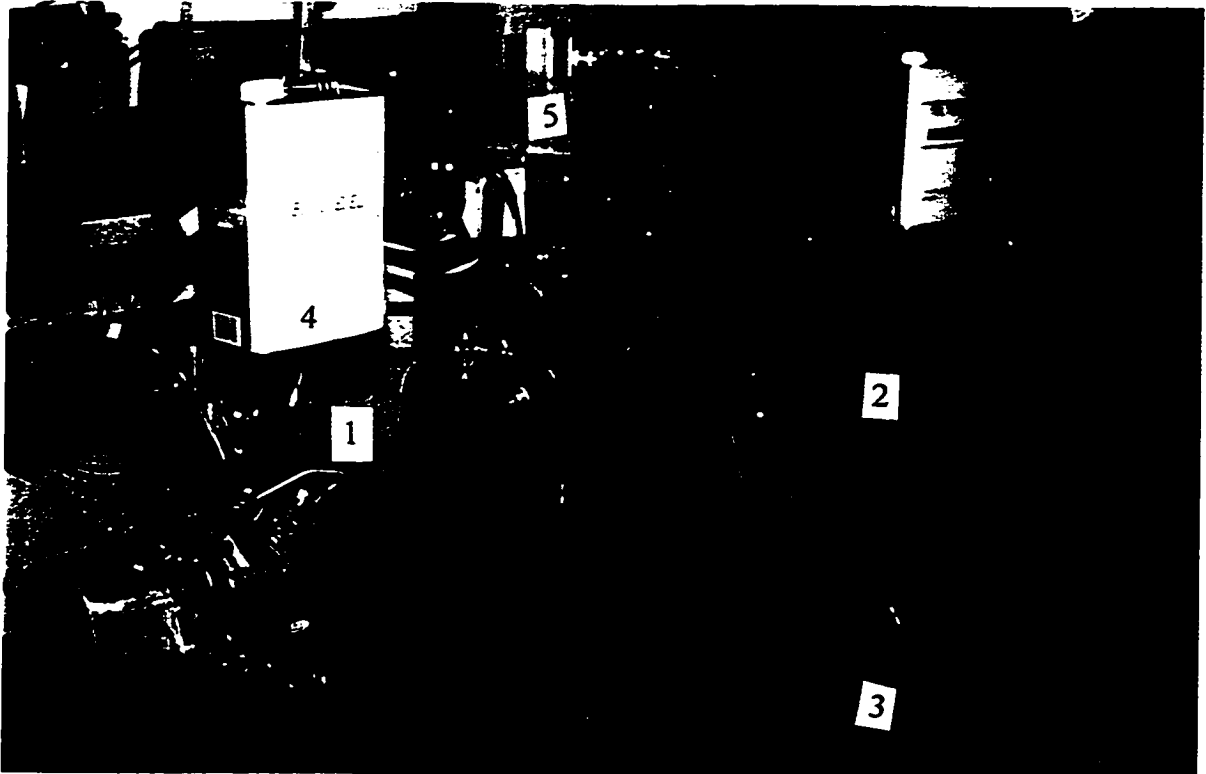


Figure A.3 Schematic Layout of Test Unit



1- DI Engine, 2- IDI Engine, 3- DC Machine, 4- Fuel Tank, 5- Electronics for rpm

Figure A.4 Overall View of the Engine and D.C Motor Setup

APPENDIX B

Sensitivity Analysis of Thermal Properties

The model used for the determination of the burning rate constant K_b (also called the evaporation constant) of a fuel is summarized by Williams (1973). This incorporates the thermal conductivity, latent heat, specific heat capacity, density and boiling point of the fuel.

Following a relatively straight forward, non-trivial analysis [Williams, 1973] it was shown that the burning rate constant K_b (m^2/s) can be given by:

$$K_b = \frac{8 \lambda}{C_p \rho_f} \ln (1 + B_{ev}) \quad (B.1)$$

and

$$B_{ev} = \frac{C_p (T_g - T_b)}{L} \quad (B.2)$$

where:

- λ - thermal conductivity of fuel (W/m.K)
- L - latent heat of vaporization of fuel (J/kg)
- C_p - specific heat capacity of fuel (J/kg.K)
- ρ_f - density of fuel (kg/m^3)
- T_b - boiling point of fuel (K)
- T_g - gas atmosphere temperature (K)

The sensitivity analysis procedure described in Chapter 3 was followed to determine to what extent the thermal properties of biodiesel fuels affect their burning rate. The mean values of the properties used in the analysis are given in Table B.1. The results of the sensitivity

analysis for the thermal properties are shown graphically in Figures B.1 to B.4 for normalized burning rate constant (Kb_i / Kb_{max}).

For $\pm 5\%$ variation in **density** the results show that there was 9% variation in Kb from its maximum. For a $\pm 5\%$ variation in **latent heat**, **specific heat**, and **thermal conductivity**, the variation in the burning rate constant (Kb) from their individual maximum values were 7%, 2%, and 9% respectively. These results are in agreement with what is expected based on the theory of vaporization of a droplet. That is, a droplet is first heated through conduction to its boiling point, then additional heat has to be provided to vaporize the droplet. It is the vapour of the droplet which eventually mixes with the surrounding oxygen and, if the conditions are suitable, results in a run-away chain reaction or autoignition.

Table B.1 Mean Value of Thermal Properties used for Sensitivity Analysis

Property	Mean value
Density	871.4 kg/m ³
*Heat of Vaporization	297 J/g
*Thermal Conductivity	0.17 W/m.K
*Specific Heat Capacity	2.47 J/g.K
*Boiling Point	609 K

* From Vander Griend *et al.* (1988) based on Rape Oil Methyl Ester.

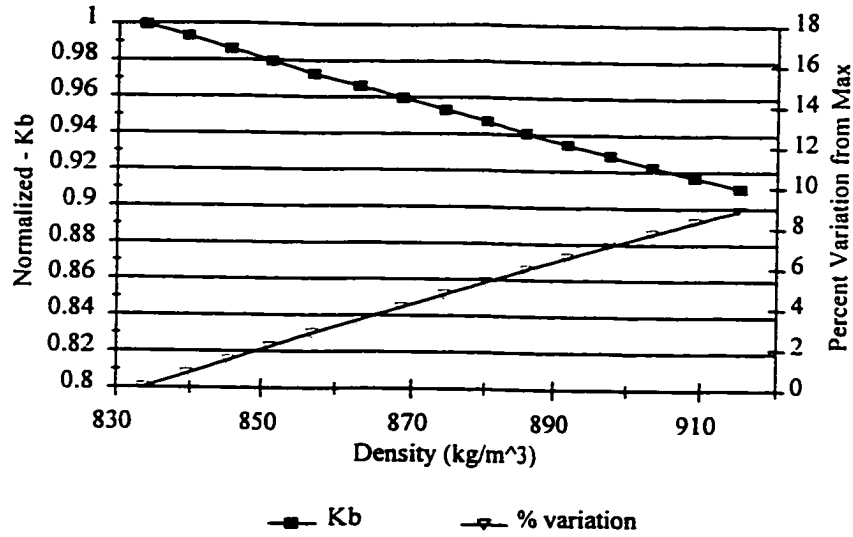


Figure B.1 Variation of Normalized Burning Rate Constant (Kb_i / Kb_{max}) with 5% Variation of Density for Constant Specific Heat Capacity, Thermal Conductivity and Latent Heat of Vaporization

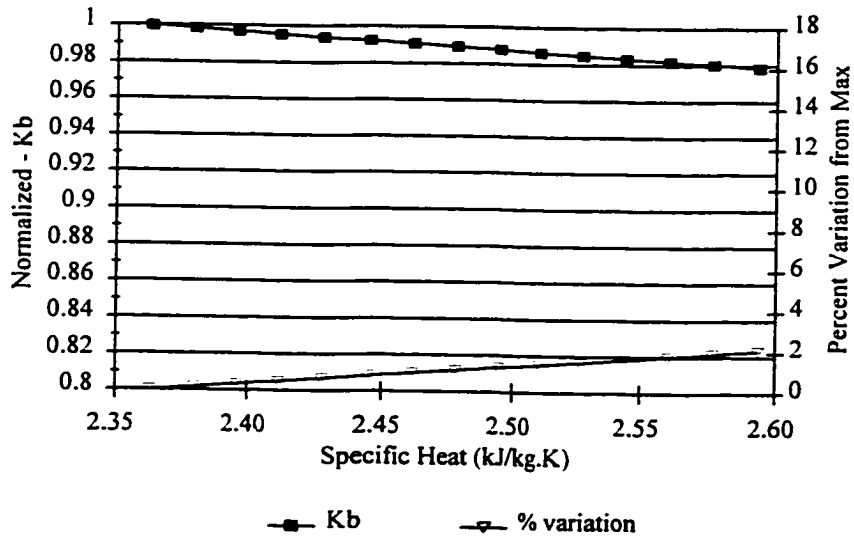


Figure B.2 Variation of Normalized Burning Rate Constant (Kb_i / Kb_{max}) with 5% Variation of Specific Heat Capacity for Constant Density, Thermal Conductivity and Latent Heat of Vaporization

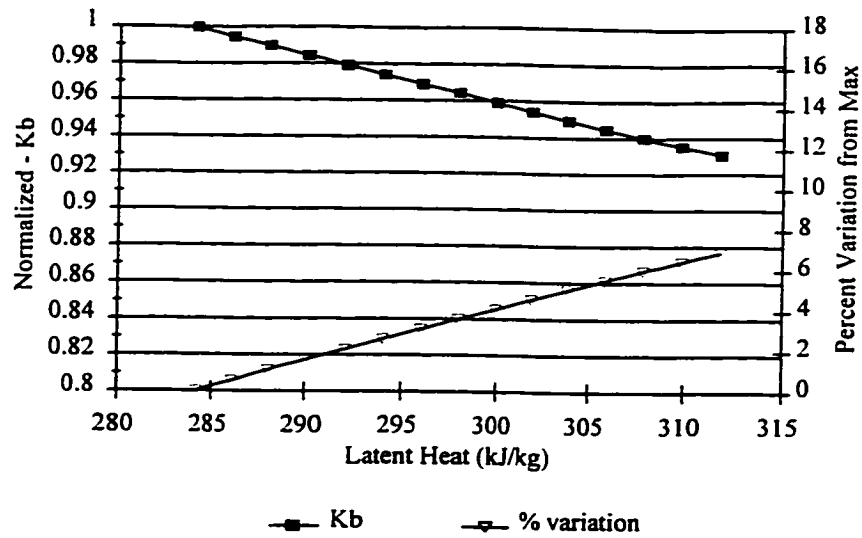


Figure B.3 Variation of Normalized Burning Rate Constant (Kb_i / Kb_{max}) with 5% Variation of Latent Heat of Vaporization for Constant Density, Thermal Conductivity and Specific Heat Capacity

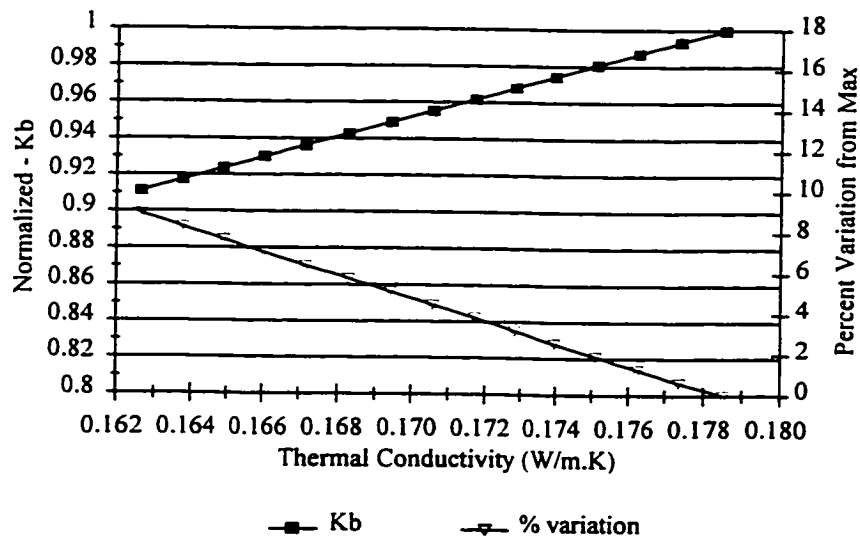


Figure B.4 Variation of Normalized Burning Rate Constant (Kb_i / Kb_{max}) with 5% Variation of Thermal Conductivity for Constant Density, Latent Heat of Vaporization and Specific Heat Capacity

APPENDIX C

C - Programs Used to Carry Out Sensitivity Analysis on Biodiesel Properties

Atomization Properties

/* C - program to carry out sensitivity analysis of atomization properties*/

```
#include <stdio.h>
#include <math.h>
#include <stdlib.h>
#define maxarry 50
#define nstep 15
```

```
main()
{
```

```
double rho[maxarry], rhobar, dtrho, rhomax, rhomin, rho_l, rhogas;
double sigma[maxarry], sigmabr, dtsigma, sigmamx, sigmamn, sigma_l;
double mubar, mu[maxarry], mumax, mumin, dtmu, mu_l, mugas, nu, nugas;
double vel[maxarry], velbar, vel_l, dia, dia_l;
double pline, patm, pgas, tatm, tgas, vary_r, vary_s, vary_m;
double nozeff, poly, cr, molwgt, unigas, rgas;
double weber_1[maxarry], weber_2[maxarry], webar;
double reynolds_1[maxarry], reynolds_2[maxarry], rebar;
double const1_k[maxarry], const2_k[maxarry], const3_k[maxarry], visc_crit;
double smd_1[maxarry], smd_2[maxarry], smd_3[maxarry], smd_ls, smd_hs;
double rhos, rhogs, mus, sigmas, dias, vels;
double sqrt(double), pow(double, double);
double weber_cal(double, double, double, double);
double reynolds_cal(double, double, double, double);
double atomiz_cal1(double, double);
double atomiz_cal2(double, double, double, double);
double smdls_cal(double, double, double, double, double, double);
double smdhs_cal(double, double, double, double, double, double);
double smd2_cal(double, double, double, double, double, double);
int i=1;
```

```
FILE *infile, *outfile, *fopen();
infile=fopen("atomizin.dat", "r"); /* open input data file */
outfile=fopen("atomiout.dat", "w"); /* open output data file */
fscanf(infile, "%lf,%lf,%lf,%lf", &rhobar, &sigmabr, &mubar, &dia);
/*density, surf tens, viscosity, noz dia */
fscanf(infile, "%lf,%lf,%lf", &pline, &patm, &tatm); /*press line & gas, atm tempt */
fscanf(infile, "%lf,%lf,%lf", &poly, &cr, &nozeff); /* polytropic index, compres ratio, nozzle eff */
fscanf(infile, "%lf,%lf,%lf", &vary_r, &vary_s, &vary_m); /*percentage variation on variables */
fscanf(infile, "%lf,%lf", &molwgt, &unigas); /*molecular wgt, gas constant*/
printf("%s\n", "reading file done:\n");
printf("%g,%g,%g,%g\n\n", rhobar, sigmabr, mubar, dia);
printf("%g,%g,%g\n\n", pline, patm, tatm);
```

```

printf("%g,%g,%g\n\n",vary_r,vary_s,vary_m);
printf("%g,%g,%g,%g\n\n",poly,cr,nozeff);
printf("%g,%g,%g\n\n",molwgt,unigas);

/* cal max, min & increment density */
rhomax = rhobar + rhobar*vary_r/100.0;
rhomin = rhobar - rhobar*vary_r/100.0;
dtrho= (rhomax - rhomin)/((double)nstep);

/* cal max, min & increment surface tension */
sigmamx = sigmabr + sigmabr*vary_s/100.0;
sigmamn = sigmabr - sigmabr*vary_s/100.0;
dtsigma= (sigmamx - sigmamn)/((double)nstep);

/* cal max, min & increment viscosity */
mumax = mubar + mubar*vary_m/100.0;
mumin = mubar - mubar*vary_m/100.0;
dtmu= (mumax - mumin)/((double)nstep);

/* cal gas pressure in cylinder ==> p2/p1 = (v1/v2)^n */
pgas = patm * pow(cr,poly);

/*Calculate gas temperature in cylinder ==> T2/T1=(p2/p1)^(n-1/n)*/
tgas = tatm * pow( (pgas/patm), ((poly - 1.0)/poly) );

/*Calculate gas density & viscosity in cylinder */
rgas = unigas / molwgt * 1000.0; /* (J/kg.K) */
rhogas = pgas / (rgas * tgas); /* kg/m^3 */
mugas = 2.86429e-5 + ( 3.14651e-8 * (tgas-273.0) ); /* Pa.s */
printf("going to loop #1:\n");

/*Calculate parameters vector */
i=1;
while (i <= nstep) {
    /*printf("%s%d\n","i = ",i);*/
    rho[i] = rhomin + ((double) i)*dtrho ;
    mu[i] = mumin + ((double) i)*dtmu;
    sigma[i] = sigmamn + ((double) i)*dtsigma ;
    vel[i] = sqrt( 2.0 * nozeff*(pline-pgas)/rho[i]);

    ++i ;
}

/* ***Constant Surface Tension Weber #*** */
fprintf(outfile,"%s\n\n","For constant Surface Tension");
fprintf(outfile,"%s,%s,%s\n","Density ","Velocity ","Weber # ");
printf("%s,%f\n","const s.t d=","dia);
for (i=1; i <= (nstep); ++i) {
    weber_1[i]=weber_cal(rho[i],sigmabr,vel[i],dia);
    printf("%f,%f,%f\n",rho[i],vel[i],weber_1[i]);
}

```

```

        fprintf(outfile,"%f,%f,%f\n",rho[i],vel[i],weber_1[i]);
    }

/* ***Constant Density Weber #*** */
fprintf(outfile,"%s\n\n","For constant Density");
fprintf(outfile,"%s,%s\n","Surface Tension ","Weber #");
printf("const den:\n");
velbar= sqrt(2.0 * nozeff*(pline-pgas)/rhubar);
for (i=1; i <= (nstep); ++i) {
    weber_2[i]=weber_cal(rhubar,sigma[i],velbar,dia);
    printf("%f,%f\n",sigma[i],weber_2[i]);
    fprintf(outfile,"%f,%f\n",sigma[i],weber_2[i]);
}

/* ***Constant Viscosity *** */
fprintf(outfile,"%s\n\n","For constant Viscosity");
fprintf(outfile,"%s,%s,%s\n","Density ","Velocity ","Reynolds # ");
printf("%s,%f\n","const s.t d=" ,dia);
for (i=1; i <= (nstep); ++i) {
    reynolds_1[i]=reynolds_cal(rho[i],mubar,vel[i],dia);
    printf("%6.3f,%6.3f,%10.3f\n",rho[i],vel[i],reynolds_1[i]);
    fprintf(outfile,"%f,%f,%f\n",rho[i],vel[i],reynolds_1[i]);
}

/*Constant Density Reynolds #*/
fprintf(outfile,"%s\n\n","For constant Density");
fprintf(outfile,"%s,%s\n","Viscosity ","Reynolds #");
printf("const den:\n");
velbar= sqrt(2.0 * nozeff*(pline-pgas)/rhubar);
for (i=1; i <= (nstep); ++i) {
    reynolds_2[i]=reynolds_cal(rhubar,mu[i],velbar,dia);
    printf("%10.5f,%10.3f\n",mu[i],reynolds_2[i]);
    fprintf(outfile,"%f,%f\n",mu[i],reynolds_2[i]);
}

/* *****Determine atomization characteristics - K ***** */
rebar=rhubar * velbar * dia / mubar;
webar=rhubar * pow(velbar,2.0) * dia / sigmabr;

/* **Constant density and viscosity ==> rhobar,mubar,sigma(i),Rebar & Weber_2** */

printf("%s\n","K_value for atomization ==>const dens and visc:\n");
fprintf(outfile,"%s\n","K_value for atomization ==>const dens and visc:\n");
fprintf(outfile,"%s,%s,%s\n","Visc_crit","sigma","Const l_k");
for (i=1; i<=nstep; ++i) {
    if( ( rhobar/rhogas * pow((rebar/weber_2[i]),2.0) ) > 1.0) {
        constl_k[i]=atomiz_call(rhubar,rhogas);
        visc_crit=1.0;
    }
}

```

```

        else {
            const1_k[i]=atomiz_cal2(rhobar,rhogas,weber_2[i],rebar);
            visc_crit=0.0;
        }
    fprintf(outfile,"%f,%f,%f\n",visc_crit,sigma[i],const1_k[i]);
}

/* **Constant density and surf tens ==> rhobar,mu[i],sigmabr,Reynolds_2 & We_bar** */

printf("K - value from aotmozation characteristics -- Const Dens & Surf tens\n ");
fprintf(outfile,"K - value from aotmozation characteristics -- Const Dens & Surf tens\n ");
fprintf(outfile,"%s,%s,%s\n","Visc_crit","Mu","Const2_k");
for (i=1; i<=nstep; ++i) {
    if( ( rhobar/rhogas * pow((reynolds_2[i]/webar),2.0) ) > 1.0) {
        const2_k[i]=atomiz_cal1(rhobar,rhogas);
        visc_crit=1.0;
    }
    else {
        const2_k[i]=atomiz_cal2(rhobar,rhogas,webar,reynolds_2[i]);
        visc_crit=0.0;
    }
    fprintf(outfile,"%f,%f,%f\n",visc_crit,mu[i],const2_k[i]);
}

/* **Constant visc and surf tens ==> rho[i],mubar,sigmabr,Reynolds_1 & weber_1** */

printf("K - value from aotmozation characteristics -- Const visc & Surf tens\n ");
fprintf(outfile,"K - value from aotmozation characteristics -- Const Visc & Surf tens\n ");
fprintf(outfile,"%s,%s,%s\n","Visc_crit","rho","Const2_k");
for (i=1; i<=nstep; ++i) {
    if( ( rho[i]/rhogas * pow((reynolds_1[i]/weber_1[i]),2.0) ) > 1.0) {
        const3_k[i]=atomiz_cal1(rho[i],rhogas);
        visc_crit=1.0;
    }
    else {
        const3_k[i]=atomiz_cal2(rho[i],rhogas,weber_1[i],reynolds_1[i]);
        visc_crit=0.0;
    }
    fprintf(outfile,"%f,%f,%f\n",visc_crit,rho[i],const3_k[i]);
}

/* *****Calculate Sauter Mean Diameter - SMD ***** */

/* **Constant density and viscosity ==> rhobar,mubar,sigma(i),Rebar & Weber_2** */

printf("%s\n","Sauter Mean Diameter ==>Varying Surface Tension:\n");
fprintf(outfile,"%s\n","SMD ==> Varying Surface Tension:\n");
fprintf(outfile,"%s,%s\n","sigma","SMD_1");
for (i=1; i<=nstep; ++i) {

```



```

/*      nu=mubar/rhobar;
      smd_ls=smdl_cal(rhobar,rhogas,nu,nugas,rebar,weber_2[i]);
      smd_hs=smdhs_cal(rhobar,rhogas,nu,nugas,rebar,weber_2[i]);
if (smd_hs > smd_ls){
      smd_1[i]= smd_hs;}
else{
      smd_1[i]= smd_ls;
      }
      */
      smd_1[i]=1.0e6 * smd2_cal(dia,velbar,sigma[i],rhogas,rhobar,mubar) ;
      fprintf(outfile,"%f,%g\n",sigma[i],smd_1[i]);
}

/* **Constant density and surf tens ==> rhobar,mu[i],sigmabr,Reynolds_2 & Webar** */

printf("%s\n","Sauter Mean Diameter ==>Varying Viscosity:\n");
fprintf(outfile,"%s\n","SMD ==>Varying Viscosity:\n");
fprintf(outfile,"%s,%s\n","mu","SMD_2");
for (i=1; i<=nstep; ++i) {
/*      nu=mu[i]/rhobar;
      smd_ls=smdl_cal(rhobar,rhogas,nu,nugas,reynolds_2[i],webar);
      smd_hs=smdhs_cal(rhobar,rhogas,nu,nugas,reynolds_2[i],webar);
      if (smd_hs > smd_ls){
      smd_2[i]= smd_hs;}
else{
      smd_2[i]= smd_ls ;
      }
      */
      smd_2[i]=1.0e6 * smd2_cal(dia,velbar,sigmabr,rhogas,rhobar,mu[i]) ;
      fprintf(outfile,"%f,%g\n",mu[i],smd_2[i]);
}

/* **Constant visc and surf tens ==> rho[i],mubar,sigmabr,Reynolds_1 & weber_1** */

printf("%s\n","Sauter Mean Diameter ==>Varying Density:\n");
fprintf(outfile,"%s\n","SMD ==> Varying Density:\n");
fprintf(outfile,"%s,%s\n","rho","SMD_3");
for (i=1; i<=nstep; ++i) {
/*      nu=mubar/rho[i];
      smd_ls=smdl_cal(rho[i],rhogas,nu,nugas,reynolds_1[i],weber_1[i]);
      smd_hs=smdhs_cal(rho[i],rhogas,nu,nugas,reynolds_1[i],weber_1[i]);
      if (smd_hs > smd_ls){
      smd_3[i]= smd_hs;}
else{
      smd_3[i]= smd_ls;
      }
      */
      smd_3[i]= 1.0e6 * smd2_cal(dia,vel[i],sigmabr,rhogas,rho[i],mubar) ;
      fprintf(outfile,"%f,%g\n",rho[i],smd_3[i]);
}
fprintf(outfile,"\n\n%s\n","Properties:");
fprintf(outfile,"%s,%s,%s\n","rhobar","sigmabar","mubar");
fprintf(outfile,"%f,%f,%f\n",rhobar,sigmabr,mubar);

```

```

fprintf(outfile, "%s,%s,%s\n", "%vary-rho", "%vary-sigma", "%vary-mu");
fprintf(outfile, "%f,%f,%f\n", vary_r, vary_s, vary_m);
fprintf(outfile, "%s,%s,%s,%s\n", "rhogas", "mugas", "Pgas", "Tgas");
fprintf(outfile, "%f,%f,%f,%f\n", rhogas, mugas, pgas, tgas);
fprintf(outfile, "%s,%s\n", "Weber_bar", "Reynolds_bar");
fprintf(outfile, "%f,%f\n", webar, rebar);
fprintf(outfile, "%s,%s\n", "vel_bar", "diameter");
fprintf(outfile, "%f,%f\n", velbar, dia);
fclose(infile);
fclose(outfile);
}
/* **function atomiz_call** */

double atomiz_call(double rho_a, double rhogas_a) {

double atomiz1;

atomiz1 = sqrt(rho_a / rhogas_a);
return atomiz1;
}

/* **function atomiz_cal2** */

double atomiz_cal2(double rho_a, double rhogas_a, double we_a, double re_a) {
double atomiz2;
atomiz2 = pow( ((rho_a * we_a) / (rhogas_a * re_a)), (1.0/3.0) );
return atomiz2;
}

/* ***Function Reynolds_cal*** */

double reynolds_cal(double rhow, double muw, double velw, double diaw)
{
double reynolds;
printf("%f,%f,%f,%f\n", rhow, velw, muw, diaw);*/
reynolds= (rho_w * vel_w * dia_w) / mu_w;
return reynolds;
}

/* ***function weber_cal*** */

double weber_cal(double rhow, double sigmaw, double velw, double diaw)
{
double weber;
printf("%f,%f,%f,%f\n", rhow, velw, sigmaw, diaw);*/
weber= (rho_w * pow(vel_w, 2.0) * dia_w) / sigmaw;
return weber;
}

/* *****function smdls_cal***** */

```

```

double smdls_cal(double rhos,double rhogs,double nus,double nugs,double res,double wes)
{
double smdls;
smdls=4.12*pow(res,1.2)*pow(wes,-0.75)*pow((nus/nugs),0.54)*pow((rhos/rhogs),0.18) ;
return smdls;
}

/* *****function smdhs_cal***** */

double smdhs_cal(double rhos,double rhogs,double nus,double nugs,double res,double wes)
{
double smdhs;
smdhs=0.38*pow(res,0.25)* pow(wes,-0.32)*pow((nus/nugs),0.37)* pow((rhos/rhogs),-0.47);
return smdhs;
}

/* *****function smd2_cal***** */

double smd2_cal(double dias,double vels,double sigmas,double rhogs,double rhos,double mus)
{
double temp;
double smd2;
double sqrt(double);
temp = 1.331e5 * mus /sqrt( (sigmas*rhos*dias) );
smd2= 47.0e-3 * (dias/vels) * pow( (sigmas/rhogs),0.25 ) * pow(9.81,0.2) * temp ;
printf("%s,%g\n","smd2",smd2);
return smd2;
}

```

Evaporation Properties

```

/* A C - program to carry out sensivity analysis on thermal properties */

#include <stdio.h>
#include <math.h>
#define maxarray 50
#define nstep 15

main() {

double tgas, tboil, tatm, patm, pgas, cr, poly;
double cp[maxarray],cpbar,cpmax,cpmin,dtcp,vary_cp;
double cond[maxarray],condbar,condmax,condmin,dtcond,vary_co;
double rho[maxarray],rhobar,rhobar,rhomin,dtrho,vary_rh;
double laten[maxarray],latenbar,latenmax,latenmin,dlaten,vary_la;
double brate_1[maxarray],brate_2[maxarray],brate_3[maxarray], brate_4[maxarray];
double pow(double,double), log(double), b_param[maxarray];
int i;
FILE *infile, *outfile, *fopen();
infile = fopen("bratein.dat","r");
outfile = fopen("brateout.dat","w");
fscanf(infile, "%lf,%lf,%lf,%lf,%lf",&tatm,&tboil,&patm,&cr,&poly);
fscanf(infile, "%lf,%lf,%lf,%lf",&cpbar,&condbar,&rhobar,&latenbar);
fscanf(infile, "%lf,%lf,%lf,%lf",&vary_cp,&vary_co,&vary_rh,&vary_la);
printf("%f,%f,%f,%f,%f\n",tatm,tboil,patm,cr,poly);
printf("%f,%f,%f,%f\n",cpbar,condbar,rhobar,latenbar);
printf("%f,%f,%f,%f\n",vary_cp,vary_co,vary_rh,vary_la);

/* cal max, min & increment */
rhobar = rhobar + rhobar*vary_rh/100.0;
rhomin = rhobar - rhobar*vary_rh/100.0;
dtrho = (rhobar - rhomin)/((double)nstep);
cpmax = cpbar + cpbar*vary_cp/100.0 ;
cpmin = cpbar - cpbar*vary_cp/100.0 ;
dtcp = (cpmax - cpmin) / ( (double)nstep) ;
condmax = condbar + condbar*vary_co/100.0 ;
condmin = condbar - condbar*vary_co/100.0 ;
dtcond = (condmax - condmin) / ( (double)nstep) ;
latenmax = latenbar + latenbar*vary_la/100.0 ;
latenmin = latenbar - latenbar*vary_la/100.0 ;
dlaten = (latenmax - latenmin) / ( (double)nstep);

/* assign values to property array */
i=1;
while (i <= nstep) {
    rho[i]= rhomin + (double)i * dtrho ;
    cond[i] = condmin + (double)i * dtcond ;
    laten[i] = latenmin + (double)i * dlaten ;
    cp[i] = cpmin + (double)i * dtcp ;
}
}

```

```

    ++i;
}

/* cal gas pressure in cylinder ==> p2/p1 = (v1/v2)^n */
pgas = patm * pow(cr,poly);

/*Calculate gas temperature in cylinder ==> T2/T1=(p2/p1)^(n-1/n)*/
tgas = tatm * pow( (pgas/patm), ((poly - 1.0)/poly) );

/* *****Calculate burning rate constant***** */

fprintf(outfile,"%s\n\n","Buring Rate Constant");

/* *****for varying density***** */

fprintf(outfile,"\n%s\n","Density Varying");
fprintf(outfile,"%s,%s\n","rho","B_Rate");
for (i=1; i<=nstep; ++i) {
    printf("%s,%d\n","step_1 ",i);
    b_param[i] = cpbar*(tgas - tboil)/latenbar;
    brate_1[i] = 8.0 * 1.0e6 * condbar/( rho[i]*cpbar ) * log( (1.0 + b_param[i]) );
    fprintf(outfile,"%f,%f\n",rho[i],brate_1[i]);
}

/* *****for varying heat capacity***** */

fprintf(outfile,"\n%s\n","Heat Capacity Varying");
fprintf(outfile,"%s,%s\n","cp","B_Rate");
for (i=1; i<=nstep; ++i) {
    printf("%s,%d\n","step_2 ",i);
    b_param[i] = cp[i]*(tgas - tboil)/latenbar;
    brate_2[i] = 8.0 * 1.0e6 * condbar/( rhobar*cp[i] ) * log( (1.0 + b_param[i]) );
    fprintf(outfile,"%f,%f\n",cp[i],brate_2[i]);
}

/* *****for varying latent heat***** */

fprintf(outfile,"\n%s\n","Latent Heat Varying");
fprintf(outfile,"%s,%s\n","Latent","B_Rate");

for (i=1; i<=nstep; ++i) {
    printf("%s,%d\n","step_3 ",i);
    b_param[i] = cpbar*(tgas - tboil)/laten[i];
    brate_3[i] = 8.0 * 1.0e6 * condbar/( rhobar*cpbar ) * log( (1.0 + b_param[i]) );
    fprintf(outfile,"%f,%f\n",laten[i],brate_3[i]);
}

/* *****for varying thermal conductivity***** */
fprintf(outfile,"\n%s\n","Thermal Conductivity Varying");
fprintf(outfile,"%s,%s\n","cond","B_Rate");

```

```

for (i=1; i <=nstep; ++i) {
    printf("%s,%d\n", "step_4 ", i);
    b_param[i] = cpbar*(tgas - tboil)/latenbar;
    brate_4[i] = 8.0 * 1.0e6 * cond[i]/( rhobar*cpbar ) * log ( (1.0 + b_param[i]) );
    fprintf(outfile, "%f,%f\n", cond[i], brate_4[i]);
}
fprintf(outfile, "\n\n%s\n", "Properties:");
fprintf(outfile, "%s,%s,%s,%s\n", "rhobar", "cpbar", "condbar", "latenbar");
fprintf(outfile, "%f,%f,%f,%f\n", rhobar, cpbar, condbar, latenbar);
fprintf(outfile, "%s,%s,%s,%s\n", "vary-rh", "vary-cp", "vary-co", "vary-la");
fprintf(outfile, "%f,%f,%f,%f\n", vary_rh, vary_cp, vary_co, vary_la);
fprintf(outfile, "%s,%s,%s,%s\n", "cr", "Pgas", "Tgas", "Tboil");
fprintf(outfile, "%f,%f,%f,%f\n", cr, pgas, tgas, tboil);
fclose(infile);
fclose(outfile);
}

```

APPENDIX D
Viscosities of Natural Vegetable Oil Methyl Esters Predicted using the Measured
Viscosities of GC Standards

Table D.1 Viscosities of Methyl Ester Biodiesel Fuels at 40 °C - (using measured viscosities of GC standards and lumped mass fractions)

Fatty Acid ME	Viscosity (mPa.s)	Methyl Ester Component Mass fraction				
		Coconut	Peanut	Soya	Palm	Canola
24:0	...	0.000	0.035 (0.000) ⁰	0.000 (0.000) ⁰	0.000	0.000
22:1	5.91	0.000	0.000	0.000	0.000	0.000
22:0	...	0.000	0.024 (0.000) ⁰	0.000 (0.000) ⁰	0.000	0.001 (0.000) ⁰
20:1	...	0.000	0.014 (0.000) ¹	0.016 (0.000) ¹	0.001 (0.000) ¹	0.021 (0.000) ¹
20:0	...	0.002	0.013 (0.000) ⁰	0.007 (0.000) ⁰	0.003 (0.000) ⁰	0.012 (0.000) ⁰
18:3	2.65	0.000	0.010	0.096	0.002	0.112
18:2	3.05	0.014	0.301	0.199	0.080	0.213
18:1	3.73	0.055	0.466 (0.485)	0.600 (0.623)	0.373 (0.377)	0.574 (0.599)
18:0	4.74	0.019	0.027 (0.099)	0.017 (0.023)	0.040 (0.042)	0.020 (0.033)
16:1	...	0.000	0.004 (0.000) ¹	0.008 (0.000) ¹	0.003 (0.000) ¹	0.004 (0.000) ¹
16:0	3.60	0.073	0.105	0.058	0.481	0.042
14:0	2.69	0.171	0.000	0.000	0.013	0.000
12:0	1.95	0.533	0.000	0.000	0.004	0.000
10:0	1.40	0.060	0.000	0.000	0.000	0.000
8:0	1.01	0.075	0.000	0.000	0.000	0.000
Measured Viscosity (mPa.s)		2.32	3.77	3.67	3.87	3.70
Predicted Viscosity (mPa.s)		2.13	3.55	3.44	3.44	3.60
Error (mPa.s)		0.19	0.22	0.23	0.26	0.27
Percent Error		8.13%	5.95%	6.30%	7.02%	7.07%

()⁰ - mass fraction after being lumped with 18:0
()¹ - mass fraction after being lumped with 18:1

APPENDIX E
Surface Tension of Natural Vegetable Oil Methyl Esters Predicted using the
Measured Surface Tension of GC Standards

Table E.1 Surface Tension of Methyl Ester Biodiesel Fuels at 40 °C (using measured surface tension of GC Standards)

Fatty Acid ME	Calculated Surface Tension (mN/m)	Weight Factor	Weighted Surface Tension (mN/m)	Methyl Ester Component Mass Fraction				
				Coconut	Peanut	Soya	Palm	Canola
8:0	25.40	0.955	24.26	0.075	0.000	0.000	0.000	0.000
10:0	26.30	0.965	25.34	0.060	0.000	0.000	0.000	0.000
12:0	27.20	0.973	26.44	0.533	0.000	0.000	0.004	0.000
14:0	27.90	0.979	27.31	0.171	0.000	0.000	0.013	0.000
16:0	28.40	0.984	27.94	0.073	0.105	0.058	0.481	0.046
16:1	0.000	0.004 (0.000) ¹	0.008 (0.000) ¹	0.003 (0.000) ¹	0.005
18:0	29.00	0.988	28.69	0.019	0.027 (0.099)	0.017 (0.023)	0.040 (0.042)	0.021
18:1	22.80	0.988	21.20	0.055	0.466 (0.485)	0.600 (0.623)	0.373 (0.377)	0.618
18:2	23.80	0.993	22.36	0.014	0.301	0.199	0.080	0.189
18:3	29.60	0.998	29.46	0.000	0.010	0.096	0.002	0.097
20:0	0.002	0.013 (0.000) ⁰	0.007 (0.000) ⁰	0.003 (0.000) ⁰	0.007
20:1	0.000	0.014 (0.000) ¹	0.016 (0.000) ¹	0.001 (0.000) ¹	0.017
22:0	0.000	0.024 (0.000) ⁰	0.000 (0.000) ⁰	0.000	0.000
22:1	30.10	0.999	30.10	0.000	0.000	0.000	0.000	0.000
24:0	0.000	0.035 (0.000) ⁰	0.000 (0.000) ⁰	0.000	0.000
Measures Surface Tension (mN/m)				26.11	28.79	28.20	28.50	27.88
Predicted S.T. (Mass Average) (mN/m)				26.96	24.34	24.12	24.22	25.94
Error (mN/m)				-0.85	4.42	4.08	3.66	2.56
Percent Error				-3.27%	15.35%	14.46%	13.13%	9.00%
Predicted S.T. (Weighted Mass Average)				26.17	23.08	22.79	22.91	24.97
Error (mN/m)				-0.06	5.71	5.41	4.97	3.53
Percent Error				-0.23%	19.82%	19.17%	17.82%	12.36%

APPENDIX F
Regression Analyses for Atomization Parameters SMD, 'X', and 'n'

Regression Analysis SMD Model #1 (σ^1)

Reason(s) for rejecting this model:- Failed sensitivity analyses

The regression equation is

$$\text{smd} = 0.000168 - 0.0417 \mu - 0.00618 \sigma + 1.66 \mu \cdot \sigma$$

Predictor	Coef	StDev	T	P
Constant	0.00016837	0.00000751	22.42	0.002
μ	-0.041654	0.001810	-23.01	0.002
σ	-0.0061782	0.0002919	-21.16	0.002
$\mu \cdot \sigma$	1.66314	0.07084	23.48	0.002

S = 0.000000027 R-Sq = 100.0% R-Sq(adj) = 100.0%

Analysis of Variance

Source	DF	SS	MS	F	P
Regression	3	1.15687E-11	3.85625E-12	5455.18	0.000
Error	2	1.41379E-15	7.06896E-16		
Total	5	1.15702E-11			

Source	DF	Seq SS
μ	1	1.10011E-11
σ	1	1.77985E-13
$\mu \cdot \sigma$	1	3.89612E-13

Regression Analysis for SMD - Model #2 (σ^1)

Reason(s) for rejecting this model:- High P-values

The regression equation is

$$\text{smd} = -0.00152 \mu + 0.000366 \sigma + 0.086 \mu \cdot \sigma$$

Predictor	Coef	StDev	T	P
Noconstant				
μ	-0.001522	0.003491	-0.44	0.692
σ	0.00036628	0.00005290	6.92	0.006
$\mu \cdot \sigma$	0.0864	0.1105	0.78	0.491

S = 0.000000345

Analysis of Variance

Source	DF	SS	MS	F	P
Regression	3	1.01200E-09	3.37332E-10	2836.96	0.000
Error	3	3.56718E-13	1.18906E-13		
Total	6	1.01235E-09			

Source	DF	Seq SS
μ	1	9.89927E-10
σ	1	2.19969E-11
$\mu \cdot \sigma$	1	7.27487E-14

Regression Analysis for SMD - Model #3 (σ^2)

Reason(s) for rejecting this model:- High P-values

The regression equation is

$$\text{smd} = -0.000007 + 0.000824 \mu + 0.000615 \sigma$$

Predictor	Coef	StDev	T	P
Constant	-0.00000666	0.00001227	-0.54	0.625
μ	0.0008243	0.0007302	1.13	0.341
σ	0.0006150	0.0005263	1.17	0.327

S = 0.000000361 R-Sq = 96.6% R-Sq(adj) = 94.4%

Analysis of Variance

Source	DF	SS	MS	F	P
Regression	2	1.11791E-11	5.58956E-12	42.88	0.006
Error	3	3.91026E-13	1.30342E-13		
Total	5	1.15702E-11			

Source	DF	Seq SS
μ	1	1.10011E-11
σ	1	1.77985E-13

Regression Analysis for SMD - Model #4 (σ^2)

Reason(s) for SELECTING this model:- Lowest 'S', low P-values & passed sensitivity analyses

The regression equation is

$$\text{smd} = 0.00120 \mu + 0.000330 \sigma$$

Predictor	Coef	StDev	T	P
Noconstant				
μ	0.0012037	0.0001931	6.23	0.003
σ	0.00032950	0.00002302	14.31	0.000

S = 0.000000328

Analysis of Variance

Source	DF	SS	MS	F	P
Regression	2	1.01192E-09	5.05962E-10	4712.47	0.000
Error	4	4.29467E-13	1.07367E-13		
Total	6	1.01235E-09			

Source	DF	Seq SS
μ	1	9.89927E-10
σ	1	2.19969E-11

Regression Analysis for SMD - Model #5 (σ^2)

Reason(s) for rejecting this model:- High P-values

The regression equation is
 $smd = 0.000009 - 0.00385 \mu + 0.177 \mu \cdot \sigma$

Predictor	Coef	StDev	T	P
Constant	0.00000945	0.00000128	7.36	0.005
μ	-0.003848	0.003578	-1.08	0.361
$\mu \cdot \sigma$	0.1772	0.1152	1.54	0.221

S = 0.000000326 R-Sq = 97.3% R-Sq(adj) = 95.4%

Analysis of Variance

Source	DF	SS	MS	F	P
Regression	2	1.12522E-11	5.62608E-12	53.08	0.005
Error	3	3.17998E-13	1.05999E-13		
Total	5	1.15702E-11			

Source	DF	Seq SS
μ	1	1.10011E-11
$\mu \cdot \sigma$	1	2.51013E-13

Regression Analysis for SMD - Model #6 (σ^2)

Reason(s) for rejecting this model:- Higher 'S', lower F-value

The regression equation is
 $smd = 0.0206 \mu - 0.594 \mu \cdot \sigma$

Predictor	Coef	StDev	T	P
Noconstant				
μ	0.020560	0.005068	4.06	0.015
$\mu \cdot \sigma$	-0.5938	0.1806	-3.29	0.030

S = 0.000001231

Analysis of Variance

Source	DF	SS	MS	F	P
Regression	2	1.00630E-09	5.03148E-10	332.21	0.000
Error	4	6.05812E-12	1.51453E-12		
Total	6	1.01235E-09			

Source	DF	Seq SS
μ	1	9.89927E-10
$\mu \cdot \sigma$	1	1.63683E-11

Regression Analysis for SMD - Model #7 (σ^1)

Reason(s) for rejecting this model:- Higher 'S', lower F-value

The regression equation is
 $smd = 0.000008 + 0.0535 \mu .\sigma$

Predictor	Coef	StDev	T	P
Constant	0.00000817	0.00000049	16.65	0.000
$\mu .\sigma$	0.053466	0.005319	10.05	0.001

S = 0.000000332 R-Sq = 96.2% R-Sq(adj) = 95.2%

Analysis of Variance

Source	DF	SS	MS	F	P
Regression	1	1.11295E-11	1.11295E-11	101.03	0.001
Error	4	4.40651E-13	1.10163E-13		
Total	5	1.15702E-11			

Regression Analysis for SMD - Model #8 (σ^1)

Reason(s) for rejecting this model:- Higher 'S', lower F-value

The regression equation is
 $smd = 0.139 \mu .\sigma$

Predictor	Coef	StDev	T	P
Noconstant				
$\mu .\sigma$	0.13859	0.01101	12.59	0.000

S = 0.000002489

Analysis of Variance

Source	DF	SS	MS	F	P
Regression	1	9.81373E-10	9.81373E-10	158.38	0.000
Error	5	3.09808E-11	6.19616E-12		
Total	6	1.01235E-09			

Regression Analysis for SMD - Model #1b (σ^{-1})

Reason(s) for rejecting this model:- Failed Sensitivity Analyses

The regression equation is

$$\text{smd} = -0.000165 + 0.0479 \mu + 0.000004 \ 1/\sigma - 0.00120 \ \mu / \sigma$$

Predictor	Coef	StDev	T	P
Constant	-0.00016470	0.00001026	-16.06	0.004
μ	0.047894	0.002478	19.33	0.003
$1/\sigma$	0.00000448	0.00000026	17.00	0.003
μ / σ	-0.00120320	0.00006324	-19.03	0.003

S = 0.000000033 R-Sq = 100.0% R-Sq(adj) = 100.0%

Analysis of Variance

Source	DF	SS	MS	F	P
Regression	3	1.15680E-11	3.85599E-12	3535.41	0.000
Error	2	2.18135E-15	1.09068E-15		
Total	5	1.15702E-11			

Source	DF	Seq SS
μ	1	1.10011E-11
$1/\sigma$	1	1.72007E-13
μ / σ	1	3.94822E-13

Regression Analysis for SMD - Model #2b (σ^{-1})

Reason(s) for rejecting this model:- High P-values

The regression equation is

$$\text{smd} = 0.00844 \mu + 0.000000 \ 1/\sigma - 0.000200 \ \mu / \sigma$$

Predictor	Coef	StDev	T	P
Noconstant				
μ	0.008440	0.002995	2.82	0.067
$1/\sigma$	0.00000025	0.00000003	7.50	0.005
μ / σ	-0.00020033	0.00009293	-2.16	0.120

S = 0.000000307

Analysis of Variance

Source	DF	SS	MS	F	P
Regression	3	1.01207E-09	3.37357E-10	3570.11	0.000
Error	3	2.83485E-13	9.44948E-14		
Total	6	1.01235E-09			

Source	DF	Seq SS
μ	1	9.89927E-10
$1/\sigma$	1	2.17037E-11
μ / σ	1	4.39175E-13

Regression Analysis for SMD - Model #3b (σ^{-1})

Reason(s) for rejecting this model:- High P-values

The regression equation is

$$\text{smd} = 0.000028 + 0.000773 \mu - 0.000000 \frac{1}{\sigma}$$

Predictor	Coef	StDev	T	P
Constant	0.00002798	0.00001783	1.57	0.215
μ	0.0007728	0.0007916	0.98	0.401
$1/\sigma$	-0.00000048	0.00000042	-1.14	0.337

S = 0.000000364 R-Sq = 96.6% R-Sq(adj) = 94.3%

Analysis of Variance

Source	DF	SS	MS	F	P
Regression	2	1.11731E-11	5.58657E-12	42.22	0.006
Error	3	3.97004E-13	1.32335E-13		
Total	5	1.15702E-11			

Source	DF	Seq SS
μ	1	1.10011E-11
$1/\sigma$	1	1.72007E-13

Regression Analysis for SMD - Model #4b (σ^{-1})

Reason(s) for rejecting this model:- Higher 'S', lower F-value

The regression equation is

$$\text{smd} = 0.00199 \mu + 0.000000 \frac{1}{\sigma}$$

Predictor	Coef	StDev	T	P
Noconstant				
μ	0.0019902	0.0001825	10.90	0.000
$1/\sigma$	0.00000018	0.00000002	10.96	0.000

S = 0.000000425

Analysis of Variance

Source	DF	SS	MS	F	P
Regression	2	1.01163E-09	5.05815E-10	2799.74	0.000
Error	4	7.22659E-13	1.80665E-13		
Total	6	1.01235E-09			

Source	DF	Seq SS
μ	1	9.89927E-10
$1/\sigma$	1	2.17037E-11

Regression Analysis for SMD - Model #5b (σ^{-1})

Reason(s) for rejecting this model:- High P-values

The regression equation is

$$\text{smd} = 0.000010 + 0.00608 \mu - 0.000140 \mu / \sigma$$

Predictor	Coef	StDev	T	P
Constant	0.00000958	0.00000135	7.07	0.006
μ	0.006079	0.002873	2.12	0.125
μ / σ	-0.00013990	0.00009065	-1.54	0.220

S = 0.000000325 R-Sq = 97.3% R-Sq(adj) = 95.4%

Analysis of Variance

Source	DF	SS	MS	F	P
Regression	2	1.12529E-11	5.62647E-12	53.21	0.005
Error	3	3.17206E-13	1.05735E-13		
Total	5	1.15702E-11			

Source	DF	Seq SS
μ	1	1.10011E-11
μ / σ	1	2.51805E-13

Regression Analysis for SMD - Model #6b (σ^{-1})

Reason(s) for rejecting this model:- Higher 'S', lower F-value

The regression equation is

$$\text{smd} = -0.0121 \mu + 0.000450 \mu / \sigma$$

Predictor	Coef	StDev	T	P
Noconstant				
μ	-0.012140	0.004634	-2.62	0.059
μ / σ	0.0004496	0.0001298	3.46	0.026

S = 0.000001184

Analysis of Variance

Source	DF	SS	MS	F	P
Regression	2	1.00675E-09	5.03374E-10	359.20	0.000
Error	4	5.60547E-12	1.40137E-12		
Total	6	1.01235E-09			

Source	DF	Seq SS
μ	1	9.89927E-10
μ / σ	1	1.68209E-11

Regression Analysis for SMD - Model #7b (σ^{-1})

Reason(s) for rejecting this model:- Higher 'S', lower F-value

The regression equation is
 $smd = 0.000007 + 0.000052 \mu / \sigma$

Predictor	Coef	StDev	T	P
Constant	0.00000701	0.00000082	8.55	0.001
μ / σ	0.00005157	0.00000698	7.39	0.002

S = 0.000000445 R-Sq = 93.2% R-Sq(adj) = 91.5%

Analysis of Variance

Source	DF	SS	MS	F	P
Regression	1	1.07798E-11	1.07798E-11	54.55	0.002
Error	4	7.90383E-13	1.97596E-13		
Total	5	1.15702E-11			

Regression Analysis for SMD - Model #8b (σ^{-1})

Reason(s) for rejecting this model:- Higher 'S', lower F-value

The regression equation is
 $smd = 0.000110 \mu / \sigma$

Predictor	Coef	StDev	T	P
Noconstant				
μ / σ	0.00010977	0.00000607	18.10	0.000

S = 0.000001745

Analysis of Variance

Source	DF	SS	MS	F	P
Regression	1	9.97129E-10	9.97129E-10	327.47	0.000
Error	5	1.52248E-11	3.04497E-12		
Total	6	1.01235E-09			

Regression Analysis for 'X' - Model #1 (σ^1)

Reason(s) for rejecting this model:- High P-values

The regression equation is

$$X = 0.000232 - 0.0589 \mu - 0.00816 \sigma + 2.35 \mu . \sigma$$

Predictor	Coef	StDev	T	P
Constant	0.0002322	0.0001720	1.35	0.310
μ	-0.05888	0.04146	-1.42	0.291
σ	-0.008161	0.006687	-1.22	0.347
$\mu . \sigma$	2.353	1.623	1.45	0.284

S = 0.000000609 R-Sq = 98.3% R-Sq(adj) = 95.7%

Analysis of Variance

Source	DF	SS	MS	F	P
Regression	3	4.23150E-11	1.41050E-11	38.04	0.026
Error	2	7.41658E-13	3.70829E-13		
Total	5	4.30567E-11			

Source	DF	Seq SS
μ	1	4.05457E-11
σ	1	9.89409E-13
$\mu . \sigma$	1	7.79907E-13

Regression Analysis for 'X' - Model #2 (σ^1)

Reason(s) for rejecting this model:- High P-values

The regression equation is

$$X = -0.00353 \mu + 0.000865 \sigma + 0.179 \mu . \sigma$$

Predictor	Coef	StDev	T	P
Noconstant				
μ	-0.003532	0.006959	-0.51	0.647
σ	0.0008645	0.0001054	8.20	0.004
$\mu . \sigma$	0.1786	0.2203	0.81	0.477

S = 0.000000687

Analysis of Variance

Source	DF	SS	MS	F	P
Regression	3	4.88725E-09	1.62908E-09	3447.90	0.000
Error	3	1.41746E-12	4.72486E-13		
Total	6	4.88867E-09			

Source	DF	Seq SS
μ	1	4.76097E-09
σ	1	1.25971E-10
$\mu . \sigma$	1	3.10474E-13

Regression Analysis for 'X' - Model #3 (σ^2)

Reason(s) for rejecting this model:- High P-values

The regression equation is

$$X = -0.000015 + 0.00122 \mu + 0.00145 \sigma$$

Predictor	Coef	StDev	T	P
Constant	-0.00001543	0.00002420	-0.64	0.569
μ	0.001220	0.001440	0.85	0.459
σ	0.001450	0.001038	1.40	0.257

S = 0.000000712 R-Sq = 96.5% R-Sq(adj) = 94.1%

Analysis of Variance

Source	DF	SS	MS	F	P
Regression	2	4.15351E-11	2.07676E-11	40.95	0.007
Error	3	1.52157E-12	5.07188E-13		
Total	5	4.30567E-11			

Source	DF	Seq SS
μ	1	4.05457E-11
σ	1	9.89409E-13

Regression Analysis for 'X' - Model #4 (σ^2)

Reason(s) for SELECTING this model:- Lowest 'S', high F-value, low P-values

The regression equation is

$$X = 0.00210 \mu + 0.000789 \sigma$$

Predictor	Coef	StDev	T	P
Noconstant				
μ	0.0020993	0.0003873	5.42	0.006
σ	0.00078852	0.00004618	17.08	0.000

S = 0.000000657

Analysis of Variance

Source	DF	SS	MS	F	P
Regression	2	4.88694E-09	2.44347E-09	5656.40	0.000
Error	4	1.72793E-12	4.31983E-13		
Total	6	4.88867E-09			

Source	DF	Seq SS
μ	1	4.76097E-09
σ	1	1.25971E-10

Regression Analysis for 'X' - Model #5 (σ^1)

Reason(s) for rejecting this model:- High P-values

The regression equation is

$$X = 0.000022 - 0.00894 \mu + 0.390 \mu .\sigma$$

Predictor	Coef	StDev	T	P
Constant	0.00002228	0.00000259	8.60	0.003
μ	-0.008939	0.007217	-1.24	0.304
$\mu .\sigma$	0.3902	0.2323	1.68	0.192

S = 0.000000657 R-Sq = 97.0% R-Sq(adj) = 95.0%

Analysis of Variance

Source	DF	SS	MS	F	P
Regression	2	4.17626E-11	2.08813E-11	48.41	0.005
Error	3	1.29409E-12	4.31364E-13		
Total	5	4.30567E-11			

Source	DF	Seq SS
μ	1	4.05457E-11
$\mu .\sigma$	1	1.21688E-12

Regression Analysis for 'X' - Model #6 (σ^1)

Reason(s) for rejecting this model:- Higher 'S', lower F-value

The regression equation is

$$X = 0.0486 \mu - 1.43 \mu .\sigma$$

Predictor	Coef	StDev	T	P
Noconstant				
μ	0.04859	0.01186	4.10	0.015
$\mu .\sigma$	-1.4270	0.4227	-3.38	0.028

S = 0.000002880

Analysis of Variance

Source	DF	SS	MS	F	P
Regression	2	4.85549E-09	2.42774E-09	292.70	0.000
Error	4	3.31775E-11	8.29437E-12		
Total	6	4.88867E-09			

Source	DF	Seq SS
μ	1	4.76097E-09
$\mu .\sigma$	1	9.45211E-11

Regression Analysis for 'X' - Model #7 (σ^1)

Reason(s) for rejecting this model:- Higher 'S', lower F-value

The regression equation is

$$X = 0.000019 + 0.103 \mu .\sigma$$

Predictor	Coef	StDev	T	P
Constant	0.00001931	0.00000103	18.67	0.000
$\mu .\sigma$	0.10275	0.01121	9.17	0.001

S = 0.000000699 R-Sq = 95.5% R-Sq(adj) = 94.3%

Analysis of Variance

Source	DF	SS	MS	F	P
Regression	1	4.11008E-11	4.11008E-11	84.06	0.001
Error	4	1.95585E-12	4.88963E-13		
Total	5	4.30567E-11			

Regression Analysis for 'X' - Model #8 (σ^1)

Reason(s) for rejecting this model:- Higher 'S', lower F-value

The regression equation is

$$X = 0.304 \mu .\sigma$$

Predictor	Coef	StDev	T	P
Noconstant				
$\mu .\sigma$	0.30382	0.02597	11.70	0.000

S = 0.000005871

Analysis of Variance

Source	DF	SS	MS	F	P
Regression	1	4.71631E-09	4.71631E-09	136.82	0.000
Error	5	1.72358E-10	3.44717E-11		
Total	6	4.88867E-09			

Regression Analysis for 'X' - Model #1b (σ^{-1})

Reason(s) for rejecting this model:- High P-values

The regression equation is

$$X = -0.000205 + 0.0676 \mu + 0.000006 \frac{1}{\sigma} - 0.00170 \mu / \sigma$$

Predictor	Coef	StDev	T	P
Constant	-0.0002050	0.0001894	-1.08	0.392
μ	0.06757	0.04577	1.48	0.278
$1/\sigma$	0.00000585	0.00000487	1.20	0.352
μ / σ	-0.001698	0.001168	-1.45	0.283

S = 0.000000610 R-Sq = 98.3% R-Sq(adj) = 95.7%

Analysis of Variance

Source	DF	SS	MS	F	P
Regression	3	4.23124E-11	1.41041E-11	37.90	0.026
Error	2	7.44302E-13	3.72151E-13		
Total	5	4.30567E-11			

Source	DF	Seq SS
μ	1	4.05457E-11
$1/\sigma$	1	9.80525E-13
μ / σ	1	7.86147E-13

Regression Analysis for 'X' - Model #2b (σ^{-1})

Reason(s) for rejecting this model:- High P-values

The regression equation is

$$X = 0.0184 \mu + 0.000001 \frac{1}{\sigma} - 0.000449 \mu / \sigma$$

Predictor	Coef	StDev	T	P
Noconstant				
μ	0.018446	0.006111	3.02	0.057
$1/\sigma$	0.00000058	0.00000007	8.65	0.003
μ / σ	-0.0004493	0.0001896	-2.37	0.099

S = 0.000000627

Analysis of Variance

Source	DF	SS	MS	F	P
Regression	3	4.88749E-09	1.62916E-09	4140.90	0.000
Error	3	1.18030E-12	3.93432E-13		
Total	6	4.88867E-09			

Source	DF	Seq SS
μ	1	4.76097E-09
$1/\sigma$	1	1.24309E-10
μ / σ	1	2.20895E-12

Regression Analysis for 'X' - Model #3b (σ^{-1})

Reason(s) for rejecting this model:- High P-values

The regression equation is

$$X = 0.000067 + 0.00107 \mu - 0.000001 \frac{1}{\sigma}$$

Predictor	Coef	StDev	T	P
Constant	0.00006684	0.00003502	1.91	0.152
μ	0.001073	0.001554	0.69	0.540
$1/\sigma$	-0.00000115	0.00000083	-1.39	0.260

S = 0.000000714 R-Sq = 96.4% R-Sq(adj) = 94.1%

Analysis of Variance

Source	DF	SS	MS	F	P
Regression	2	4.15262E-11	2.07631E-11	40.70	0.007
Error	3	1.53045E-12	5.10150E-13		
Total	5	4.30567E-11			

Source	DF	Seq SS
μ	1	4.05457E-11
$1/\sigma$	1	9.80525E-13

Regression Analysis for 'X' - Model #4b (σ^{-1})

Reason(s) for rejecting this model:- Higher 'S', lower F-value

The regression equation is

$$X = 0.00398 \mu + 0.000000 \frac{1}{\sigma}$$

Predictor	Coef	StDev	T	P
Noconstant				
μ	0.0039811	0.0003953	10.07	0.001
$1/\sigma$	0.00000043	0.00000004	12.11	0.000

S = 0.000000920

Analysis of Variance

Source	DF	SS	MS	F	P
Regression	2	4.88528E-09	2.44264E-09	2882.81	0.000
Error	4	3.38925E-12	8.47312E-13		
Total	6	4.88867E-09			

Source	DF	Seq SS
μ	1	4.76097E-09
$1/\sigma$	1	1.24309E-10

Regression Analysis for 'X' - Model #5b (σ^1)

Reason(s) for rejecting this model:- High P-values

The regression equation is
 $X = 0.000023 + 0.0130 \mu - 0.000309 \mu / \sigma$

Predictor	Coef	StDev	T	P
Constant	0.00002257	0.00000272	8.29	0.004
μ	0.012953	0.005776	2.24	0.111
μ / σ	-0.0003091	0.0001822	-1.70	0.188

S = 0.000000654 R-Sq = 97.0% R-Sq(adj) = 95.0%

Analysis of Variance

Source	DF	SS	MS	F	P
Regression	2	4.17750E-11	2.08875E-11	48.89	0.005
Error	3	1.28164E-12	4.27213E-13		
Total	5	4.30567E-11			

Source	DF	Seq SS
μ	1	4.05457E-11
μ / σ	1	1.22933E-12

Regression Analysis for 'X' - Model #6b (σ^1)

Reason(s) for rejecting this model:- Higher 'S', lower F-value

The regression equation is
 $X = -0.0300 \mu + 0.00108 \mu / \sigma$

Predictor	Coef	StDev	T	P
Noconstant				
μ	-0.02998	0.01083	-2.77	0.050
μ / σ	0.0010799	0.0003034	3.56	0.024

S = 0.000002768

Analysis of Variance

Source	DF	SS	MS	F	P
Regression	2	4.85802E-09	2.42901E-09	317.06	0.000
Error	4	3.06444E-11	7.66111E-12		
Total	6	4.88867E-09			

Source	DF	Seq SS
μ	1	4.76097E-09
μ / σ	1	9.70541E-11

Regression Analysis for 'X' - Model #7b (σ^{-1})

Reason(s) for rejecting this model:- High P-values

The regression equation is
 $X = 0.000017 + 0.000099 \mu / \sigma$

Predictor	Coef	StDev	T	P
Constant	0.00001709	0.00000171	10.01	0.001
μ / σ	0.00009888	0.00001455	6.80	0.002

S = 0.000000926 R-Sq = 92.0% R-Sq(adj) = 90.0%

Analysis of Variance

Source	DF	SS	MS	F	P
Regression	1	3.96266E-11	3.96266E-11	46.21	0.002
Error	4	3.43007E-12	8.57517E-13		
Total	5	4.30567E-11			

Regression Analysis for 'X' - Model #8b (σ^{-1})

Reason(s) for rejecting this model:- Higher 'S', lower F-value

The regression equation is
 $X = 0.000241 \mu / \sigma$

Predictor	Coef	StDev	T	P
Noconstant				
μ / σ	0.00024082	0.00001469	16.39	0.000

S = 0.000004226

Analysis of Variance

Source	DF	SS	MS	F	P
Regression	1	4.79937E-09	4.79937E-09	268.73	0.000
Error	5	8.92974E-11	1.78595E-11		
Total	6	4.88867E-09			

Regression Analysis for 'n' - Model #1 (σ^2)

Reason(s) for rejecting this model:- High P-values

The regression equation is

$$n = 6.81 - 1206 \mu - 204 \sigma + 48408 \mu \cdot \sigma$$

Predictor	Coef	StDev	T	P
Constant	6.813	6.373	1.07	0.397
μ	-1206	1536	-0.78	0.515
σ	-203.8	247.7	-0.82	0.497
$\mu \cdot \sigma$	48408	60115	0.81	0.505

S = 0.02256 R-Sq = 70.1% R-Sq(adj) = 25.1%

Analysis of Variance

Source	DF	SS	MS	F	P
Regression	3	0.0023819	0.0007940	1.56	0.414
Error	2	0.0010181	0.0005090		
Total	5	0.0034000			

Source	DF	Seq SS
μ	1	0.0020347
σ	1	0.0000171
$\mu \cdot \sigma$	1	0.0003301

Regression Analysis for 'n' - Model #2 (σ^2)

Reason(s) for rejecting this model:- High P-values

The regression equation is

$$n = 418 \mu + 61.1 \sigma - 15397 \mu \cdot \sigma$$

Predictor	Coef	StDev	T	P
Noconstant				
μ	418.2	233.8	1.79	0.172
σ	61.080	3.543	17.24	0.000
$\mu \cdot \sigma$	-15397	7401	-2.08	0.129

S = 0.02309

Analysis of Variance

Source	DF	SS	MS	F	P
Regression	3	16.3368	5.4456	10210.96	0.000
Error	3	0.0016	0.0005		
Total	6	16.3384			

Source	DF	Seq SS
μ	1	15.4078
σ	1	0.9267
$\mu \cdot \sigma$	1	0.0023

Regression Analysis for 'n' - Model #3 (σ^1)

Reason(s) for rejecting this model:- High P-values

The regression equation is
 $n = 1.72 + 30.6 \mu - 6.0 \sigma$

Predictor	Coef	StDev	T	P
Constant	1.7190	0.7202	2.39	0.097
μ	30.58	42.88	0.71	0.527
σ	-6.04	30.90	-0.20	0.858

S = 0.02120 R-Sq = 60.3% R-Sq(adj) = 33.9%

Analysis of Variance

Source	DF	SS	MS	F	P
Regression	2	0.0020519	0.0010259	2.28	0.250
Error	3	0.0013481	0.0004494		
Total	5	0.0034000			

Source	DF	Seq SS
μ	1	0.0020347
σ	1	0.0000171

Regression Analysis for 'n' - Model #4 (σ^1)

Reason(s) for SELECTING this model:- Low 'S'; As the dominant predictor μ increases the predicted parameter 'n' decreases as would be the case in practice.

The regression equation is
 $n = - 67.3 \mu + 67.6 \sigma$

Predictor	Coef	StDev	T	P
Noconstant				
μ	-67.32	18.42	-3.65	0.022
σ	67.632	2.196	30.80	0.000

S = 0.03126

Analysis of Variance

Source	DF	SS	MS	F	P
Regression	2	16.3345	8.1672	8359.25	0.000
Error	4	0.0039	0.0010		
Total	6	16.3384			

Source	DF	Seq SS
μ	1	15.4078
σ	1	0.9267

Regression Analysis for 'n' - Model #5 (σ^2)

Reason(s) for rejecting this model:- High P-values

The regression equation is
 $n = 1.57 + 41 \mu - 599 \mu \cdot \sigma$

Predictor	Coef	StDev	T	P
Constant	1.57240	0.08409	18.70	0.000
μ	41.0	234.2	0.18	0.872
$\mu \cdot \sigma$	-599	7538	-0.08	0.942

S = 0.02131 R-Sq = 59.9% R-Sq(adj) = 33.2%

Analysis of Variance

Source	DF	SS	MS	F	P
Regression	2	0.0020376	0.0010188	2.24	0.254
Error	3	0.0013624	0.0004541		
Total	5	0.0034000			

Source	DF	Seq SS
μ	1	0.0020347
$\mu \cdot \sigma$	1	0.0000029

Regression Analysis for 'n' - Model #6 (σ^2)

Reason(s) for rejecting this model:- Higher 'S', lower F-value

The regression equation is
 $n = 4101 \mu - 128838 \mu \cdot \sigma$

Predictor	Coef	StDev	T	P
Noconstant				
μ	4100.6	824.0	4.98	0.008
$\mu \cdot \sigma$	-128838	29369	-4.39	0.012

S = 0.2001

Analysis of Variance

Source	DF	SS	MS	F	P
Regression	2	16.1783	8.0891	202.05	0.000
Error	4	0.1601	0.0400		
Total	6	16.3384			

Source	DF	Seq SS
μ	1	15.4078
$\mu \cdot \sigma$	1	0.7705

Regression Analysis for 'n' - Model #7 (σ^1)

Reason(s) for rejecting this model:- High F-values, low F-value

The regression equation is
 $n = 1.59 + 721 \mu .\sigma$

Predictor	Coef	StDev	T	P
Constant	1.58606	0.02743	57.81	0.000
$\mu .\sigma$	721.0	297.3	2.43	0.072

S = 0.01855 R-Sq = 59.5% R-Sq(adj) = 49.4%

Analysis of Variance

Source	DF	SS	MS	F	P
Regression	1	0.0020236	0.0020236	5.88	0.072
Error	4	0.0013764	0.0003441		
Total	5	0.0034000			

Regression Analysis for 'n' - Model #8 (σ^1)

Reason(s) for rejecting this model:- Higher 'S', lower F-value

The regression equation is
 $n = 17241 \mu .\sigma$

Predictor	Coef	StDev	T	P
Noconstant				
$\mu .\sigma$	17241	2123	8.12	0.000

S = 0.4799

Analysis of Variance

Source	DF	SS	MS	F	P
Regression	1	15.187	15.187	65.94	0.000
Error	5	1.152	0.230		
Total	6	16.338			

Regression Analysis for 'n' - Model #1b (σ^{-1})

Reason(s) for rejecting this model:- High P-values

The regression equation is

$$n = -4.24 + 1399 \mu + 0.149 \frac{1}{\sigma} - 34.9 \mu / \sigma$$

Predictor	Coef	StDev	T	P
Constant	-4.241	6.982	-0.61	0.605
μ	1399	1687	0.83	0.494
$1/\sigma$	0.1494	0.1795	0.83	0.493
μ / σ	-34.89	43.05	-0.81	0.503

S = 0.02248 R-Sq = 70.3% R-Sq(adj) = 25.7%

Analysis of Variance

Source	DF	SS	MS	F	P
Regression	3	0.0023890	0.0007963	1.58	0.411
Error	2	0.0010110	0.0005055		
Total	5	0.0034000			

Source	DF	Seq SS
μ	1	0.0020347
$1/\sigma$	1	0.0000223
μ / σ	1	0.0003321

Regression Analysis for 'n' - Model #2b (σ^{-1})

Reason(s) for rejecting this model:- High P-values

The regression equation is

$$n = 383 \mu + 0.0404 \frac{1}{\sigma} - 9.07 \mu / \sigma$$

Predictor	Coef	StDev	T	P
Noconstant				
μ	383.2	194.6	1.97	0.144
$1/\sigma$	0.040411	0.002139	18.89	0.000
μ / σ	-9.073	6.039	-1.50	0.230

S = 0.01998

Analysis of Variance

Source	DF	SS	MS	F	P
Regression	3	16.3372	5.4457	13643.52	0.000
Error	3	0.0012	0.0004		
Total	6	16.3384			

Source	DF	Seq SS
μ	1	15.4078
$1/\sigma$	1	0.9285
μ / σ	1	0.0009

Regression Analysis for 'n' - Model #3b (σ^{-1})

Reason(s) for rejecting this model:- High P-values

The regression equation is
 $n = 1.35 + 32.5 \mu + 0.0055 \ 1/\sigma$

Predictor	Coef	StDev	T	P
Constant	1.347	1.037	1.30	0.285
μ	32.45	46.04	0.70	0.532
$1/\sigma$	0.00548	0.02460	0.22	0.838

S = 0.02116 R-Sq = 60.5% R-Sq(adj) = 34.2%

Analysis of Variance

Source	DF	SS	MS	F	P
Regression	2	0.0020570	0.0010285	2.30	0.248
Error	3	0.0013430	0.0004477		
Total	5	0.0034000			

Source	DF	Seq SS
μ	1	0.0020347
$1/\sigma$	1	0.0000223

Regression Analysis for 'n' - Model #4b (σ^{-1})

Reason(s) for rejecting this model:- Best statistical model but the effects of the dominant predictor μ is slightly contrary to what occurs in practice.

The regression equation is
 $n = 91.1 \mu + 0.0374 \ 1/\sigma$

Predictor	Coef	StDev	T	P
Noconstant				
μ	91.079	9.836	9.26	0.001
$1/\sigma$	0.0374158	0.0008893	42.07	0.000

S = 0.02290

Analysis of Variance

Source	DF	SS	MS	F	P
Regression	2	16.3363	8.1682	15570.75	0.000
Error	4	0.0021	0.0005		
Total	6	16.3384			

Source	DF	Seq SS
μ	1	15.4078
$1/\sigma$	1	0.9285

Regression Analysis for 'n' - Model #5b (σ^{-1})

Reason(s) for rejecting this model:- High P-values

The regression equation is
 $n = 1.57 + 5 \mu + 0.56 \mu / \sigma$

Predictor	Coef	StDev	T	P
Constant	1.57076	0.08871	17.71	0.000
μ	4.7	188.2	0.02	0.982
μ / σ	0.562	5.939	0.09	0.931

S = 0.02130 R-Sq = 60.0% R-Sq(adj) = 33.3%

Analysis of Variance

Source	DF	SS	MS	F	P
Regression	2	0.0020388	0.0010194	2.25	0.253
Error	3	0.0013612	0.0004537		
Total	5	0.0034000			

Source	DF	Seq SS
μ	1	0.0020347
μ / σ	1	0.0000041

Regression Analysis for 'n' - Model #6b (σ^{-1})

Reason(s) for rejecting this model:- Higher 'S', lower F-value

The regression equation is
 $n = -2983 \mu + 97.2 \mu / \sigma$

Predictor	Coef	StDev	T	P
Noconstant				
μ	-2983.5	741.7	-4.02	0.016
μ / σ	97.25	20.77	4.68	0.009

S = 0.1895

Analysis of Variance

Source	DF	SS	MS	F	P
Regression	2	16.1948	8.0974	225.52	0.000
Error	4	0.1436	0.0359		
Total	6	16.3384			

Source	DF	Seq SS
μ	1	15.4078
μ / σ	1	0.7870

Regression Analysis for 'n' - Model #7b (σ^{-1})

Reason(s) for rejecting this model:- High P-values

The regression equation is
 $n = 1.57 + 0.709 \mu / \sigma$

Predictor	Coef	StDev	T	P
Constant	1.56878	0.03403	46.10	0.000
μ / σ	0.7092	0.2898	2.45	0.071

S = 0.01845 R-Sq = 60.0% R-Sq(adj) = 49.9%

Analysis of Variance

Source	DF	SS	MS	F	P
Regression	1	0.0020385	0.0020385	5.99	0.071
Error	4	0.0013615	0.0003404		
Total	5	0.0034000			

Regression Analysis for 'n' - Model #8b (σ^{-1})

Reason(s) for rejecting this model:- Higher 'S', lower F-value

The regression equation is
 $n = 13.7 \mu / \sigma$

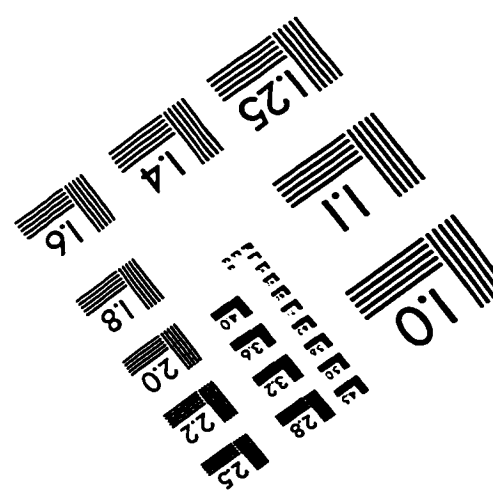
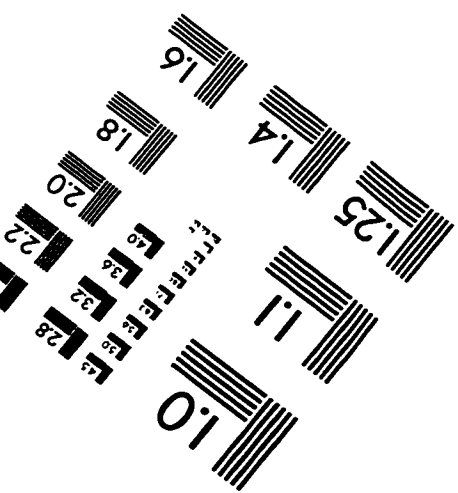
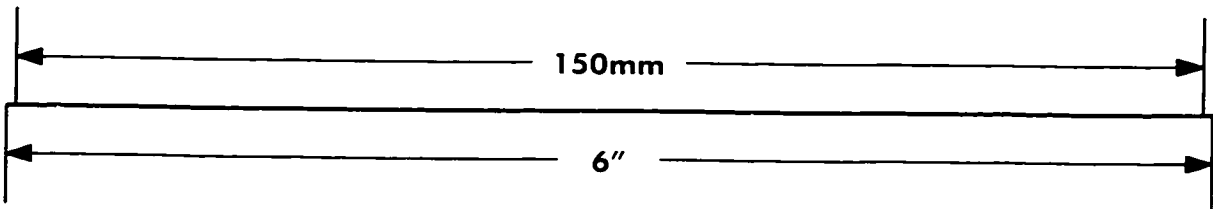
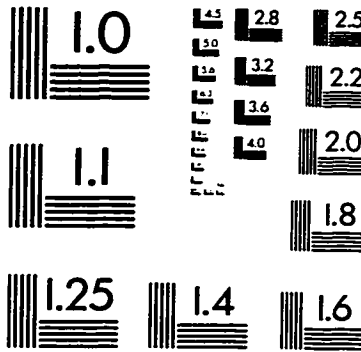
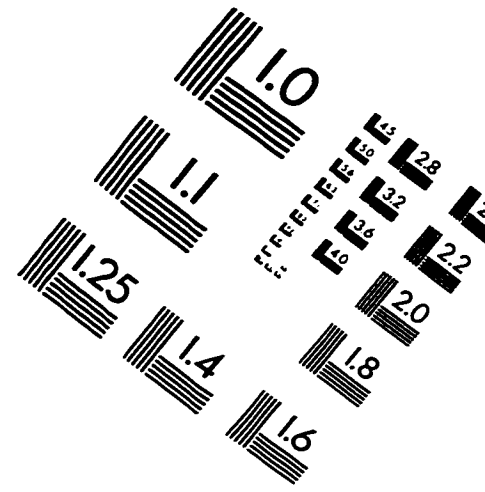
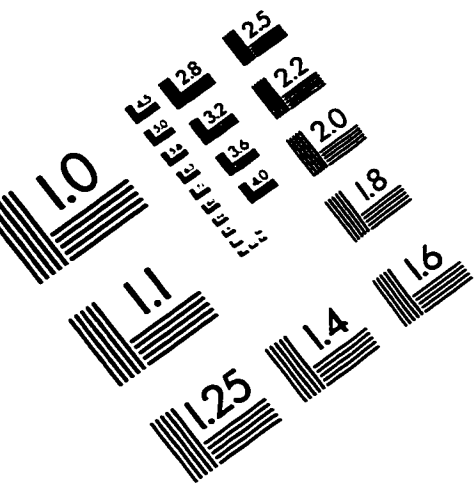
Predictor	Coef	StDev	T	P
Noconstant				
μ / σ	13.736	1.323	10.38	0.000

S = 0.3807

Analysis of Variance

Source	DF	SS	MS	F	P
Regression	1	15.614	15.614	107.74	0.000
Error	5	0.725	0.145		
Total	6	16.338			

IMAGE EVALUATION TEST TARGET (QA-3)



APPLIED IMAGE, Inc
1653 East Main Street
Rochester, NY 14609 USA
Phone: 716/482-0300
Fax: 716/288-5989

© 1993, Applied Image, Inc., All Rights Reserved